(2)

Bioluminescence in the Western Alboran Sea in April 1991

D. M. Lavoie
D. K. Young
M. S. Hulbert
Oceanography Division
Ocean Science Directorate

Original contains color plates: All DTIC reproductions will be in black and white

DISCLAIMER NOTICE

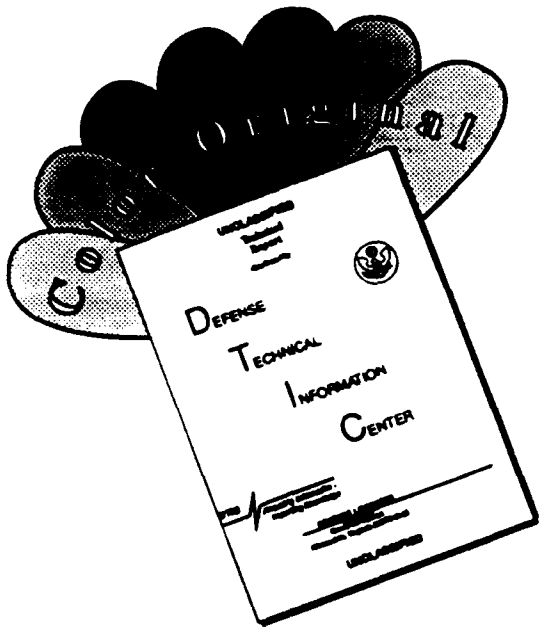

THIS DOCUMENT IS BEST QUALITY AVAILABLE. THE COPY FURNISHED TO DTIC CONTAINED A SIGNIFICANT NUMBER OF COLOR PAGES WHICH DO NOT REPRODUCE LEGIBLY ON BLACK AND WHITE MICROFICHE.

THIS
PAGE
IS
MISSING
IN
ORIGINAL
DOCUMENT

ABSTRACT

This document reports on the results of an expedition to study bioluminescence in the western Alboran Sea of the Mediterranean in April of 1991. Two oceanographic research vessels and a research submersible were involved in making extensive measurements of bioluminescence and optical properties as well as related biological and physical parameters. The primary research tool used was the HIDEX, a high resolution, state-of-the-art bathyphotometer. The results reported here cover only bioluminescence and related biological measurements made from the USNS Bartlett. Recommendations are given for survey requirements needed to extend measurements seasonally and geographically in this region of the Mediterranean.

Bioluminescence was high in this region of the Mediterranean Sea during this study, ranging on the order of 10^{11} to 10^{13} photons $s^{-1}L^{-1}$ in the upper 200 m of the water column. The bioluminescence depth profile usually exhibited several well-defined peaks, and total light and numbers of events generally decreased quickly below the bottom of the thermocline. The variability in intensity of bioluminescence over the night cycle and with depth at any one station was greater than the variability between adjacent stations.

The high intensity of bioluminescence appeared to be due to the abundance and variety of sources rather than due to any one bright taxon. The dominant organisms in terms of light production were heterotrophic dinoflagellates and small crustacean zooplankton rather than chlorophyll-containing organisms. This fact plus the depth distribution of chlorophyll-bearing organisms imply that bioluminescence would not be predictable from surface chlorophyll.

The regional pattern of bioluminescence can be separated into three groups: low values along the Spanish coast in the predominant Atlantic surface water flowing in through the Strait of Gibraltar; high values along the Moroccan coast due to upwelling; and intermediate values in the divergence region at the N-S oceanic front area near Isla de Alboran.

The results confirmed the historical observations of high bioluminescence in this region, but they did not confirm the phenomenology of the MED 3-88 observations.

ACKNOWLEDGMENTS

The authors would like to thank Mr. Kenneth M. Ferer for encouraging and funding this wide-ranging, cooperative study of an important phenomenon. We also appreciate the collaboration of our colleagues on the program, including Rudy Hollman, Richard Ray, Pat Wagner, and Irene DePalma on the USNS Bartlett and James Case, Stephen Bernstein, and Edith Widder on the R/V Seward Johnson; the often tedious data analysis and reduction performed by our shore-based technicians Kevin Hart, Mary Simmons, and Scott Heitzman; typing by our secretaries Elaine McNeil, Leona Cole, and Roxanne Read; and editorial assistance of Jaime Ratliff and the rest of the Technical Publications staff. Our thanks to Mark Geiger for the loan of the underway sampling system and to CDR Thomas Donaldson for his help. And we salute the officers and crew of the USNS Bartlett, the R/V Seward Johnson.

This work was sponsored by CNO (OP-096) ASW Oceanography under Program Element 0603704N, Mr. Kenneth M. Ferer, Program Manager.

The mention of commercial products or the use of company names does not in any way imply endorsement by the U.S. Navy or NOARL.

CONTENTS

1. INTRODUCTION 1
2. BACKGROUND 1
3. STUDY AREA 3
4. PROCEDURES 5
    4.1 HIDEX 5
    4.2 PLANKTON NET HAULS 9
    4.3 PHOTOGRAPHIC SURVEY 9
    4.4 ALGAL PIGMENTS 9
    4.5 UNDERWAY DATA 10
5. RESULTS 10
    5.1 HIDEX 11
    5.2 PLANKTON NET HAULS 13
    5.3 PHOTOGRAPHIC SURVEY 14
    5.4 ALGAL PIGMENTS 14
    5.5 UNDERWAY DATA 14
6. DISCUSSION 14
    6.1 BIOLUMINESCENCE INTENSITIES AND SOURCES 14
    6.2 BIOLUMINESCENCE DISTRIBUTION 16
    6.3 RELATION OF BIOLUMINESCENCE TO ALGAL PIGMENTS 18
7. CONCLUSIONS 20
8. RECOMMENDATIONS 22
9. REFERENCES 23

Appendix A Multiparameter Profiles
Appendix B Bioluminescence Profile Overlays
Appendix C Integrated Bioluminescence Intensities and Events
Appendix D Plankton Counts
    D-1: Zooplankton, 200-0 m
    D-2: Dinoflagellates at station 7
    D-3: Dinoflagellates at station 12
Appendix E Photographic Survey
Appendix F Extractable Algal Pigments
Appendix G Underway Data

FIGURES

Figure 1a: IR image of Alboran Gyre with float track.....4
Figure 1b: IR image of Alboran Gyre with cruise track.....4
Figure 2: HIDEX cut-away drawing.....8
Figure 3: Integrated light and peak intensities by station.....11
Figure 4: Physical provinces in the western Alboran Sea.....17

TABLES

Table 1: Station locations and dates.....5
Table 2: Bioluminescence operations summary.....7

BIOLUMINESCENCE IN THE WESTERN ALBORAN SEA IN APRIL 1991

1. INTRODUCTION

The objective of this experiment was to address EUROCEAN 89-03 Oceanographic Requirements with respect to bioluminescence and related optical properties in the Mediterranean Sea. Specifically, we intended to examine the variability of bioluminescence with depth, over the region, and throughout the nighttime cycle in the western Alboran Sea. In addition, we intended to determine the contribution by dinoflagellates and small zooplankton to the total bioluminescence.

The approach was to make profiles at closely spaced stations using the HIDEX (High Intake, Defined EXitation) bathyphotometer, following the nighttime cycle of bioluminescence by continual profiles from dusk until dawn. These measurements were coordinated with the daytime activities of the optical and physical oceanography group aboard the USNS Bartlett and those of the bioluminescence group and the submersible studies group aboard the R/V Seward Johnson, whose results are reported in separate documents.

Together with infared (IR) satellite imagery and surface float tracks provided by the Operational Oceanography Center of the Naval Oceanographic Office, the data developed by this coordinated effort cover most of the physical, biological, and optical aspects of planktonic bioluminescence in this region of the Mediterranean.

2. BACKGROUND

Donaldson (1989) reported on 974 measurements of bioluminescence at 35-ft depths (via sea chest) over the length of the Mediterranean Sea between August 1988 and February 1989. The significance of these measurements is that they were the first resulting from a U.S. Navy survey of bioluminescence in the Mediterranean Sea, and that they were taken during the MED 3-88 deployment of the USS KENNEDY by military rather than civilian

personnel. The measurements showed highest levels of surface bioluminescence in the Alboran Basin of the western Mediterranean Sea. This finding confirmed previous of work by Russian scientists (Bityukov and his coworkers 1971a, 1971b, 1977, 1978, and 1982, and Gordiencko et al., 1980) who had collected between 1965 and 1979 the only previously published measurements of bioluminescence from the Mediterranean Sea.

More specifically, the extensive bioluminescence measurements by vertical profiling and towed bathyphotometers by the Russian investigators demonstrated that bioluminescence in the Mediterranean Sea increased from east to west, being weakest in the Aegean Sea and most intense near the Straits of Gibraltar in the Alboran Sea. Other geographic maxima were correlated with upwelling areas. Significant seasonal variations and vertical layering were noted throughout. Vertical maxima were correlated with planktonic biomass, thermal gradients, or both, depending on the amount of water mixing. The most intense bioluminescence in the Alboran Sea was observed in early spring (April) and lowest in winter (February). Bityukov (1971a) reported that measurements of bioluminescence from a towed bathyphotometer in the Strait of Gibraltar and east of the Azores were 600 times greater than those of the Gulf Stream off North America and 5 times greater than those in the Aegean Sea.

Independent evidence suggests that the extremely intense bioluminescence measured by Donaldson (1989) and Bityukov (1971b) in the Alboran Sea may be the result of certain gelatinous marine species (listed by Bityukov, 1971b as Medusa, Siphonophora and Tunicata) among 368 identified bioluminescent species from Atlantic and Mediterranean waters. Recent in situ measurements from a research submersible of bioluminescence produced by these gelatinous animals suggest that, once stimulated, certain species may continue flashing for periods from 90 s (E. Widder et al., 1989) to several minutes in duration (E. Widder, Harbor Branch Oceanographic Institution, Ft. Pierce, FL, personal communication, 1991).

Because the relative intensity of bioluminescence from gelatinous species is two or more orders of magnitude greater than that of dinoflagellates (the most commonly reported source of oceanic bioluminescence), the bioluminescence potential of a water column dominated by such organisms would be greater accordingly. Further, since the residence time of stimulated organisms in the chambers of

all existing bathyphotometers is on the order of several seconds or less, the full flash times of gelatinous species would not be recorded; thus, the bioluminescence potential of a water column dominated by gelatinous species measured by existing bathyphotometers may be greatly underestimated.

The approach taken in the field experiment was to characterize the bioluminescence, as well as the physical and optical properties of this area, to determine the relative importance of the different taxa to the production of light and to examine the nature of the physical controls on the organisms' distribution, development, and the propagation of their light.

3. STUDY AREA

The circulation of the surface waters of the western Alboran Sea is dominated by the inflow of modified Atlantic Water through the Straits of Gibraltar. As described by Arnone et al. (1990), the flow forms an anticyclonic gyre between the Strait and the Isla de Alboran. A cyclonic gyre exists immediately to the east, forming an area of shear and upwelling around the 3°W meridian. The anticyclonic western gyre was well developed during this experiment, as seen in the satellite IR imagery in Figure 1a. Superimposed on this image is the track of a drifter buoy whose positions were plotted every 24 h (image and track courtesy of the Operational Oceanography Center, Naval Oceanographic Office).

Bioluminescent layers of high intensity (Bityukov, 1977) and extensive upwelling of nutrient-rich water and high productivity are known to occur in the frontal areas adjacent to the Moroccan coast in the Alboran basin (Lohrenz et al., 1988). The cruise track and station locations were chosen to be counter to the prevailing transport of the western Alboran Gyre, with the rationale of sampling the maximum variability in the region. The biological variability was expected to be due to population dynamics, as well as physical mixing of the seawater. The cruise track is also shown superimposed on the IR imagery in Figure 1b.

The moon phases at the time of the study were as follows: full moon 30 March; last quarter 7 April; new moon 14 April; and first quarter 21 April.

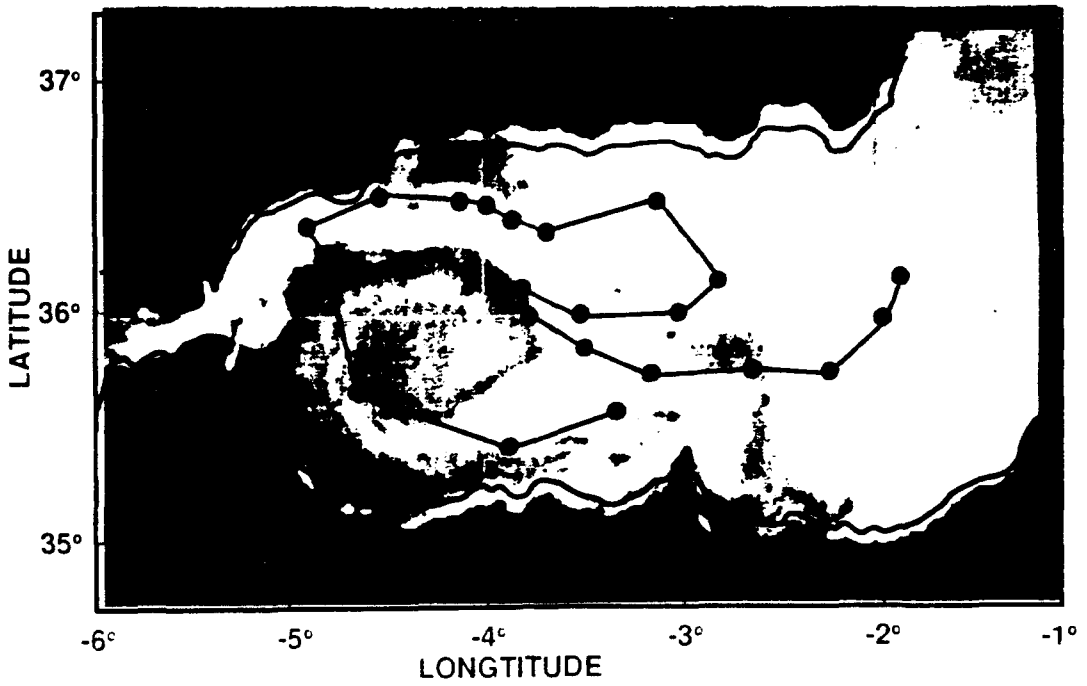

Figure 1a. Satellite IR imagery of the western Alboran Sea in April 1991. The superimposed track is the path of a drifter buoy released at approximately 3° 30' W whose positions were plotted every 24 h. The inflowing Atlantic Water flows along the Spanish coast before turning south near the 3° meridian to form an anticyclonic gyre. Isla de Alboran appears near 36° N, 3° W.

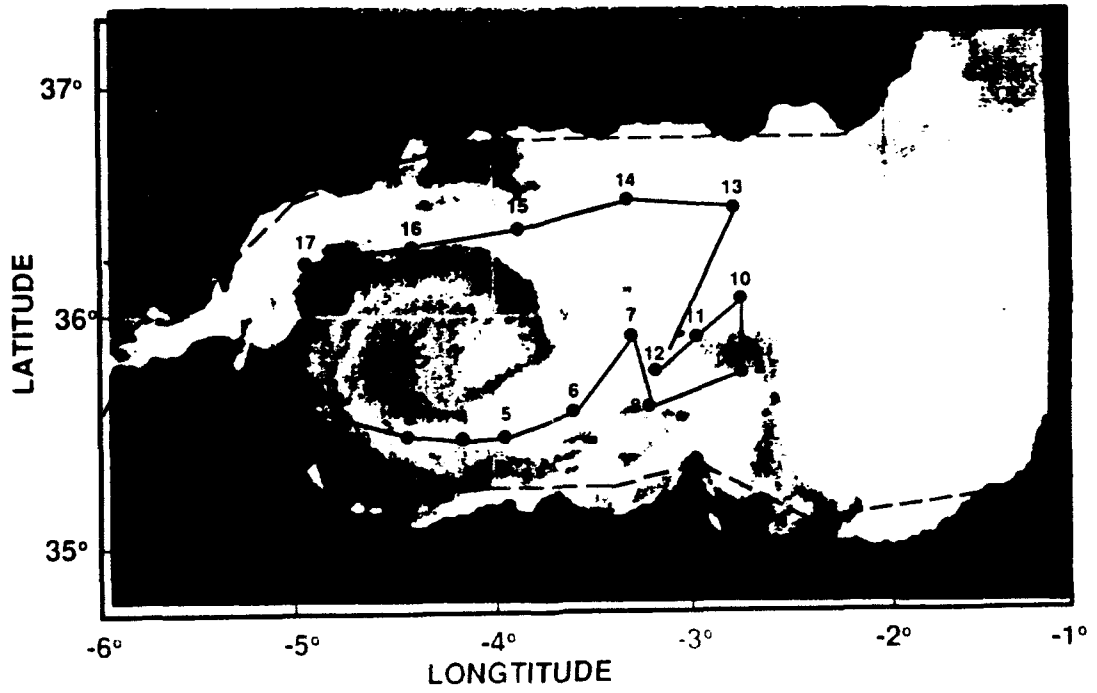

Figure 1b. The same IR imagery with the cruise track of the USNS Bartlett superimposed. Note that the track ran counter to the direction of the gyre.

4. PROCEDURES

Table 1 lists the station locations and dates. Stations were generally occupied for 22 h, except for station 12, which was occupied for 4 days. Optics studies were conducted during daylight, and bioluminescence studies were conducted during the nighttime. The ship was allowed to drift a maximum of 2 nmi away from the station during measurements, and then it was maneuvered back to position. A summary of the bioluminescence operations is shown in Table 2, and details of the bioluminescence activities are described below.

Table 1. Station locations and dates for MED-OP 91. (USNS Bartlett cruise 1306-91, 2-21 April 1991)

Station Number	North Latitude	West Longitude	Date (April)
1	35° 49.5'	5° 03.8'	2
2	35° 33.5'	4° 48.7'	3
5	35° 28.0'	4° 00.0'	6
6	35° 34.0'	3° 39.0'	7
7	35° 54.0'	3° 21.0'	8
8	35° 35.0'	3° 16.0'	9
9	35° 44.0'	2° 48.0'	10
10	36° 03.0'	2° 48.0'	11
11	35° 53.0'	3° 01.0'	12
12	35° 45.0'	3° 14.0'	13,14,15,16
13	36° 27.0'	2° 57.0'	17
15	36° 21.0'	3° 55.0'	19
16	36° 17.0'	4° 27.0'	20

4.1 HIDEX: HIDEX (Figure 2) is an advanced bathyphotometer developed with Navy funding by Dr. James Case of the University of California at Santa Barbara. The design incorporates a high-volume pump to stimulate maximum bioluminescence intensity within a

region of defined turbulence provided by a grid. The numbers of flashes stimulated by this turbulence are counted, and the total, calibrated light intensity is measured. The decay characteristics of the flashes are determined using a photometer array connected to a line of fiber optic pickups spaced along the length of the chamber, which is 1 m long and has a volume of 16 L. In addition to the bioluminescence measurements, the package also includes instrumentation for the simultaneous measurement of depth, temperature, salinity, fluorometry, transmissometry, and tilt and roll of the package. The data are telemetered up the wire, displayed in real time, and recorded on magnetic disk.

Bioluminescence operations generally began at 1800 h local time, just before sunset, and ended at 0400 h, just before sunrise. Generally, three series of multiple profiles were recorded: the "dusk" series from 1800 to 2100 h, the "midnight" series from 2200 to 0100 h, and the "dawn" series from 0200 to 0400 h. In order to observe both short-term variability on the scale of minutes and variability over the entire nightly cycle, from two to four profiles were taken approximately 30 minutes apart during each of these series. Sampling started at 5 to 10 m and ended at a depth of 200 m. Lowering speeds were approximately 0.3 ms^{-1}. Pumping rate was held constant at 16 L s^{-1} (i.e. one volume s^{-1}) and the instrument sampled the multiple signals at a rate of 2 Hz, for an overall vertical resolution of approximately 0.15 m.

At most of the stations, one or more motor speed tests were also conducted. These were time series tests (done at the most luminous depth noted in the profile) in which the pump motor speed was increased in steps to determine the speed at which organisms began to be ejected from the measurement chamber before their bioluminescence had begun to decay. The tests provided a check on the operating parameters of the bathyphotometer, as well as giving information on the type of organisms producing light.

At station 11, a drogue with a surface marker was placed at a depth of 30 m for the purpose of following and sampling a single patch of water over the diel cycle. All operations were done within 0.2 nmi of the drifter for 24 h. Station 12 was occupied for four days in order to study long-term variability at a fixed site.

Table 2. SUMMARY OF BIOLUMINESCENCE OPERATIONS, MED-OP 91 (CRUISE 1306-91).

H=HIDEX; P=PLANKTON; C=CAMERA; W=WATER. At each station, casts are numbered consecutively according to the type (e.g. Hidex casts are 1H, 2H, 3H, etc.; Plankton casts are 1P, 2P, 3P, etc. Hidex casts are labeled L for 200m, S for <200m, MS for motor speed test at one depth, or U for upcast.)

	DATE STATION	2-3 1	3-4 2	4-5 3	5-6 4	6-7 5	7-8 6	8-9 7	9-10 8	10-11 9	11-12 10	12-13 11	13-14 12	14-15 12	15-16 12	16-17 12	17-18 13	18-19 14	19-20 15	20-21 16	21-22 17	TIME (LOCAL)
TIME (GMT)	1600	1H (L)						1W								1W						1800
	1700	3H (L)	1C 2C				1H (L)															1900
	1800	4H (L)				1H 2H (L)	2H 3H (L)	1H (L)	1H 2H (L)	1H 2H (L)	1H 2H (L)	1H (S) 2H (S) 3H (S)			14H (L) 15H (L) 16H (U)	16H (L)	1H (L)		1H (L)	1H (L) 2H (L)		2000
DUSK SERIES	1900 SUN-DOWN					3H 4H (L)	4H (S)	2H (L)	3H (L) 4H (MS)	3H (L)	3H (L) 4H (MS)	4H (S) 5H (S) 6H (S)				17H 18H (L)	2H 3H (L)		2H (L) 3H (L)	3H (L)		2100
	2000		1P 2P 3P			1C	1C		1C	1C	5H (MS) 6H (MS) 1C	1C				19H 20H (L)	4H (L)		4H (MS) 5H (MS)	4H (L) 5H (L) 6H (S)		2200
	2100					1P 2P 3P	1P 2P 3P	1C	1P 2P 3P		1P 2P 3P	1P 2P 3P				21H (L)			6H (L)	7H (MS)		2300
	2200	5H (L)	1H 2H (L)				5H (L)	3H (L)	5H	1P 2P 3P 4H (L)			1H 2H (L)	7H 8H 9H (L)		22H 23H (L)	5H 6H (L)		7H (L)	8H (L)		2400
MID-NIGHT SERIES	2300	6H 7H (L)	3H (L) 4H(MS)			5H 6H (L)		4H 5H (L)		5H 6H (L)	7H (L)	7H (S) 8H (S) 9H (S) 10H (S)	3H (L)	10H(MS)		24H (L) 25H (MS) 26H (MS)	7H (L)		8H (L) 9H (L)	10H (L) 11H (MS)		0100
	2400		5H(MS)				6H (L) 7H (S)		7H (L) 7H (U)		8H 9H (L)	11H (S) 12H (S) 13H (S)	1C	1C		1C	1C		1C	1C		0200
	0100											14H (S) 15H (S) 16H (MS)	1P 2P 3P	1P 2P 3P		1P 2P 3P	1P		1P 2P 3P	1P 2P 3P		0300
	0200	8H 9H (L)	6H 7H (L)			7H 8H (L)	8H 9H (L)	6H 7H (L)	8H (L)	7H 8K (L)	10H 11H (L)		4H 5H (L)	11H (L)		27H 28H (L)			10H (L) 11H (L)	13H (L)		0400
DAWN SERIES	0300	10H 11H (L)	8H (L)			9H (L)	10H (L) 10H (U)	8H (L)	9H (L)	9H (L)	12H (L)		6H (L)	12H 13H (L)		29H (L)			12H (L) 13H (MS)	14H (L) 15H (MS)		0500
	0400 SUNUP																					0600

																		TOTALS
HIDEX	10	8 (2MS)		9	11 (1S,1U)	8	9 (1MS1U)	9	12 (3MS)	16 (1MS)	6	7 (1MS)	3 (1S, 1U)	14 (2MS)	7		13 (3MS)	13 (3MS)	155
CAMERA	0	2		1	1	1	1	1	1	1	1	1	0	1	1		1	1	15
PLANKTON	0	3		3	3	0	3	3	3	3	3	3	0	3	1		3	3	37
WATER	0	0		0	0	1	0	0	0	0	0	0	0	1	0		0	0	2
TOTAL	10	14		13	14	10	13	13	16	20	10	11	3	19	9		17	17	209

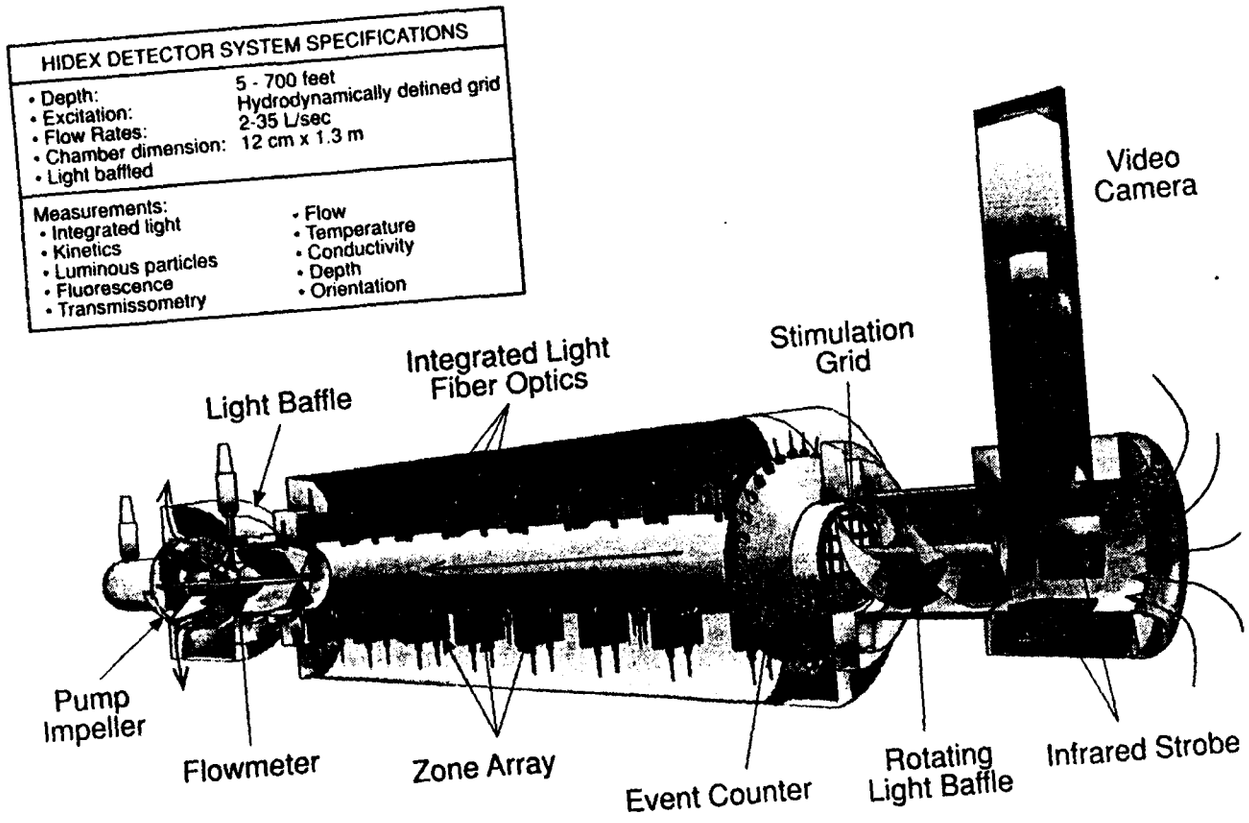

Figure 2. HIDEX cut-away drawing. The Model 3 HIDEX used in this study was identical to the one depicted here except that the video camera and IR strobe were not installed. Seawater is drawn through the rotating light baffle without significant turbulance until the stimulation grid is encountered. Here, bioluminescence is stimulated in a defined turbulance field and the intensity and number of flashes is counted. The decay of each individual flash is detected as the organisms pass through the zone array of fiber optic pickups (these are led to photomultipliers in the electronics bottle—not shown). The water passes through another light baffle and a flowmeter before being ejected. An external CTD with an in situ fluorometer and a 2-cm beam transmissometer complete the package. Drawing courtesy of Dr. Stephen Bernstein.

4.2 PLANKTON NET HAULS: At most stations, vertical hauls were made from standardized depths of 200 m, 100 m, and 50 m to the surface. Hauls were made with a 70 cm diameter net having a mesh of 62 μm and fitted with a 20 μm mesh cod end. These collections were examined briefly with a binocular microscope for qualitative impressions before being preserved in borate-buffered, 2% formaldehyde. The counts made on these samples provided semi-quantitative estimates of plankton abundance and vertical distribution.

At stations 7 and 12, the net tows were supplemented by collections using 10 L Niskin bottles mounted on the optics profiler during the evening optics hydrocast. Sampling depths were chosen based on the in situ fluorescence measurements made by the optics package during the downcast. The entire contents of each Niskin bottle were poured through a 20 μm cod end, and the approximately 100 mL of concentrate was preserved for quantitative counts of the organisms using an inverted microscope and the standard Utermöhl technique (Utermöhl, 1958).

4.3 PHOTOGRAPHIC SURVEY: On all but stations 1 and 2, a photographic survey of the water column was carried out. The photographic package consisted of a 70 mm undersea stereo camera (Photosea, Inc., San Diego, CA) mounted on a frame holding two strobe lights oriented to provide a cone of light 45° off the camera axis. The camera and strobes were set to fire automatically every 30 s, and the infocus field encompassed a volume of approximately 0.125 m^{-3}. The camera was held at each depth from 5 to 15 min, depending on the amount of bioluminescence observed in the preceding HIDEX cast. The resulting films were developed on board to provide immediate feedback to the camera operations, and they were later examined to determine the semiquantitative distributions of zooplankton down to the size of approximately 1 cm.

4.4 ALGAL PIGMENTS: Total extractable chlorophyll and phaeopigment measurements were made by standard techniques (Strickland and Parsons, 1972) with slight modifications. Seawater aliquots of 1100 mL were drawn from 10 L Niskin bottles mounted on the Optics sampling package, which collected water samples during the Optics casts. Sampling depths were chosen after examining the in situ fluorescence profile of the downcast, and the bottles were tripped during pauses in the upcast. The water samples

were filtered through 0.2 μm pore size Nuclepore™ (Nuclepore, Corp., Pleasanton, CA) membrane filters under a vacuum of 15 cm Hg or less. The filter was then placed in 90% acetone at 4° C for 24 h, and the fluorescence of the supernatent was read in a fluorometer (Model 10, Turner Designs, Mountain View, CA) calibrated against pure chlorophyll (Sigma Chemical Co., St. Louis, MO) in 90% acetone.

Two subsamples of seawater were collected from each Niskin bottle by passing the water through a 210 μm nytex mesh to remove most zooplankton. Each subsample was split into two aliquots, one of which was passed through a 20 μm nytex mesh before extraction, and the other was extracted directly. In summary, duplicate subsamples were drawn from each Niskin, and duplicate extractions were made on each of two size fractionated samples. The >20 μm fraction was calculated from the difference between the total and the <20 μm fraction. Statistics were calculated according to Dean and Dixon's (1951) procedures for small sample sets.

4.5 UNDERWAY DATA: These data were collected using a system loaned by Code OSWL, Naval Oceanographic Office. Seawater was drawn through a short length of 3 in ID stainless steel pipe inserted through the ship's portside seachest, located approximately 7 m below the waterline in the engine room. After a passage through about 30 cm of pipe, the water entered a baffled chamber that was monitored by a photometer for bioluminescence. Downstream of the photometer were a temperature sensor, a conductivity sensor, a flow-through fluorometer (Model 10, Turner Designs, Mountain View, CA), and finally a discharge pump. Data were continuously logged on magnetic tape. The system ran during the entire cruise with only minor interruptions.

5. RESULTS

The cruise was very productive. The bioluminescence potential of the 10 to 200 m water column was mapped in unprecedented detail, not only in vertical scale but also in time throughout the night cycle. These profiles were matched by profiles of related parameters, and the optical properties of the water were characterized thoroughly and in high resolution. All in all, these results are a trove of data. This document will report preliminary analyses from the cruise results, and the data will be reported more thoroughly elsewhere.

Stations were occupied for 16 out of a total of 20 nontransit days. Station 14 could not be conducted due to equipment failure, and stations 3, 4, and 17 had to be abandoned due to severe weather. Table 2 summarizes all the nighttime operations. Results are summarized below for each of the study areas.

5.1 HIDEX: A total of 134 profiles was collected. Representative individual profiles of all the parameters measured by HIDEX are presented in Appendix A, Multiparameter Profiles. One representative cast is shown for each series at each station to show the variability in all parameters throughout the night. Appendix B, Bioluminescence Profile Overlays, emphasizes the magnitude and nightly variability of the bioluminescence at each station. Each figure shows overlaid profiles in three panels corresponding to the "dusk," "midnight," and "dawn" series.

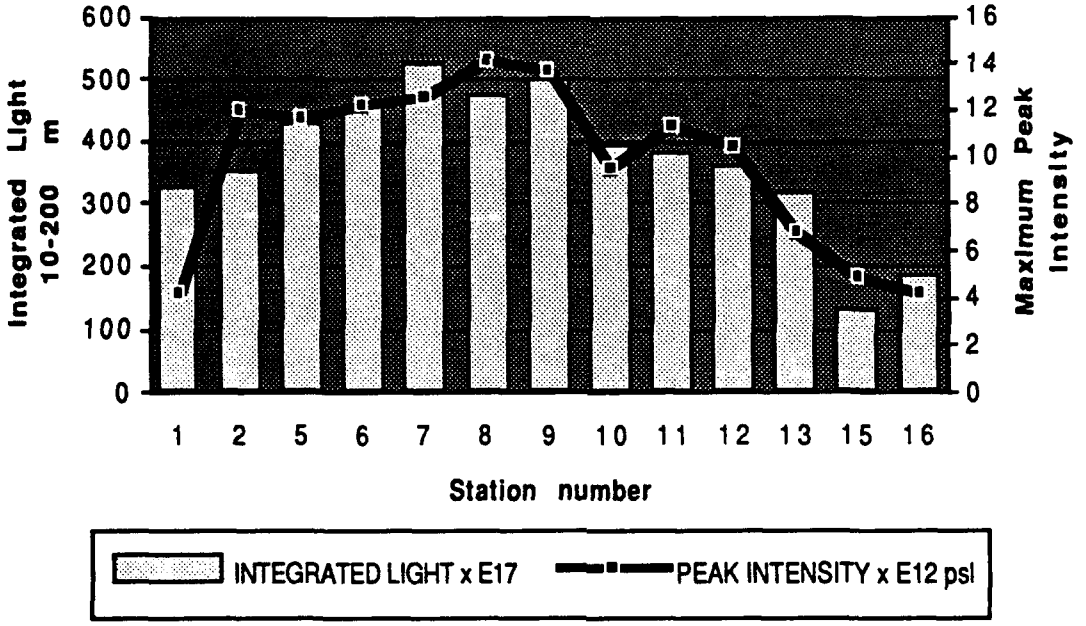

Figure 3. Bioluminescent light integrated over the 200 m water column vs. station and peak intensity of bioluminescent light vs. station. Integrated light units are 10^{17} photons $s^{-1}m^{-2}$. Peak intensity units are 10^{12} photons $s^{-1}L^{-1}$(abbreviated "psl")

Appendix C, Integrated Bioluminescence Intensities and Events, shows how the total bioluminescent light and the number of events (light flashes) in a m^2 of the 200 m water column varied throughout the night for each station. Due to technical uncertainties regarding the event counter that were unresolved as of this writing, the absolute value of the integrated events values may not be accurate; however it is believed at this time that they do reflect relative changes in total events for the water column.

In general, bioluminescence was high at all stations, with the range being roughly 10^{11} to 10^{13} photons $s^{-1}L^{-1}$ (psl). Station 1 just to the south of the strait and the 3 stations along the Spanish coast exhibited the lowest peak intensities, 4 to 5 x 10^{12} psl; the stations along the Moroccan coast generally had peak intensities on the order of 1.2 x 10^{13}, while the stations in the vicinity of Isla de Alboran were variable. Figure 3 presents the integrated light and the peak intensities by station.

Vertically, bioluminescence intensity, as well as the number of bioluminescent events, was generally highly stratified, exhibiting large and often strongly peaked values in the upper 40 to 70 m, then dropping sharply below that depth. Bioluminescence intensity peaks were often associated with the thermo/halocline at the bottom of the mixed layer. E-fold, a measure of the decay rate of the flashes, generally showed an inverse relationship with depth, indicating that bioluminescent flashes were of shorter duration in the upper layer and longer in the deeper layer. In situ fluorometry and beam attenuation were also higher and exhibited peaks in the upper 40 to 60 m compared to the water below, although their maxima did not always coincide with those of the bioluminescence profile.

Temporally and spatially, the peak intensities, integrated light, and the overall vertical pattern of bioluminescence distribution appeared to remain relatively constant over the scale of days, as was evident in both the data reported here and in the data reported by the investigators aboard the R/V Seward Johnson (which was collected 1 to 2 days later at the same station locations) and in the data taken at station 12, which was occupied for 4 days.

Over the nightly dark cycle, bioluminescence at individual stations generally exhibited significant variations. In many cases, the variable bioluminescence appeared to be due to the waxing and waning of particular layers (Appendix B, Bioluminescence Overlays).

The bioluminescence potential integrated over the 10 to 200 m water column also varied regularly through the night (Appendix C, Integrated Bioluminescence Intensity and Events).

The range of maximum intensities and total integrated light between adjacent stations was typically less than the range observed over the dark cycle and with depth at any one station.

5.2 PLANKTON NET HAULS: Data from the net hauls are presented in Appendix D, Plankton Counts. Table D-1 lists the zooplankton collected in the plankton net hauls from 200 m to surface. Table D-2 lists the results of the quantitative dinoflagellate counts done from Niskin bottles on station 7, and Table D-3 lists the counts from 3 days of collections done at station 12.

The zooplankton listed in Table D-1 are representative of most temperate pelagic areas, including the North Atlantic (the presumed source for many of the forms seen in this survey) and the Mediterranean. As a taxonomic list, Table D-1 agrees well with observations compiled by Madin (1991), for this area of the Mediterranean. It should be noted that net collections typically do not sample certain delicate organisms, such as ctenophores, most medusae, and larvaceans, so these gelatinous forms may be expected to be underrepresented in this collection.

The nonbioluminescent dinoflagellates at these stations consisted of certain *Ceratium* and *Dinophysis* species, and bioluminescent dinoflagellates were represented by *Ceratium fusus*, *Noctiluca miliaris* (=*scintillans*), and species of *Protoperidinium* (Tables D-2 and D-3). Taken together, the bioluminescent dinoflagellates numerically dominated the dinoflagellate population.

Especially intense surface bioluminescence was observed while the ship was underway during several nights of the first half of the cruise. On occasion, bright but short lived luminescence was easily visible on the crest of the bow wake while the ship steamed for 10 min or more (roughly 1500 m). When the deck lights were turned on, brownish patches were visible on the water surface. Bucket samples in these areas brought up masses of *Noctiluca miliaris* that formed a surface layer of cells in the bucket. The cursory, shipboard examination of the net hauls indicated that *Noctiluca miliaris* virtually disappeared from the plankton population in the stations along the Spanish coast, while *Protoperidinium* species remained

along the Spanish coast, while *Protoperidinium* species remained relatively plentiful. Note that both *Noctiluca* and *Protoperidinium* are heterotrophic, that is, they do not contain chlorophyll, preying instead on other plankton for nutrition.

5.3 PHOTOGRAPHIC SURVEY: The results of examining 2300 photographic frames are given in Appendix E, Photographic Survey. These results represent approximately 290 m^3 of seawater examined. Euphausid crustaceans were the most common type of organism observed. Particles that were obviously detritus were also abundant. Some of the detritus was amorphous, but the dominant form was the "stringer," an elongate aggregate with a mucous-like appearance.

5.4 ALGAL PIGMENTS: Concentrations of extracted chlorophyll "a" and phaeopigment (a breakdown product of chlorophyll) are given in Appendix F, Extractable Algal Pigments. Surface concentrations were generally greater than 1 mg m^{-3} except for stations 9, 10, and 11. This level of chlorophyll is only a bit higher than levels previously measured by this laboratory in this area (Lavoie and DePalma, 1982.) At most of the depths sampled, the majority of the algal pigments were in the <20 μm size fraction, i.e., the chlorophyll was contained in organisms smaller than most bioluminescent dinoflagellates.

5.5 UNDERWAY DATA: Because of problems with the underway measurement system, the temperature and salinity data were not useable; however, fluorescence and bioluminescence data were collected for most of the cruise. Figures G-1 and G-2 in Appendix G, Underway Data, are two examples of the data. Clearly at this depth (7 m), high fluorescence (indicating high chlorophyll concentrations) and high bioluminescence do not always co-occur.

6. DISCUSSION

6.1 BIOLUMINESCENCE INTENSITIES AND SOURCES

The measurements taken during this experiment show that high levels of bioluminescence occur in the Alboran Sea, confirming the findings of Bityukov and his coworkers and those of Donaldson. Bioluminescent light intensity levels measured by HIDEX ranged from about 10^{13} photons $s^{-1}L^{-1}$ (psl) above the bottom of the thermocline down to about 10^{11} psl from below the thermocline to

200 m. For comparison, Vestfjord, Norway, another semienclosed body of water with a high bioluminescence potential, exhibited maximum intensities on the order of 5 x 10^{11} psl in September 1990 (NOARL, unpublished data).

Preliminary results from the submersible studies (E. Widder, Harbor Branch Oceanographic Institution, Ft. Pierce, FL, personal communication, 1991) indicate that in this April timeframe, luminescent gelatinous organisms were not abundant enough to account for the amount of light measured by Donaldson in December in MED 3-88; nonetheless, Widder observed that such organisms were indeed present during the current study and exhibited bright, persistent luminescent displays (Widder, 1991).

The sampling characteristics of the HIDEX are such that the high levels measured must be attributed to dinoflagellates and smaller crustaceans, rather than to gelatinous forms. The plankton net hauls indicate that the bioluminescent dinoflagellates were abundant. Of these, *Noctiluca* was the most obvious in the collections. The light output of *Noctiluca* has been measured at 5 x 10^{9} psl (Eckert, 1965), and each organism can be stimulated to flash multiple times; however, the numerical counts (Tables D-2 and D-3) indicate that the *Protoperidinium* population actually was the source of most of the dinoflagellate bioluminescence potential. *Protoperidinium* light output has been measured at 2 to 3 x 10^{9} psl (Lapota et al., 1989). The zooplankton collected in the vertical net hauls were not examined for bioluminescence; however, many copepods, euphausids, and other crustaceans are known to be capable of bioluminescence, and the high numbers of crustaceans collected in the net hauls and seen in the photographic survey indicate that these organisms were also a probable significant source of bioluminescence.

To summarize, it would appear that the bioluminescence observed in the Alboran Sea in April 1991 was different in character from that observed in December 1988. Dinoflagellates and crustaceans were responsible for the majority of the bioluminescent light measured in April 1991, while the results of the Johnson-Sea-Link observations and measurements indicate that a high abundance of gelatinous zooplankton is the most likely explanation for the December 1988 observations. The bioluminescence potential was very high in the present study and seems to have been a result of the abundance of sources rather than the extreme intensity of one type of emitter.

6.2 BIOLUMINESCENCE DISTRIBUTION

The distribution of bioluminescence intensity across the Alboran Sea—low on the extreme western and northern edge, high on the southern edge, and intermediate and variable on the eastern edge—corresponds to the three hydrographic provinces found for this area by Hollman (1992). As seen in Figure 4, these provinces consist of Atlantic surface water flowing into the strait and along the Spanish coast, a north-south front near Isla de Alboran, and the modified Mediterranean water along the Moroccan coast. The observed hydrography of the area indicates that the increase in organisms and bioluminescence was a response to the divergence and upwelling in the frontal and Moroccan provinces.

Throughout the western Alboran Sea, bioluminescence due to dinoflagellates and small crustacean zooplankton exhibited highly structured vertical profiles. High bioluminescence was mostly confined to the upper 70 m where intensities varied by as much as a factor of 6. The high levels were often in layers only a few meters thick. At some stations, although vertical structure was pronounced, the peaks did not show a consistent pattern in depth or intensity between successive series of casts. On the other hand, at many stations, some of the bioluminescence peaks did appear consistently in successive profiles, apparently waxing toward midnight and waning toward dawn. Where this occurred, the pattern suggested an increase in light production among organisms at that depth, rather than migration of organisms from another depth. Such a pattern would be consistent with the diel periodicity that has been noted in cultured bioluminescent dinoflagellates in the laboratory (Hamman, Biggley, and Seliger, 1981) and that was first demonstrated in natural populations by NUSC and NOARL investigators in 1990 (Lapota et al., 1990). The evidence for photoperiodicity is even more obvious in the plots of bioluminescence integrated over the 200 m water column (Appendix C), in which both intensity and number of events show regular variation throughout the night; however, the pattern was not always that of a simple peak around midnight at all stations, as shown at stations 1, 6, 10, and 11 for example.

The fact that the pattern of variation—in vertical structure as well as in integrated light—differs among the stations reinforces the inference that the bioluminescence observed in this region of the Mediterranean was not attributable to a single, easily identified phenomenon. Such phenomena as migration of crustaceans, patchy

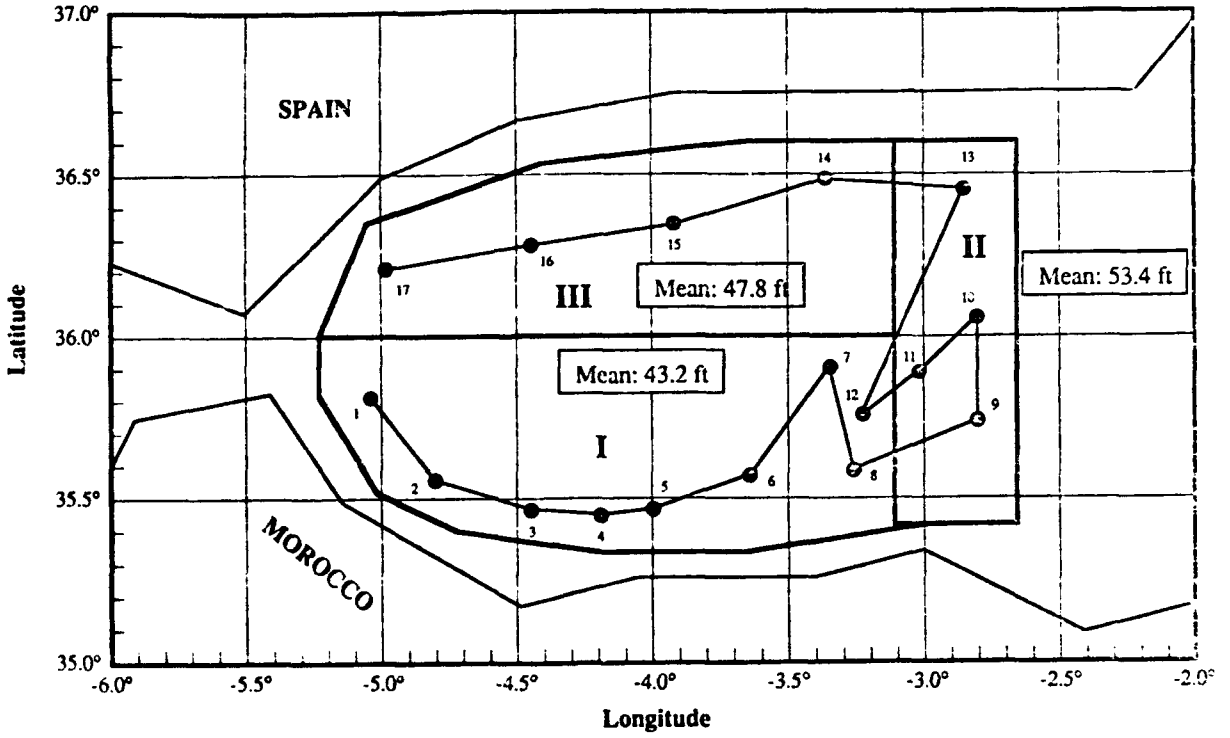

Province I & II Significantly Different (0.2%)
Province I & III Significantly Different (0.2%)
Province II & III Significantly Different (1.0%)

	AREA I	AREA II	AREA III
Surface Temperature (°C)	15.51	15.39	15.62
Surface Salinity (psu)	36.4	36.73	36.5
Temp. at 102 m (°C)	14.22	13.92	13.76
Salinity at 102 m (psu)	37.38	37.79	37.88
Attenuation Coefficient (m^{-1})	0.0759	0.0614	.0686
Attenuation Length (m)	13.17	16.28	14.58

Figure 4. Physical provinces in the western Alboran Sea as determined by optical attenuation length. Mean optical attenuation lengths (in feet) are shown for each province. Other mean physical properties for each province are listed below the figure (all from Hollman, 1992).

distributions of bioluminescent organisms, and differing proportions of dinoflagellate species with differing diel periodicities, are all biological factors that probably contributed to the variability in the results. Additional layers of complexity result from the fact that the bioluminescent community interacts with a larger, nonbioluminescent community and that these are both subject to physical controls such as the circulation of the Alboran Gyre, the upwelling of nutrients, the penetration of sunlight, and the depth of the mixed layer. The data need more extensive analysis, particularly in relation to the hydrographic processes and structure, in order to understand the controls on the bioluminescence variability.

One example of the data that requires further analysis is the relationship between bioluminescence intensity, number of events, and the light decay rate, which is parameterized by the "E-fold." E-fold is defined as the time required for an average bioluminescent event to decay by one natural log unit, or 1/e. A small E-fold value indicates that the light is produced by dinoflagellates, which typically exhibit flash durations on the order of a few tens of milliseconds, while a larger E-fold value indicates that the light is produced by organisms such as copepods, which have longer flash durations on the order of hundreds of milliseconds to several seconds (Tett and Kelly, 1973). As can be seen in this data set, the high intensities and high numbers of events in the upper 70 m are associated with low E-fold values, indicating the presence of a large number of dinoflagellates. In the deeper layers, intensity and events fall while E-fold values increase, indicating that crustaceans are the primary light producers. Thus, it appears that HIDEX detected a shift in the source population with depth, and that this shift was associated with the physical structure of the water column. This interpretation is supported by flash durations measured throughout the water column at the same HIDEX stations by the research submersible (E. Widder, Harbor Branch Oceanographic Institution, Ft. Pierce, FL, personal communication, 1991).

6.3 RELATION OF BIOLUMINESCENCE TO ALGAL PIGMENTS

There are currently efforts underway by some researchers to correlate bioluminescence with remotely sensed ocean color due to algal pigments. This data set raises some cautions about such efforts.

Algal pigments were measured three ways in this experiment: by extraction of discrete water samples (Appendix F); by continuous,

underway sampling from the seachest at 7-m depth (Appendix G); and by continuous, in situ fluorometry simultaneously with the bioluminescence measurements (Appendix A). The extracted pigment data shows that, in most cases, most of the chlorophyll in these waters was in the <20 μm range, i.e., smaller than most bioluminescent dinoflagellates (Swift et al., 1985). The predominance of the <20 μm phytoplankton has been noted in other environments as well, such as in Vestfjord, Norway (NOARL, unpublished data).

In situ fluorescence, although generally exhibiting the same trends with depth as bioluminescence, did not show coincident peaks in the profile data. This was especially evident at shallow depths. There are two immediate explanations for this observation besides the size factor mentioned previously. One is that numerous nonluminescent algae, such as diatoms, were abundant (they were noted in the vertical net collections, but they were not enumerated). The other is that the important bioluminescent organisms—*Noctiluca*, *Protoperidinium*, and the crustacea—are not pigmented and, therefore, do not fluoresce. The lack of correspondence between in situ fluorescence and bioluminescence also can be seen in the *horizontal, underway data* (Appendix G).

The preliminary conclusion is that chlorophyll and bioluminescence do not necessarily covary in time (during station keeping) or in space (during transits between stations), and that surface pigment concentrations cannot be expected to be directly related to subsurface bioluminescence. Thus, even if chlorophyll concentrations can be estimated from remote measurements of color, the estimates will not necessarily correlate with bioluminescence.

7. CONCLUSIONS

- High bioluminescence intensities (>10^{12} photons $s^{-1}L^{-1}$) were confirmed in the Alboran Sea during April.

- The variation of bioluminescence distribution across the Alboran Sea in April 1991 generally corresponded to the northern, eastern, and southern provinces found in the physical data, i.e., potential bioluminescent light was high in the southern province, low in the northern province, and intermediate and variable in the eastern province.

- Greatest spatial variability in bioluminescence occurred at the divergence zone at the southeastern boundary of the western Alboran Gyre.

- Simultaneous measurements made at stations up to 30 km apart showed similar bioluminescent intensities in the upper 300 ft (100 m) water column.

- Vertical and diel (24 h) changes in bioluminescent intensity at the same station are greater than the differences between stations. Bioluminescent intensities in the water column can vary significantly in periods of 1 h or less especially during hours surrounding dusk and dawn.

- Vertical stratification of bioluminescence can vary in intervals of a few meters. The brightest intensity of bioluminescence was normally in the upper 300 ft (100 m).

- Although continuous surface sampling is useful to define fronts and upwelling, vertical structure cannot be inferred. Subsurface water column measurements of bioluminescence, fluorescence, transmission, temperature, and salinity cannot be predicted by their surface measurements.

- Bioluminescence potential in the western Alboran Sea in April 1991 was primarily due to a mixture of large numbers of dinoflagellates and zooplankton.

- The very high bioluminescence potential was a consequence of the abundance of the sources rather than extreme intensity of any one emitter.

- The MED 3-88 phenomenology was not verified; however, shipboard and research submersible measurements suggest that high population densities of gelatinous zooplankton are the most likely explanation for the December 1988 observations and for intense, long-lasting luminescence at other times of the year.

- The research submersible was the optimal means for determining which sources were the primary emitters in these complex populations, and it was the only practical means for measuring emission parameters of fragile gelatinous sources that are destroyed by conventional sampling methods.

8. RECOMMENDATIONS

- Verification of the gelatinous zooplankton hypothesis requires the fielding of a cruise during the December timeframe.

- Periodic resampling should take place during the three times of the year when plankton bloom conditions have been reported (April, September, and December).

- Survey stations should be located in regions at each geographical extreme of the western Alboran Gyre and 3 stations at the southeastern boundary (7 total stations).

- Spatial (horizontal and vertical) variation in regions of dynamic change can be characterized rapidly and efficiently by a single ship equipped with a suite of sensors on a "Tow-Yo" package.

- Future sampling strategies should include the following:
  - A series of vertical profiles taken at the same station at least every hour during periods of twilight (3 dawn/3 dusk), at midnight (1), and at noon (1).
  - *Maximal sampling depth not to exceed* 300 ft (100 m).
  - A moored instrumental sensor suite with vertical cycling and telemetry capabilities for sampling long-term variability.

- Resampling should include nondestructive methods using submersibles, camera transects, or at least SCUBA collections in surface waters.

- Further work should be done on this data set to quantify relationships between and among bioluminescence, biological, optical, and hydrographic parameters.

9. REFERENCES

Arnone, R.A., D.A. Wiesenburg, and K. Saunders (1990). The origin and characteristics of the Algerian Current. *Journal of Geophysical Research.* 95:1587-1598.

Bityukov, E.P. (1971a). Bioluminescence in a ship wake in the Atlantic Ocean and in the Mediterranean and Black Seas. *Oceanology* 11(1):103-108.

Bityukov, E.P. (1971b). Bioluminescence in the Atlantic Ocean and the Mediterranean basin seas. In *Problemy morskoy Biologii' (Problems in Marine Biology),* V.A. Vodyanittskiy, ed. *Naukova Dumka.* (Science Publishing House), Kiev. pp. 251-257. (In Russian, summary in English).

Bityukov, E.P. (1977). Bioluminescence in the pelagic zone in the Atlantic and the seas of the Mediterranean basin. In *Issledovaniya Biologicheskikh Resursov i Ikh Okhrany y Yuzhnykh Moryakjh.* pp. 51-58. Izdatel' stvo Naukova Dumka, Kiev. (Translation CNR 78-09-083).

Bityukov, E.P., Ri.I. Vasilenko, and Yu.N. Tokarev (1978). The spectral composition of the bioluminescence field in the Black and Mediterranean. *Biologiia Morya* (Kiev) 47:40-49. (Translation DRIC-T-6619).

Bityukov, E.P. (1982). Seasonal variability and spatial nonuniformity of bioluminescence in the Mediterranean Sea. *Ekologiia Morya* (Kiev) 8:10-20 (Translation DRIC-T-6619).

Dean, R.B. and W.J. Dixon (1951). Simplified statistics for small numbers of observations. *Analytical Chemistry* 23(4):636-638.

Donaldson, T.Q. (1989). USS KENNEDY conducts bioluminescence study in the Mediterranean. *Naval Oceanography Command News* 9(11):1 and 4.

Eckert, R. (1965). Bioelectric control of bioluminescence in the dinoflagellate Noctiluca. *Science* 147:1140-1145.

Gordienko, A.P., M.N. Lebedeva, and Yu.N. Tokarev (1980). Bacterioplankton number in bioluminescence extrema in some seas of the Mediterranean Sea basin. *Ekologiia Morya* (Kiev) 80(2):15-21 (in Russian, abstract in English).

Hamman, J.P., W.H. Biggley, and H.H. Seliger (1981). Photoinhibition of stimulable bioluminescence in marine dinoflagellates. *Photochemistry and Photobiology* 33:909-914.

Hollman, R. (1992). Optical and physical characteristics of the western Alboran Sea in April 1991. NOARL Technical Note, in press.

Lapota, D., M.L. Geiger, A.V. Stiffey, D.E. Rosenberger, and D.K. Young (1989). Correlations of planktonic bioluminescence with other oceanographic parameters from a Norwegian fjord. *Marine Ecology Progress Series* 55:217-227.

Lapota, D., D.K. Young, D.M. Lavoie, I.P. DePalma, M. S. Hulbert, F.C. Stephens, and D.E. Rosenberger (1990). Bioluminescence measurements and light budget analysis in the Vestfjord, Norway in the Fall of 1989. Presented at *Fall 1990 Meeting of the American Geophysical Union*, 3-7 December, 1990, San Francisco, CA.

Lavoie, D.M. and I.P DePalma (1982). Chemical, biological, and physical measurements from the Mediterranean Sea, summer, 1980. NORDA Technical Note 138, Naval Oceanographic and Atmospheric Research Laboratory (now Naval Research Laboratory), Stennis Space Center, MS 39529-5004.

Lohrenz, S.E., R.A. Arnone, C.A. Wiesenburg, and I.P. DePalma (1988). Satellite detection of transient enhanced primary production in the western Mediterranean Sea. *Nature* 335:245-247.

Madin, L.P. (1991). Distribution and Taxonomy of Zooplankton in the Alboran Sea and Adjacent western Mediterranean: A Literature Survey and Field Guide. Woods Hole Technical Report WHOI-91-26, September 1991, Woods Hole Oceanographic Institution, Woods Hole, MA.

Strickland, J.D.H. and T.R. Parsons (1972). A practical handbook of seawater analysis. Bulletin 167 (second edition), Fisheries Research Board of Canada, Ottawa.

Swift, E., E.J. Lessard, and W.H. Biggley (1985). Organisms associated with stimulated epipelagic bioluminescence in the Sargasso Sea and the Gulf Stream. *Journal of Plankton Research* 7(6):831-848.

Tett, P.B. and M.G. Kelly (1973). Marine bioluminescence. *Oceanography and Marine Biology Annual Revue* 11:89-173.

Utermöhl, H. (1958). Zur Vervollkommung der quantitativen Phytoplankton-Methodik. *Mitteilungen der Internationale Vereinigung fuer Limnologie* 9:1-38.

Widder, E.A., S.A. Bernstein, D.F. Bracker, J.F. Case, K.R. Reisenbichler, J.J. Torres, and B.H. Robison (1989). Bioluminescence in the Monterey Submarine Canyon: image analysis of video recordings from a midwater submersible. *Marine Biology* 100(4):541-551.

Widder, E.A., 1991. Midwater bioluminescence assessment in the West Alboran Gyre (Mediterranean Sea): R/V Seward Johnson Cruise Report, April 5-25 1991. NOARL Technical Note, in press.

APPENDIX A: Multiparameter Profiles

Representative casts are presented for each profile series—dusk, midnight, and dawn—for each station. All profiles are plotted at the same scale for intercomparison. No smoothing has been performed on the data.

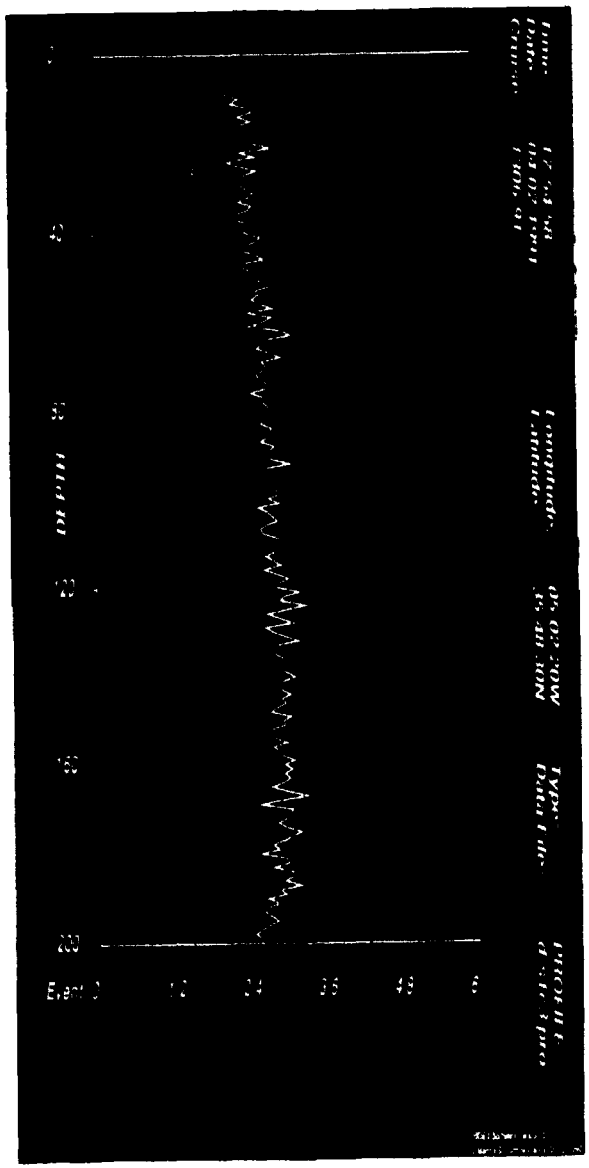

MED-OPS 91 Station 1, Dusk Figure A-1a

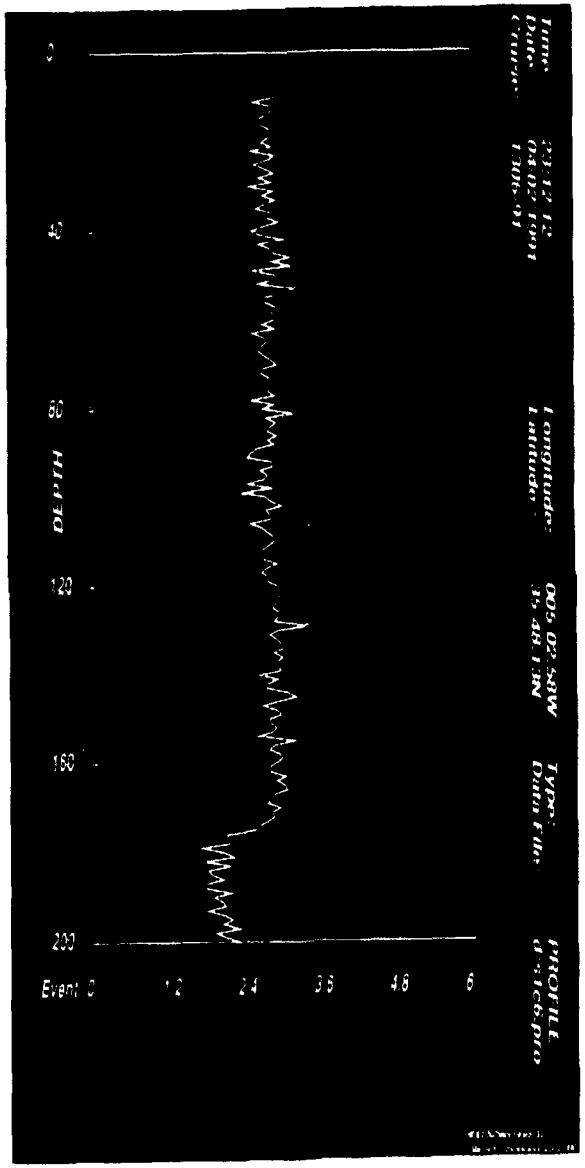

MED-OPS 91 Station 1, Midnight Figure A-1b

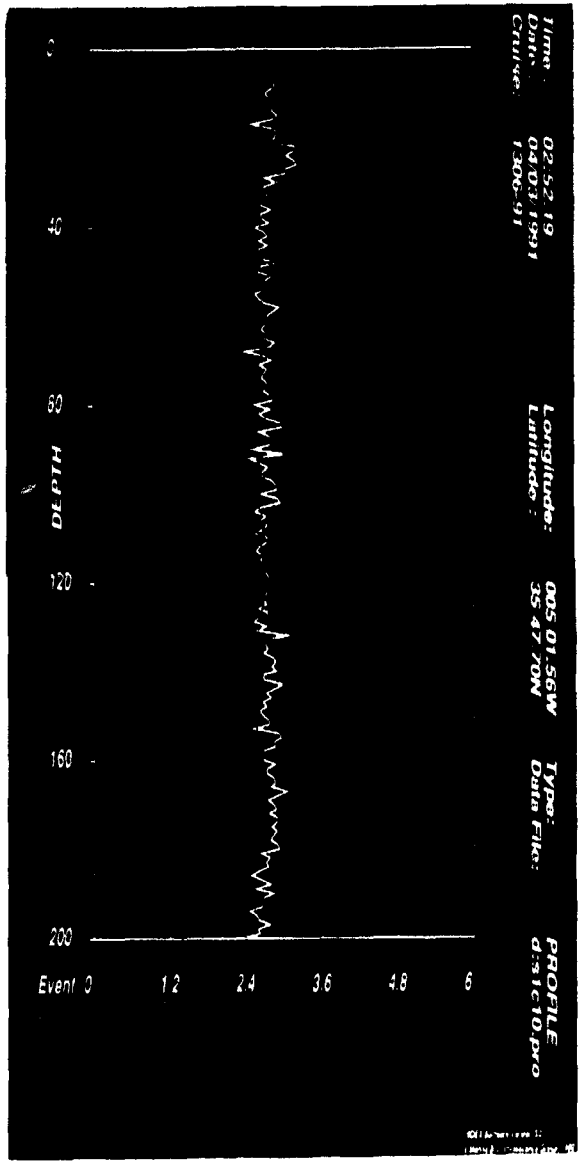

MED-OPS 91 Station 1, Dawn Figure A-1c

MED-OPS 91 Station 2, Dawn Figure A:2c

MED-OPS 91 Station 2, Midnight Figure A:2b

MED OPS 9: Station 5, Dawn Figure A 5c

MED OPS 9: Station 5, Midnight Figure A 5b

MED OPS 9: Station 5, Dusk Figure A 5a

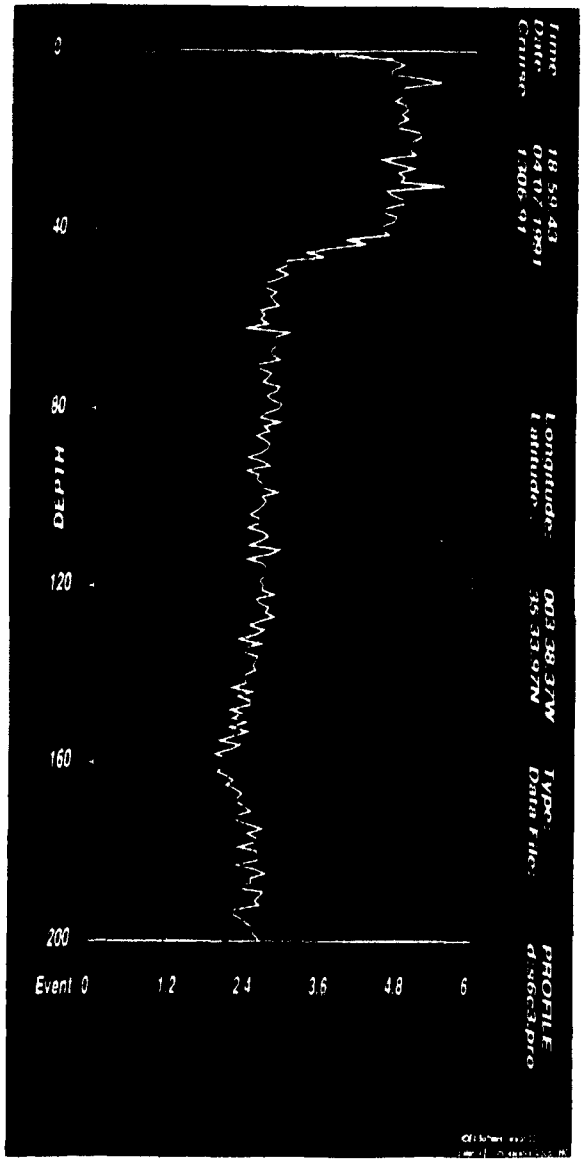

MED-OPS 91 Station 6, Dusk Figure A-6a

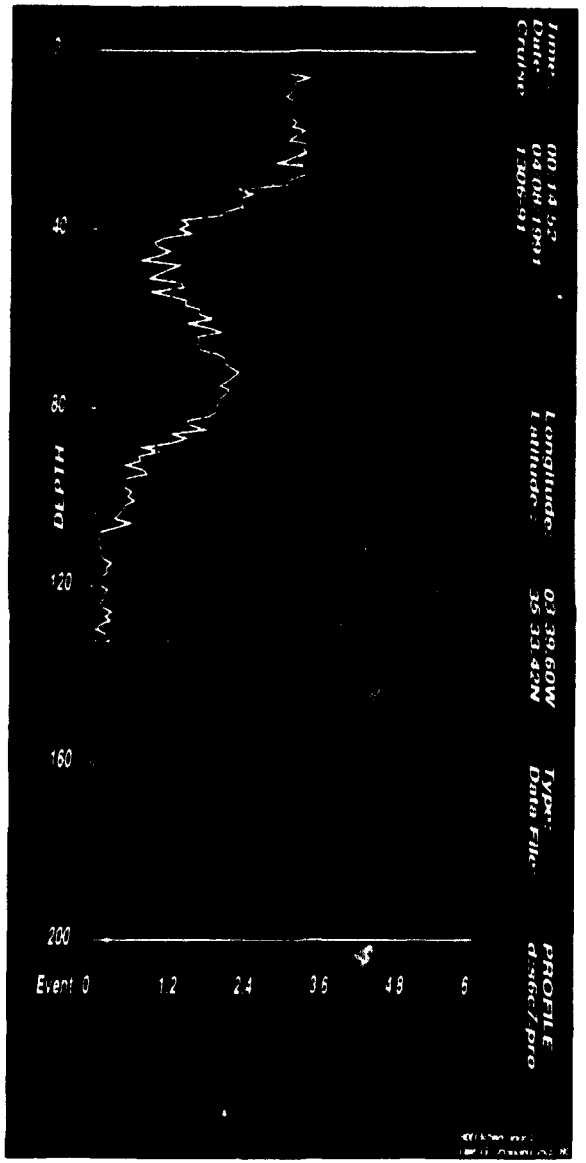

MED-OPS 91 Station 6, Midnight Figure A-6b

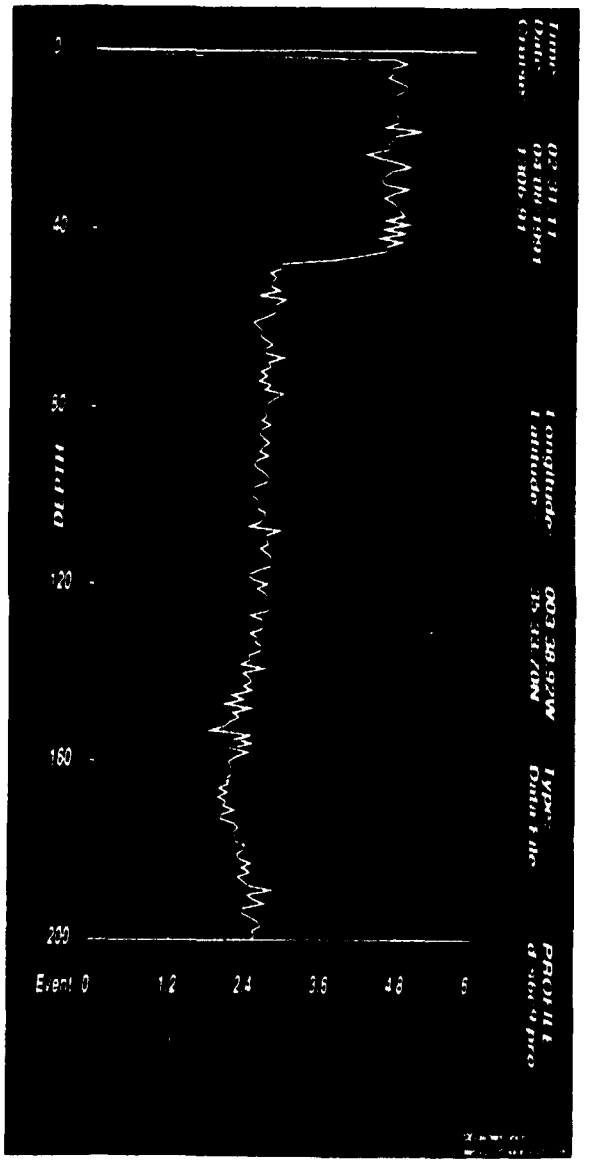

MED-OPS 91 Station 6, Dawn Figure A-6c

MED-OPS 91 Station 7, Dawn Figure A.7c

MED-OPS 91 Station 7, Midnight Figure A.7b

[illegible] Figure A.7a

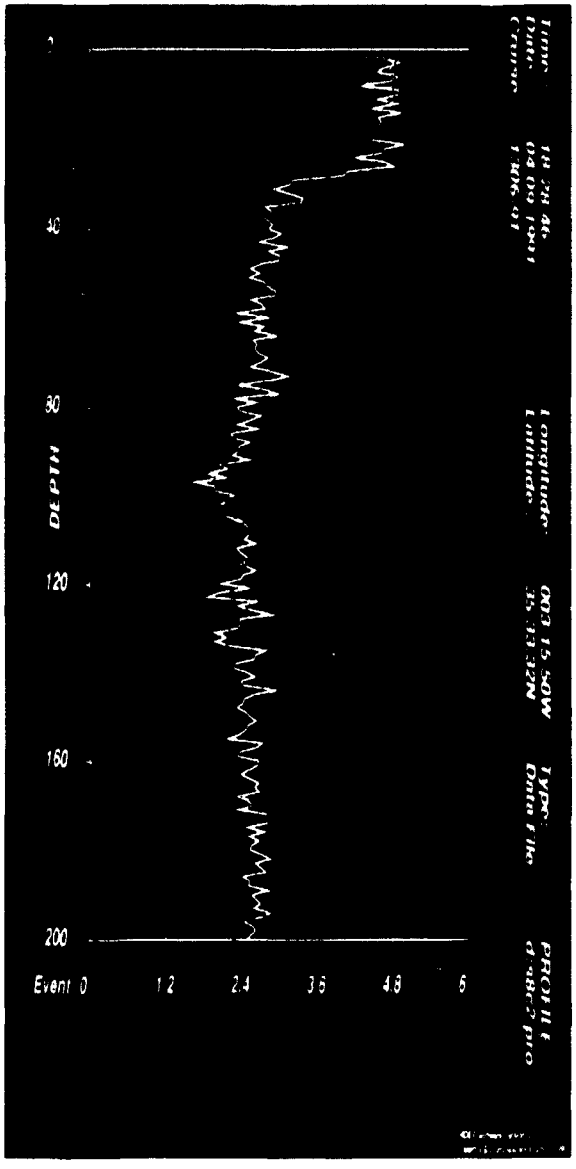

MED-OPS 91 Station 8, Dusk Figure A-8a

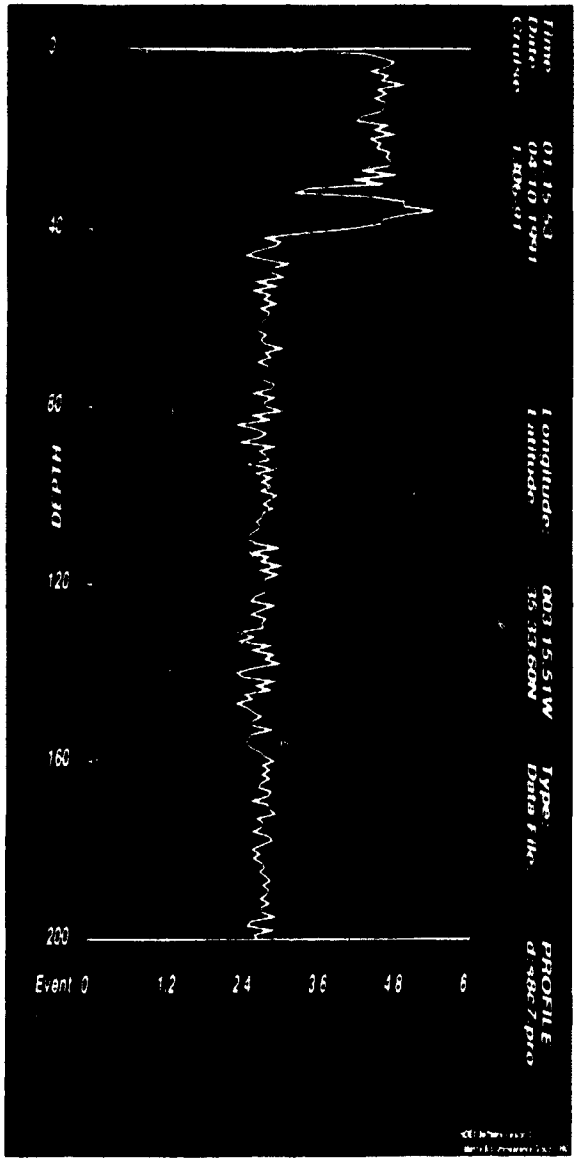

MED-OPS 91 Station 8, Midnight Figure A-8b

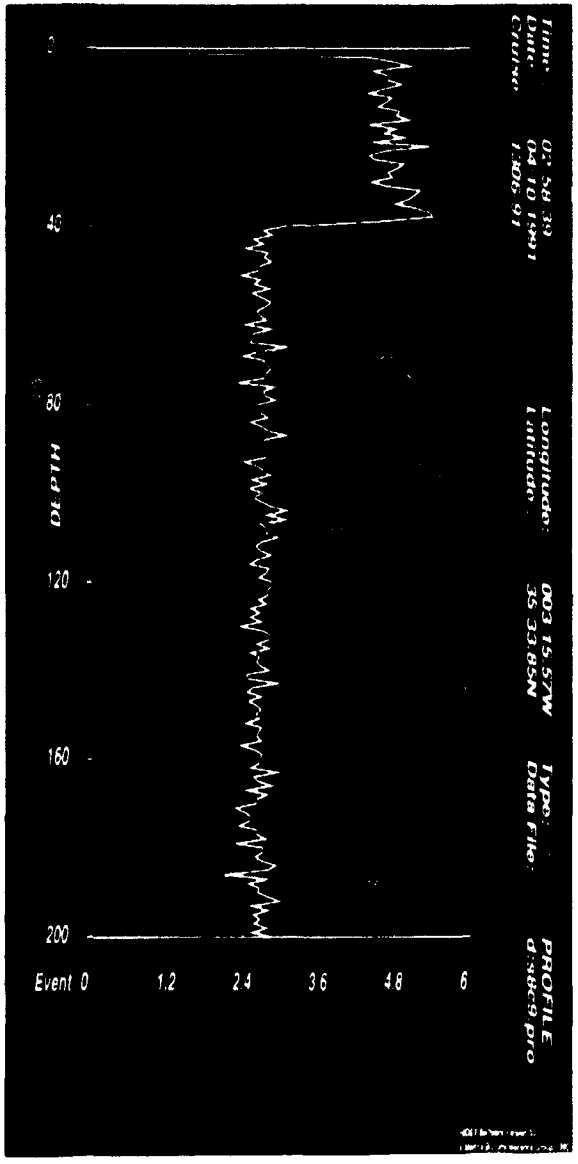

MED-OPS 91 Station 8, Dawn Figure A-8c

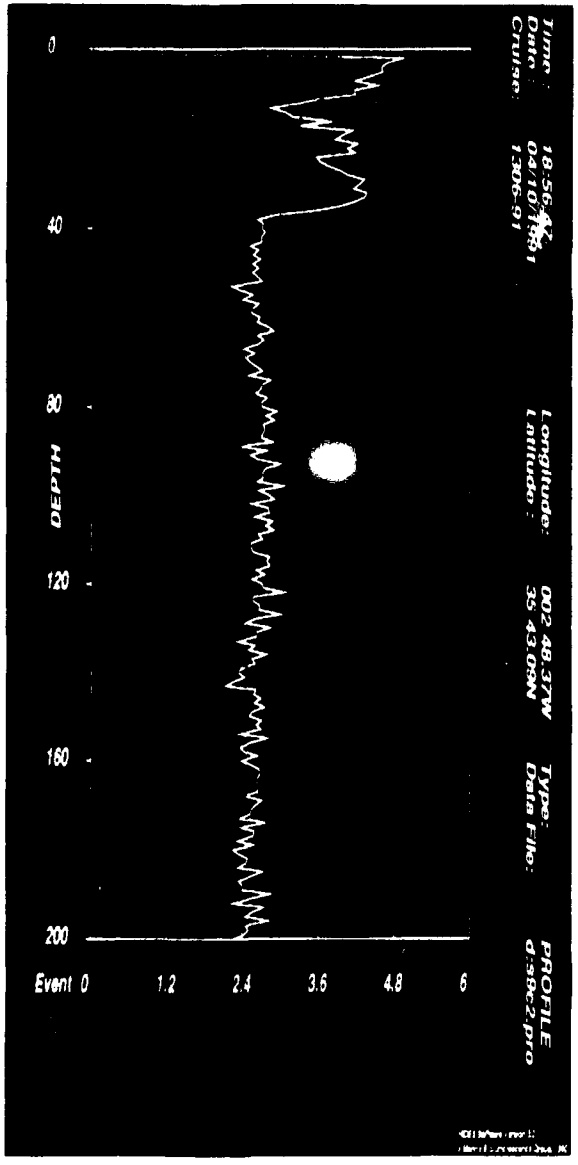

MED-OPS 91 Station 9, Dusk Figure A-9a

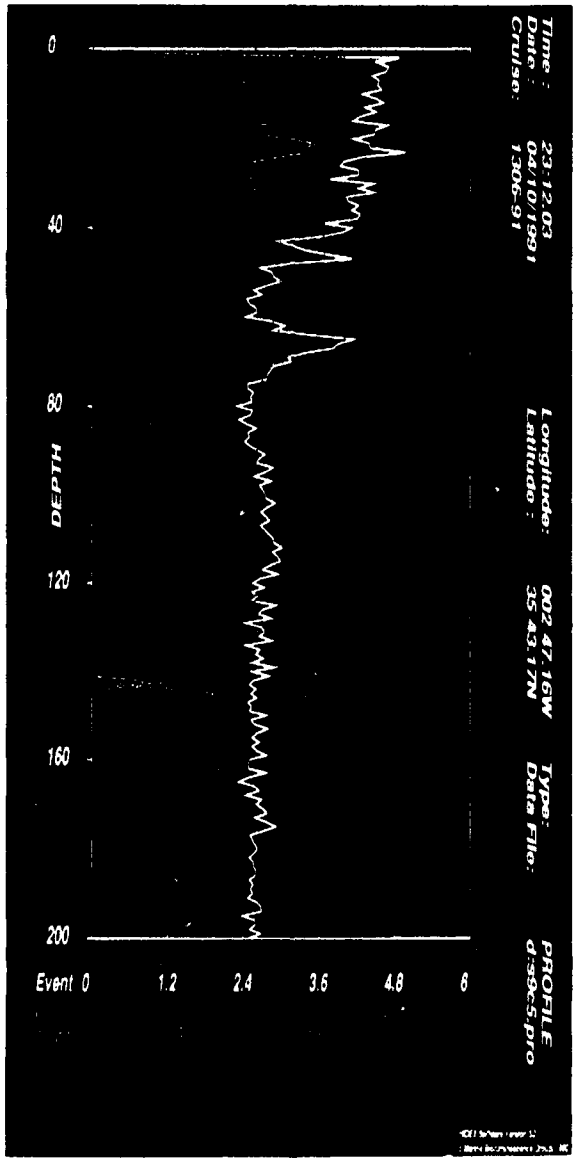

MED-OPS 91 Station 9, Midnight Figure A-9b

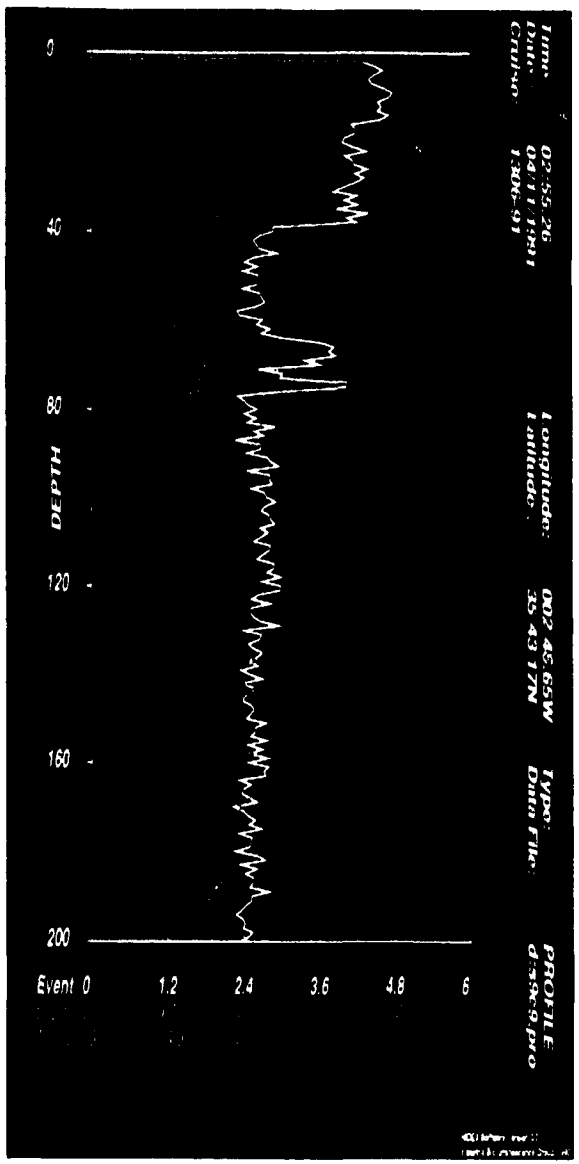

MED-OPS 91 Station 9, Dawn Figure A-9c

MED-OPS 91 Station 10, Dawn Figure A-10c

MED-OPS 91 Station 10, Midnight Figure A-10b

MED-OPS 91 Station 10, Dusk Figure A-10a

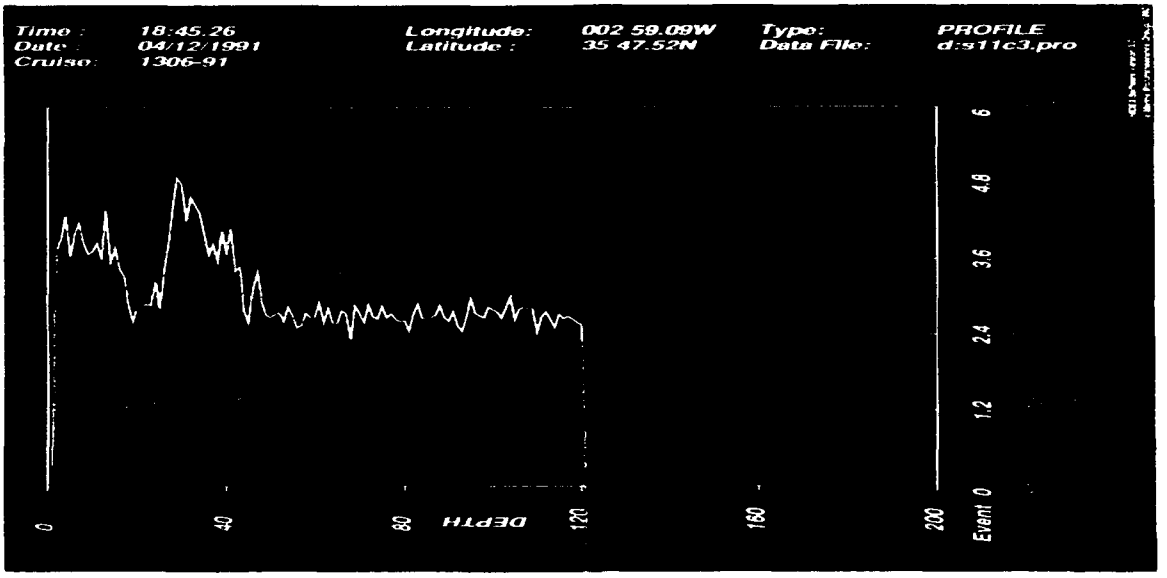

MED-OPS 91 Station 11, Dawn Figure 4-11a

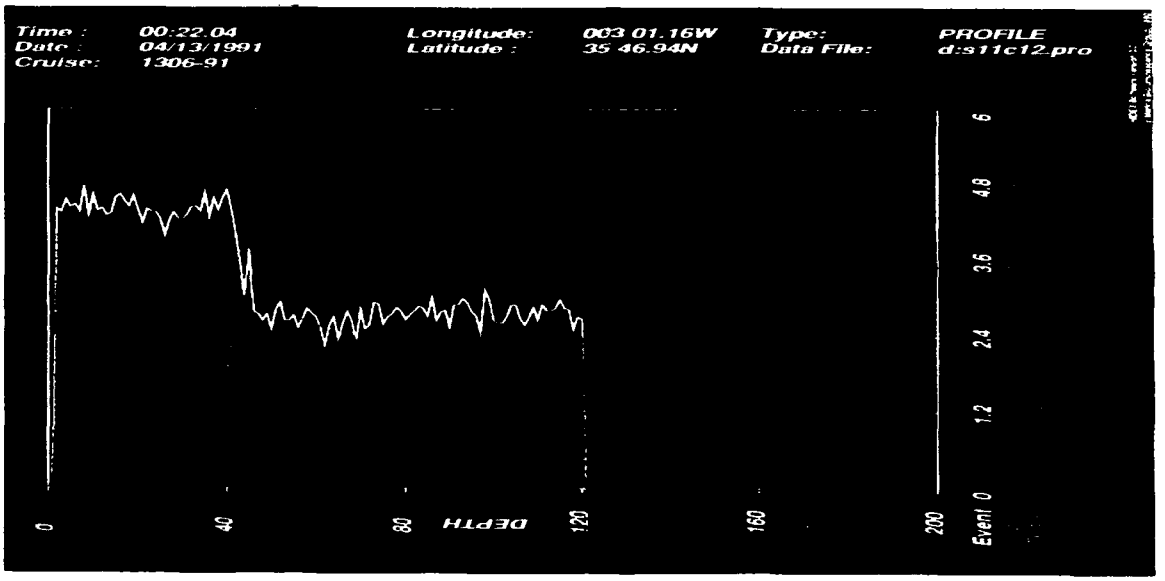

MED-OPS 91 Station 11, Midnight Figure 4-11b

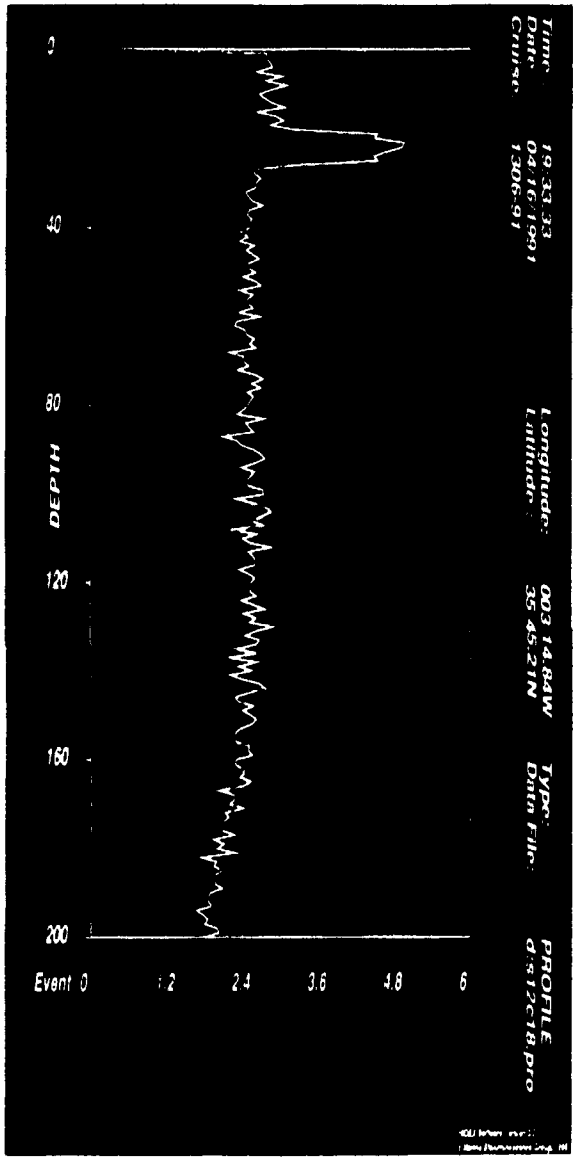

MED OPS 91 Station 12 (16-17 Apr), Dusk Figure A-12a

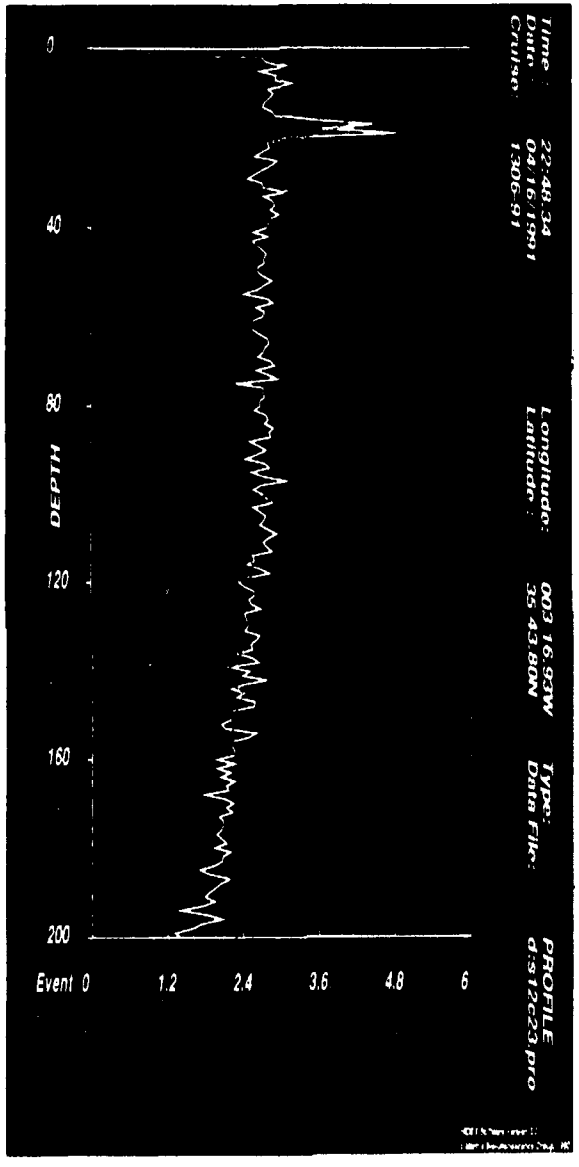

MED OPS 91 Station 12 (16-17 Apr), Midnight Figure A-12b

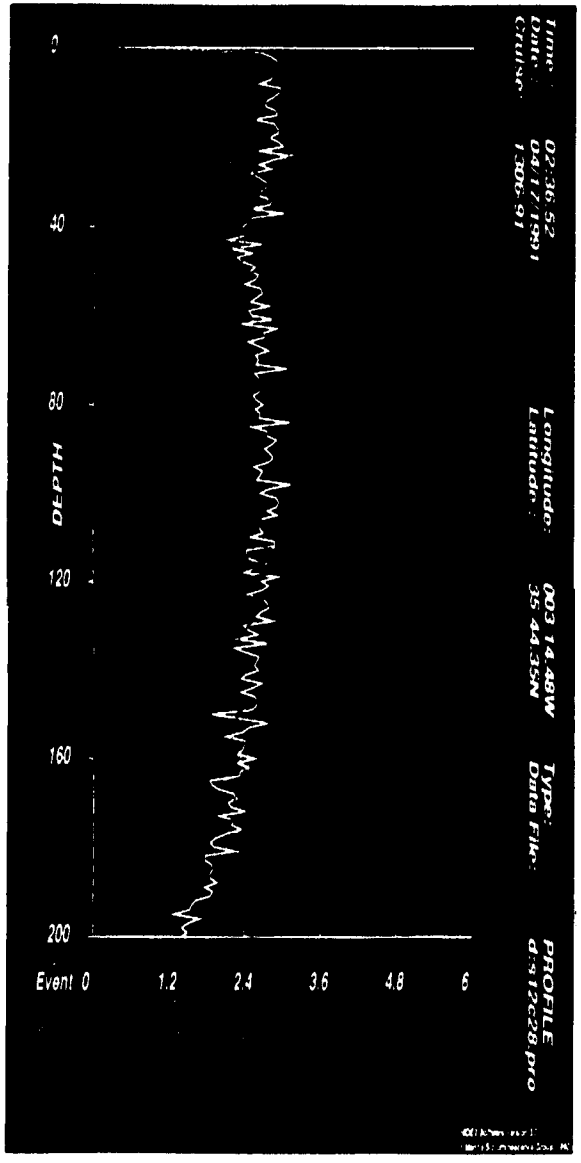

MED OPS 91 Station 12 (16-17 Apr), Dawn Figure A-12c

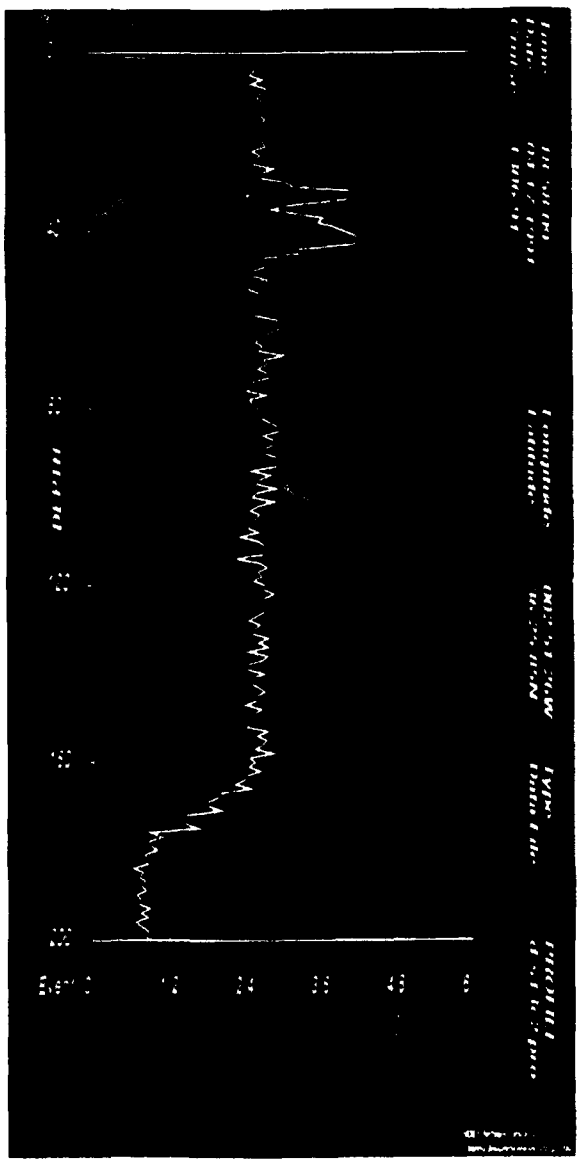

MED-OPS 9[illegible] Station 13, Dusk Figure A-13a

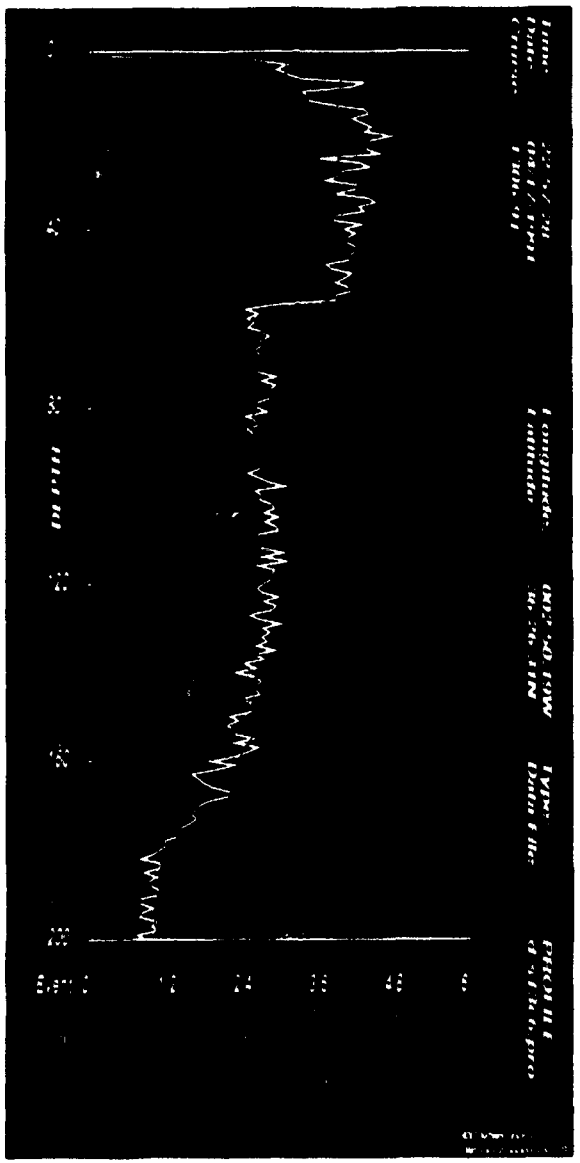

MED-OPS 91 Station 13, Midnight Figure A-13b

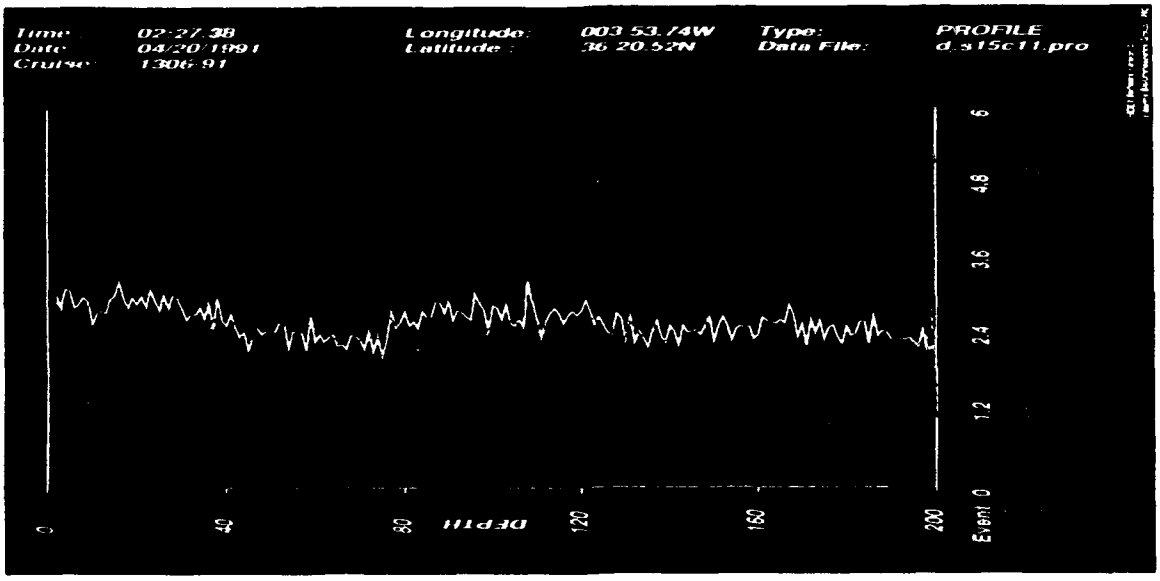

MED OPS 91 Station 15, Dawn Figure A-15c

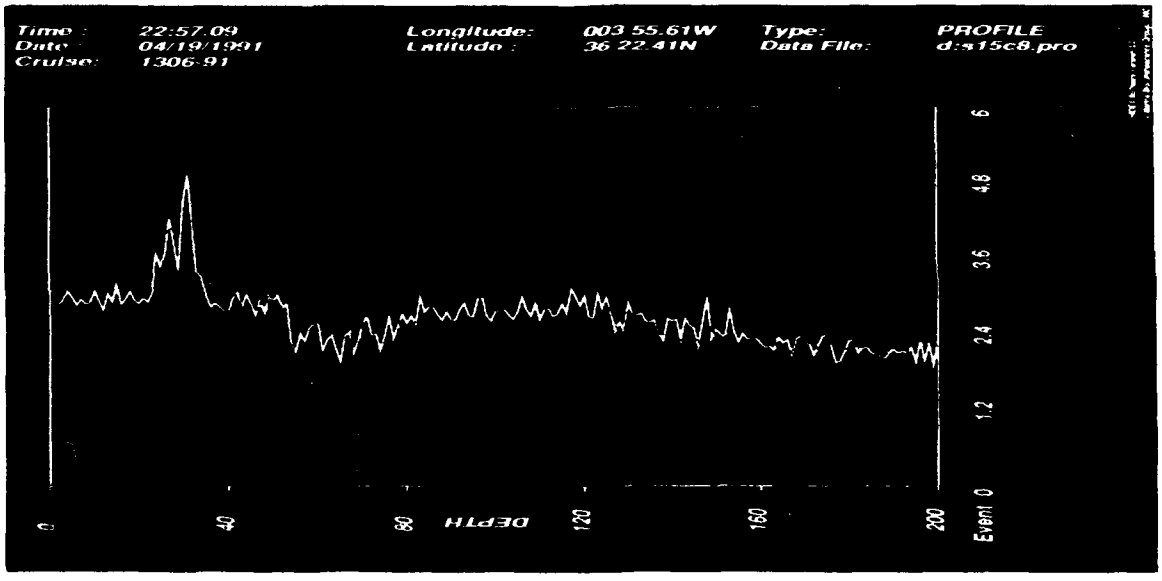

MED-OPS 91 Station 15, Midnight Figure A-15b

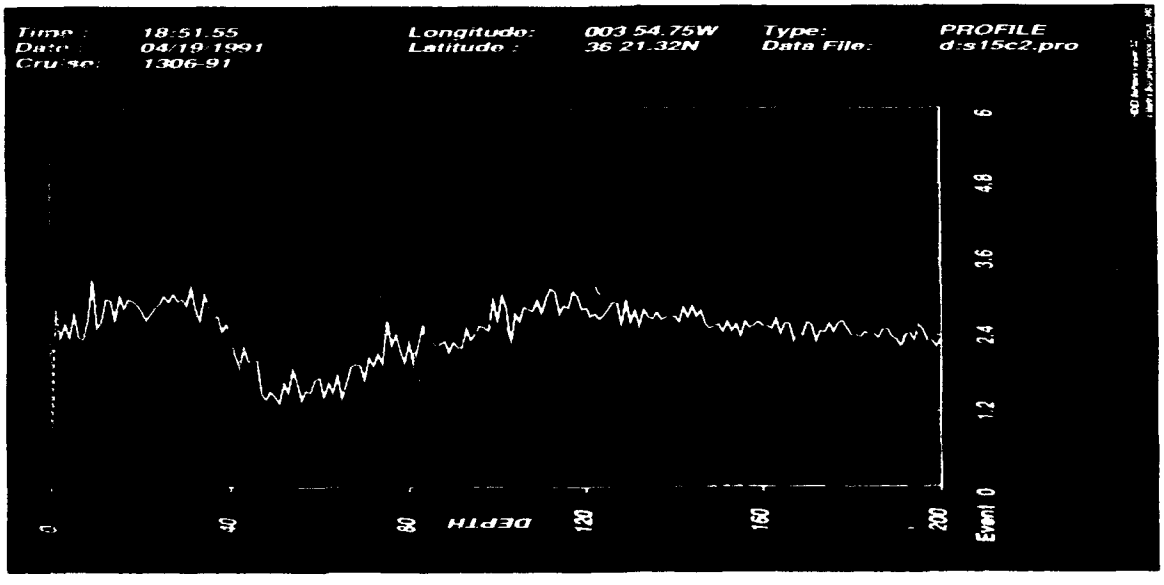

MED-OPS 91 Station 15, Dusk Figure A-15a

MED-OPS 91 Station 16, Dawn Figure A-16c

MED-OPS 91 Station 16, Midnight Figure A-16b

MED-OPS 91 Station 16, Dusk Figure A-16a

APPENDIX B: Bioluminescence Profile Overlays

Plots for the bioluminescence profiles for each series are overlaid to show the variability of bioluminescence throughout the night at each station.

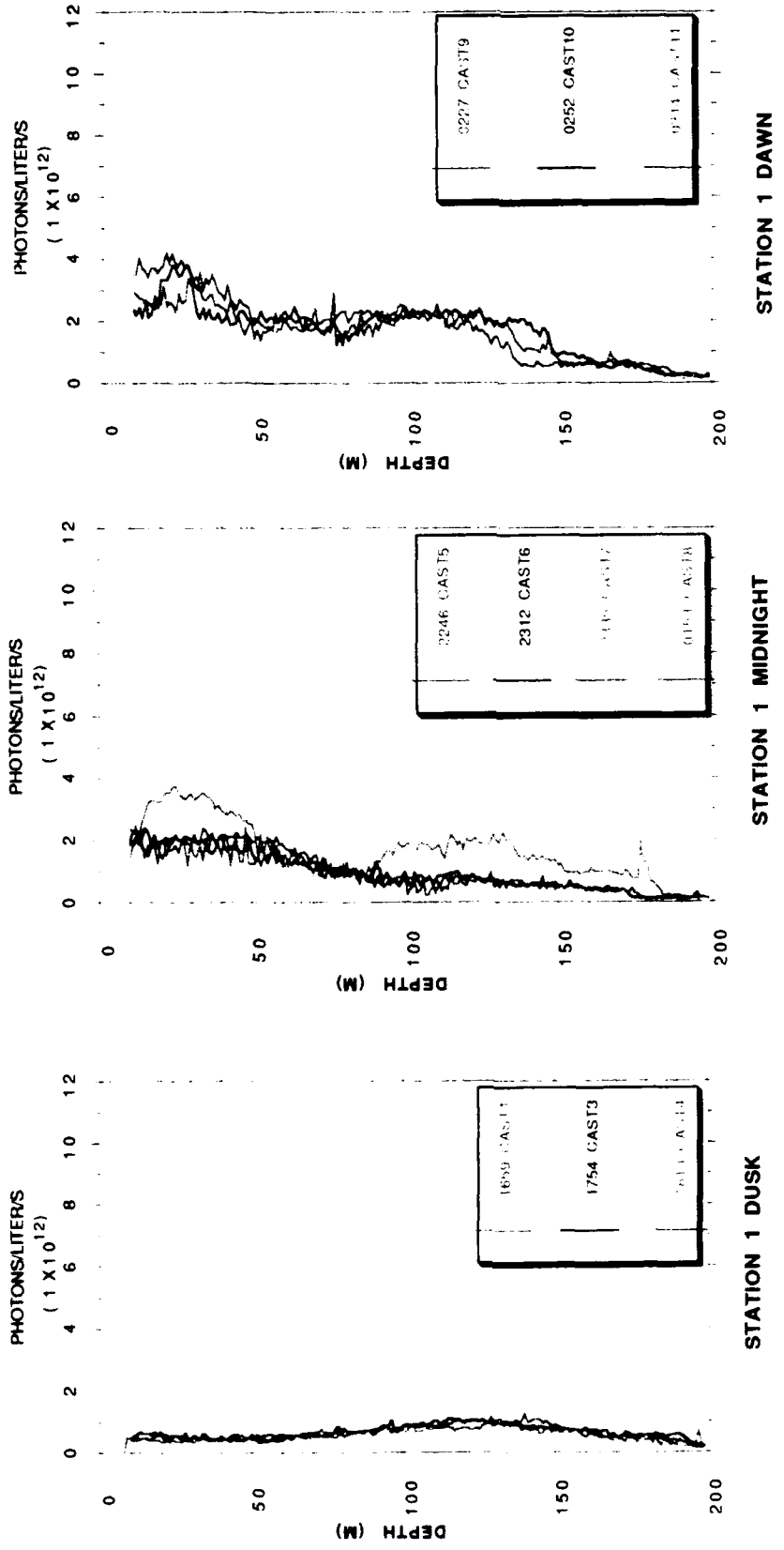

MED-OPS 91 Station 1 Figure B-1

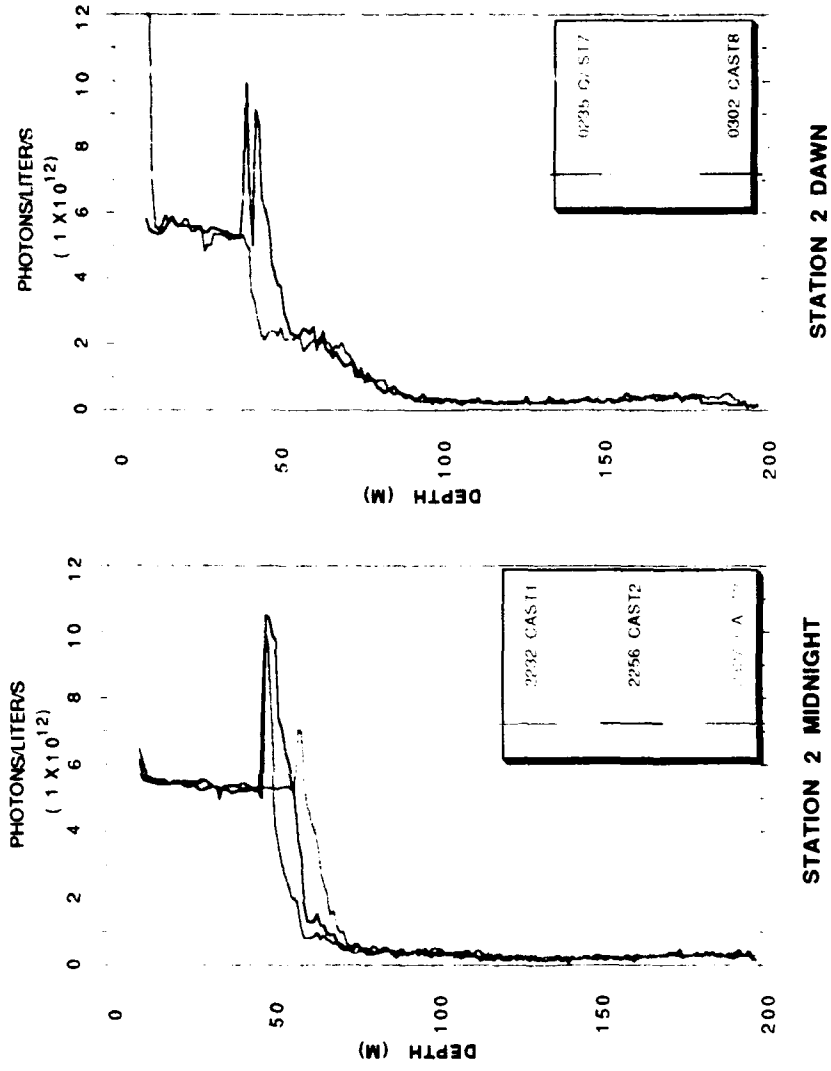

MED-OPS 91 Station 2 Figure B-2

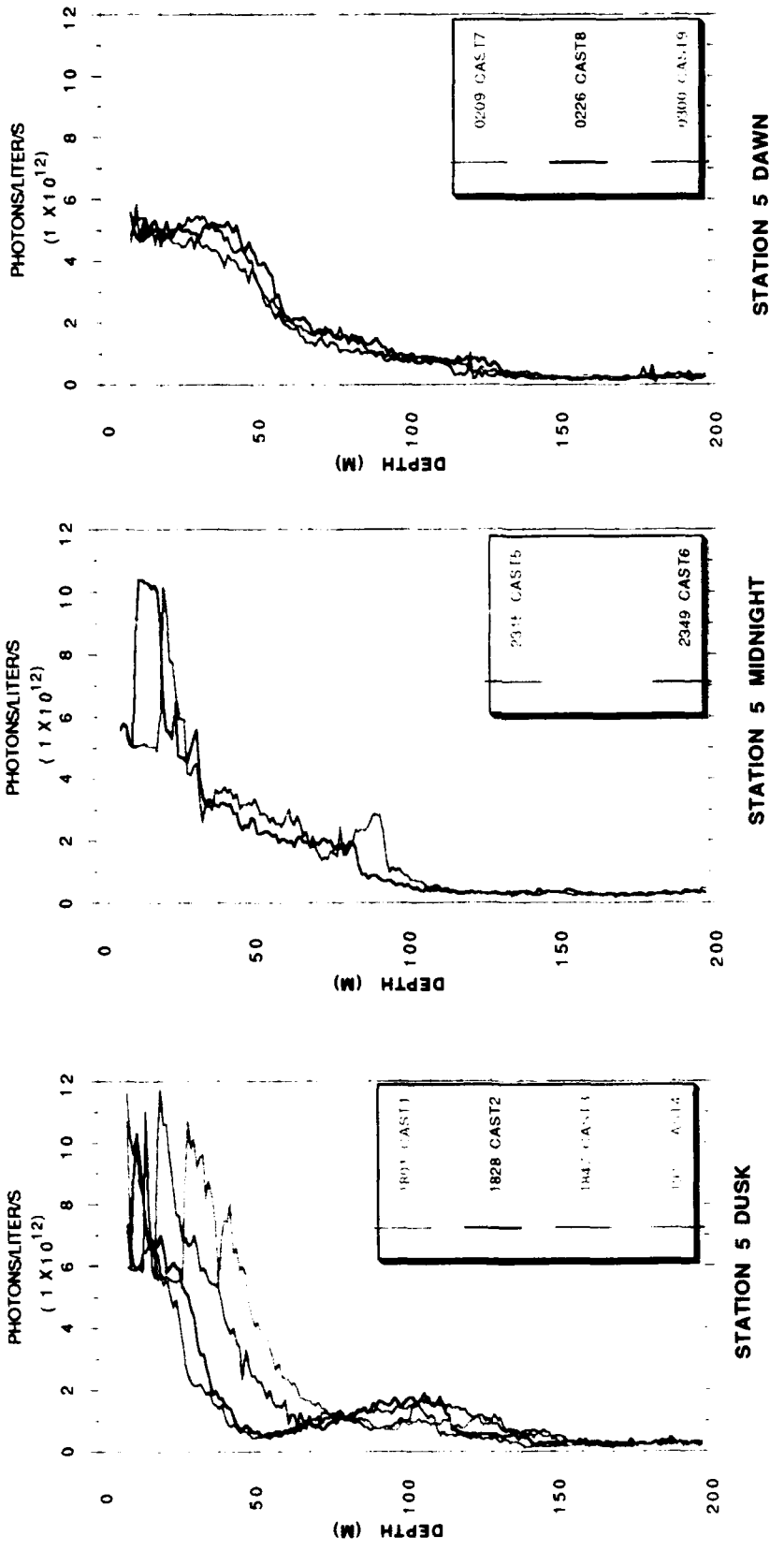

MED-OPS 91 Station 5 Figure B-5

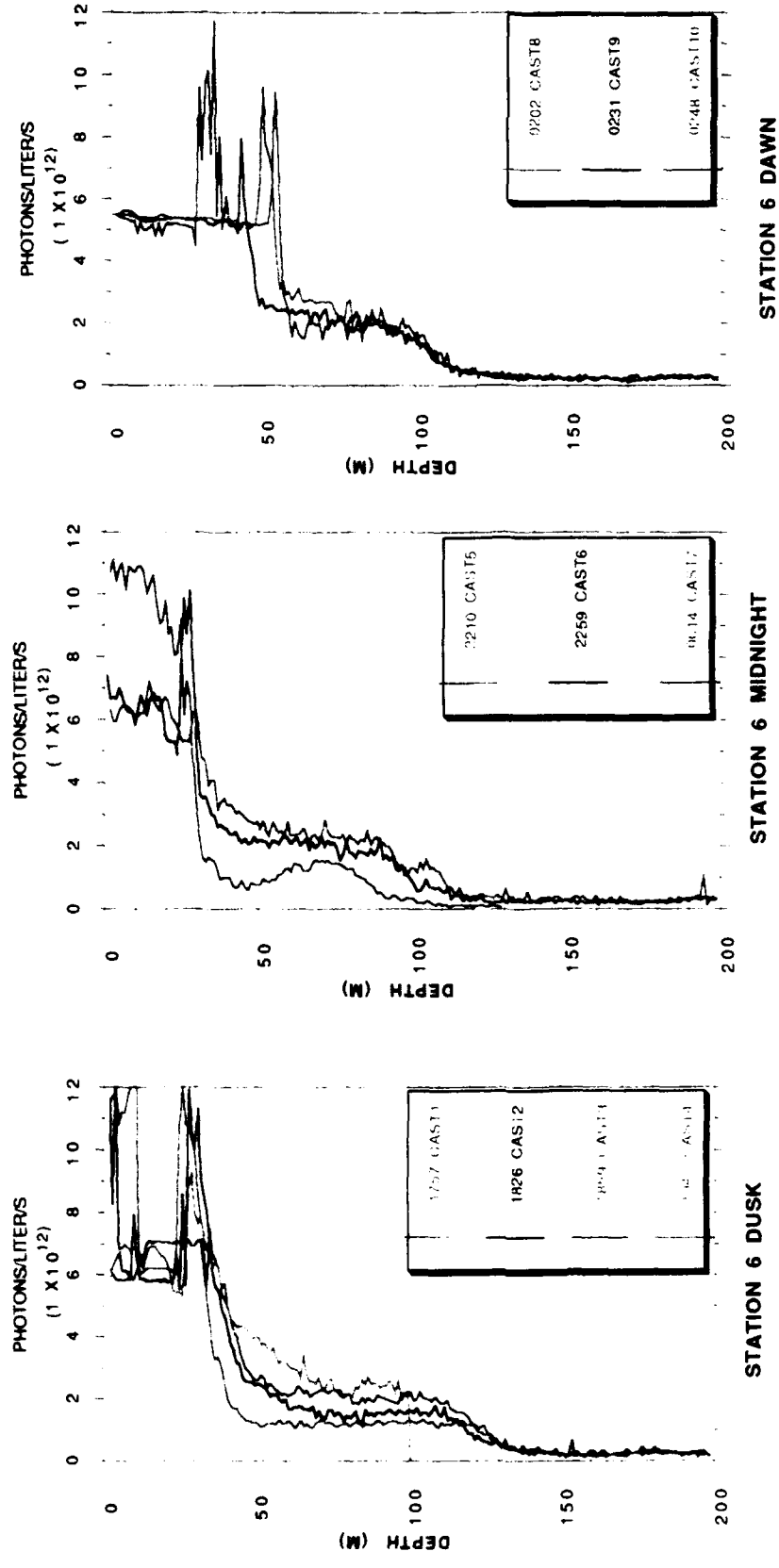

MED-OPS 91 Station 6 Figure B-6

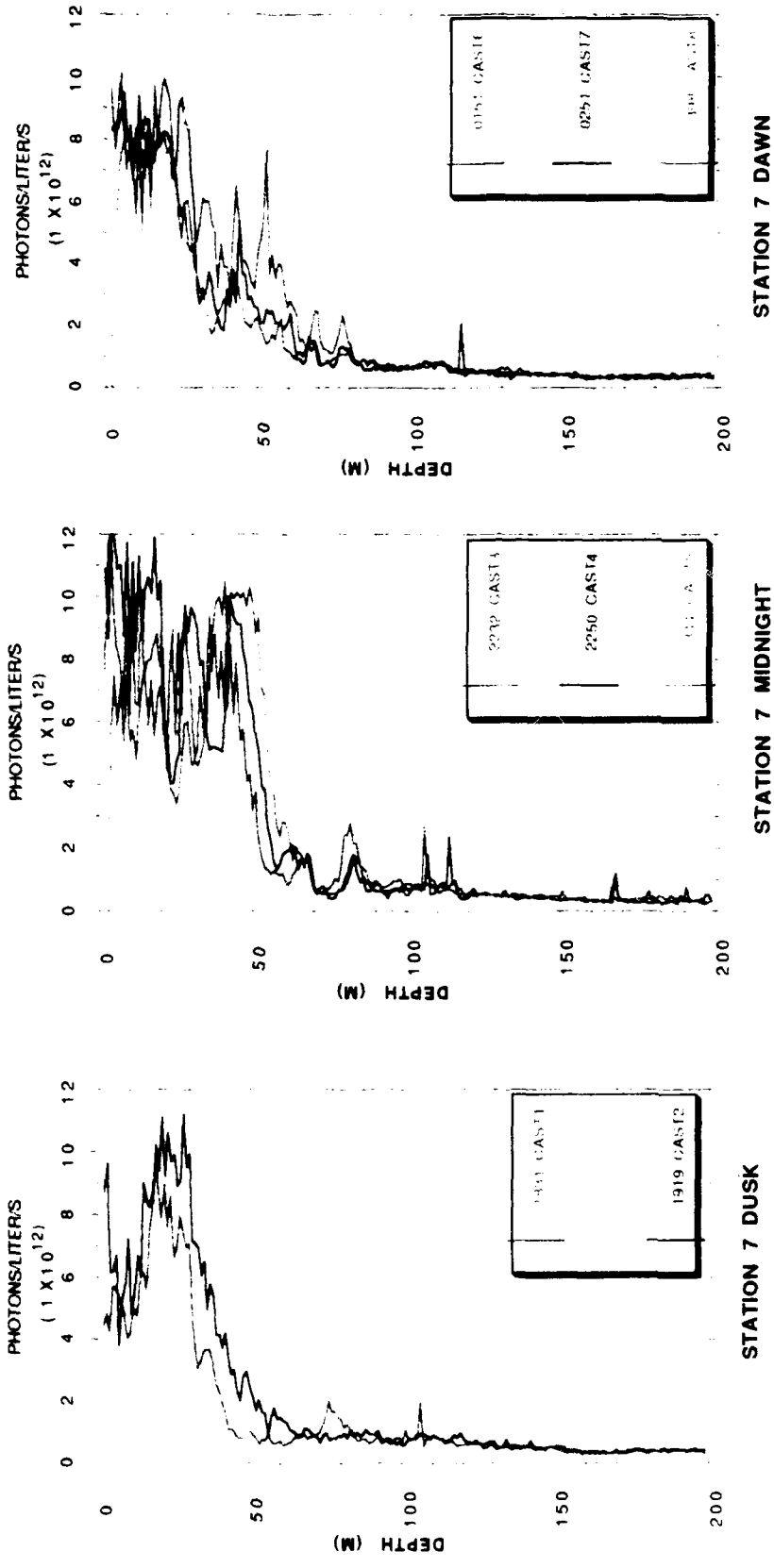

MED-OPS 91 Station 7 Figure B-7

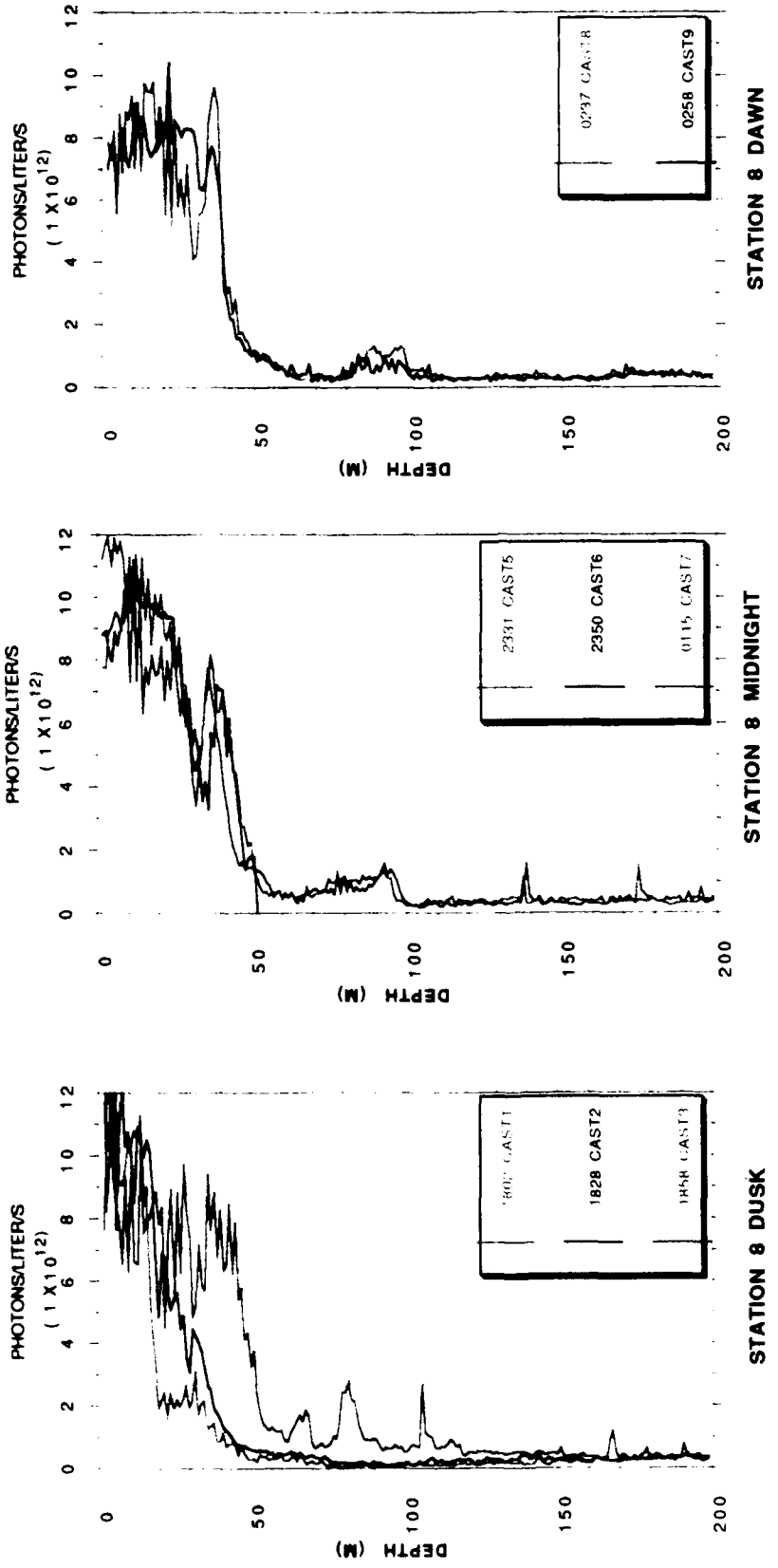

MED-OPS 91 Station 8 Figure B-8

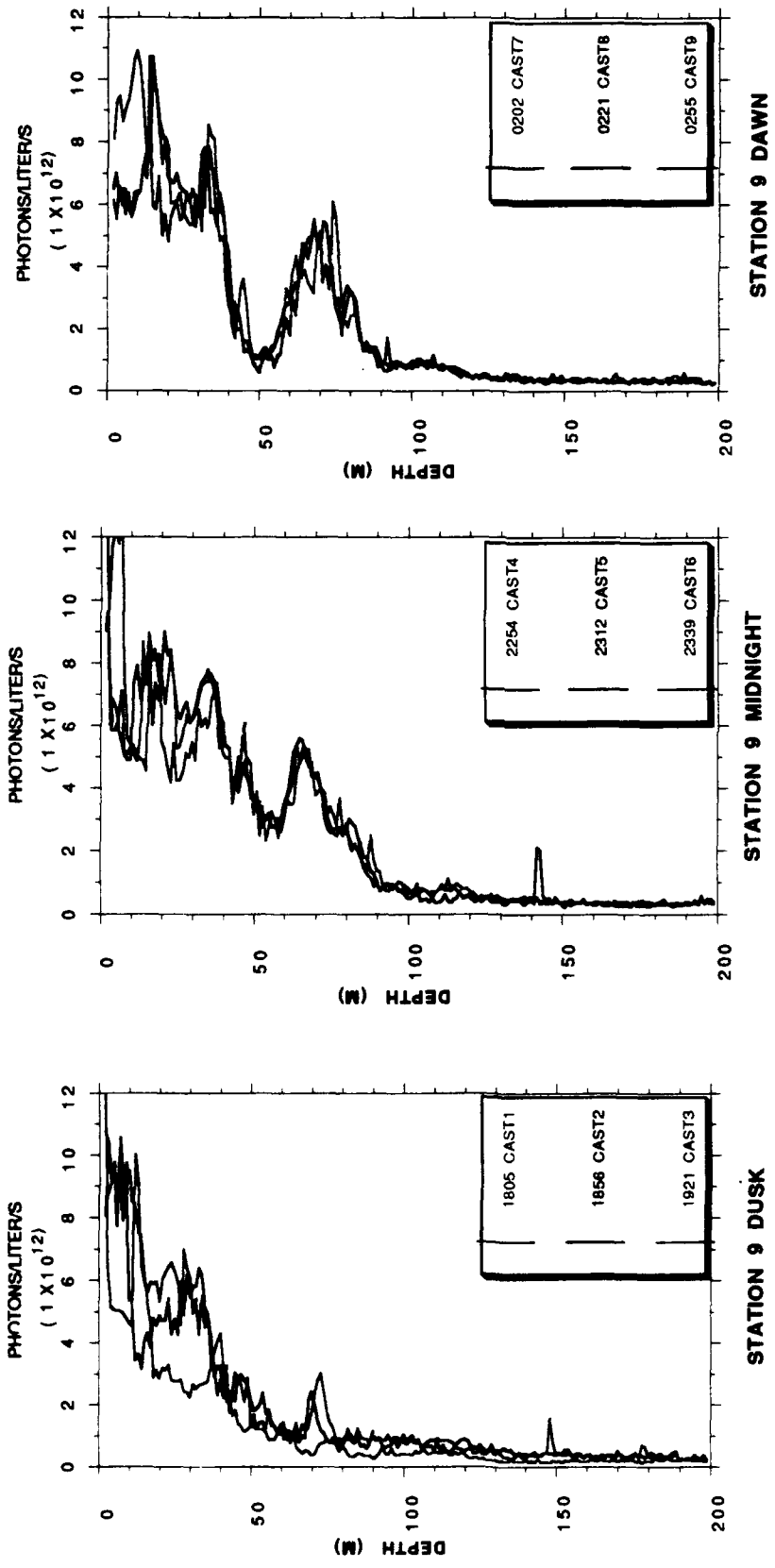

MED-OPS 91 Station 9 Figure B-9

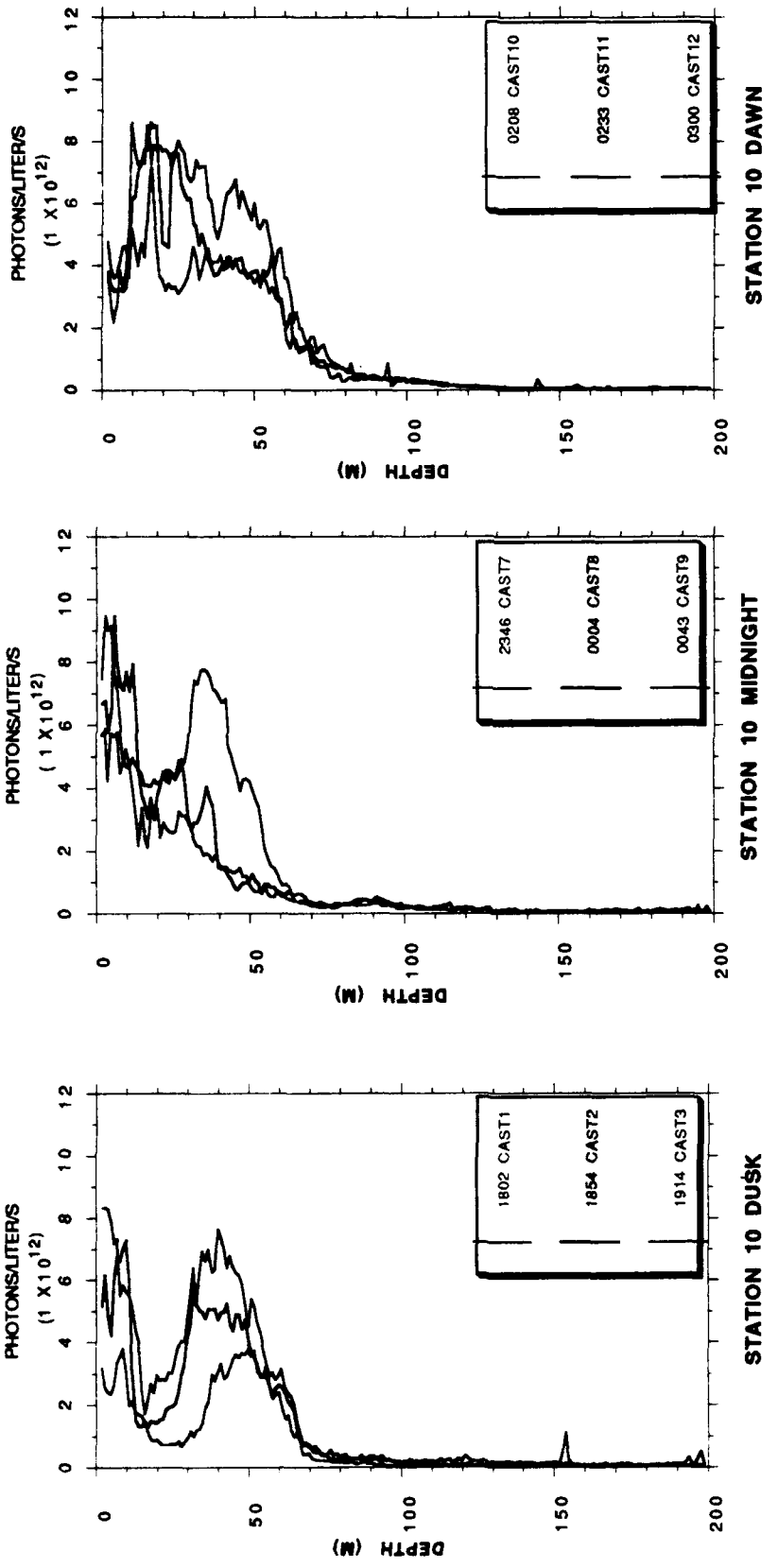

MED-OPS 91 Station 10 Figure B-10

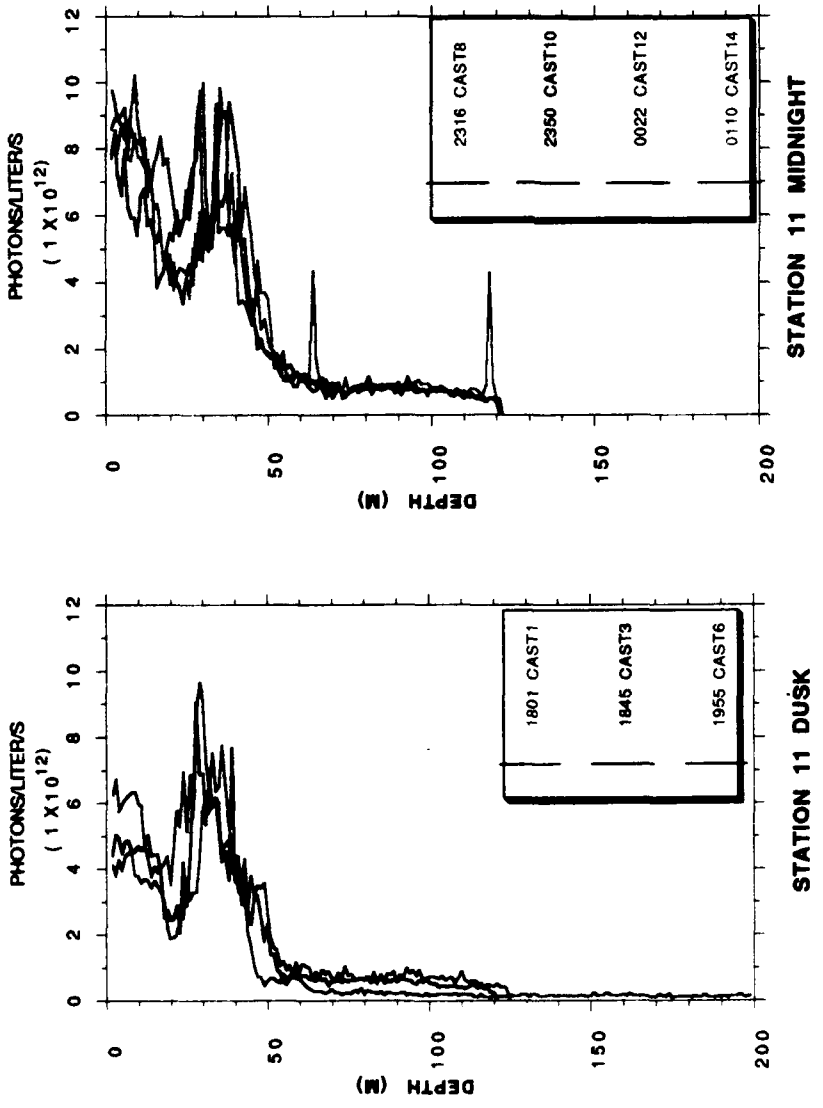

MED-OPS 91 Station 11 Figure B-11

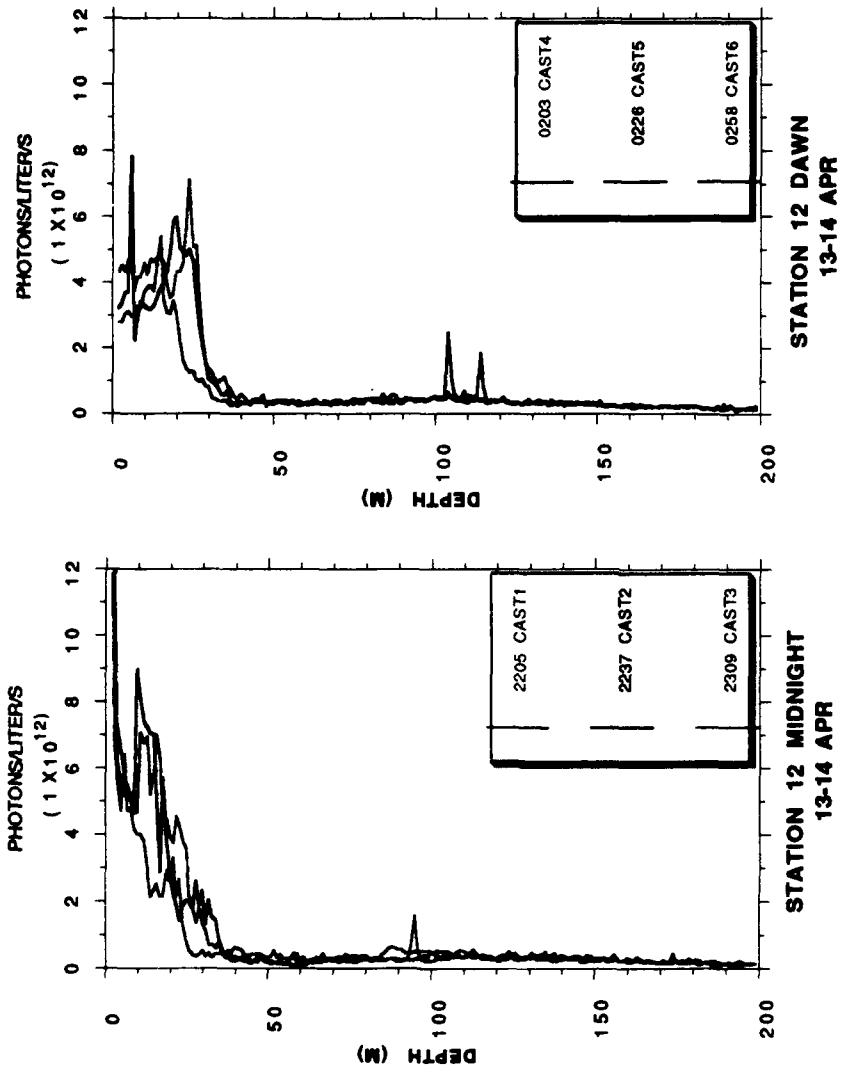

MED-OPS 91 Station 12 (13-14 Apr) Figure B-12a

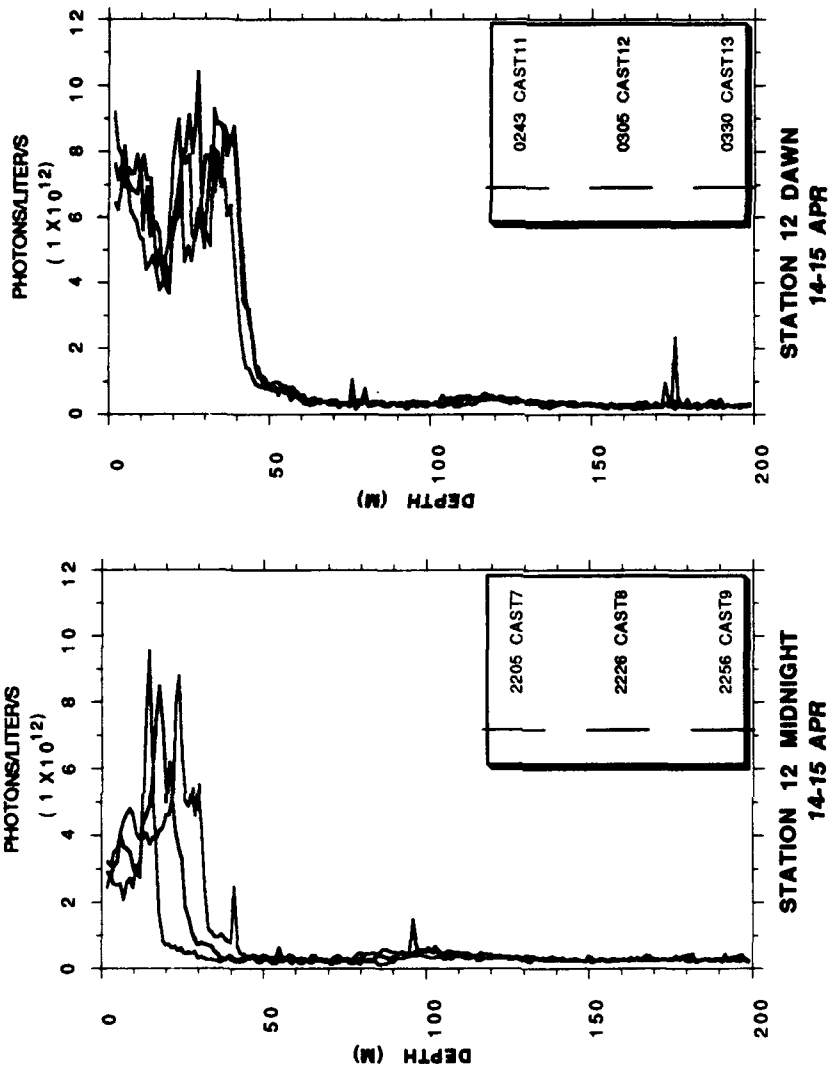

MED-OPS 91 Station 12 (14-15 Apr) Figure B-12b

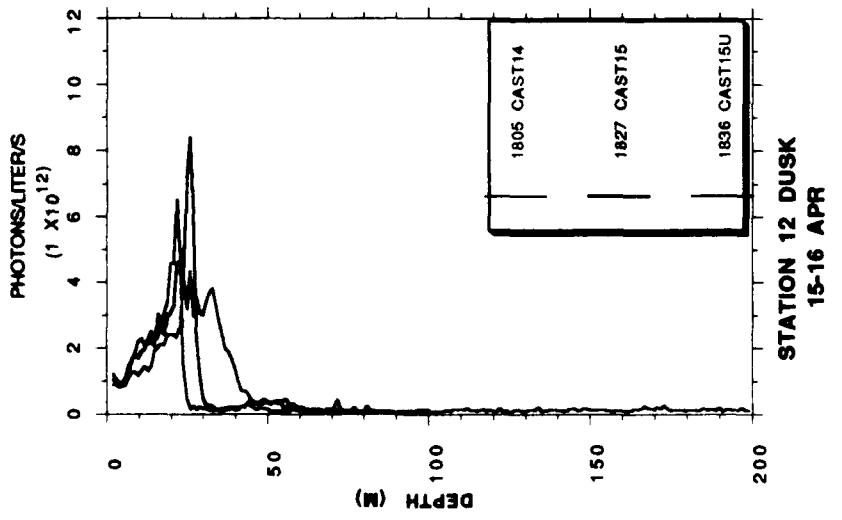

MED-OPS 91 Station 12 (15-16 Apr) Figure B-12c

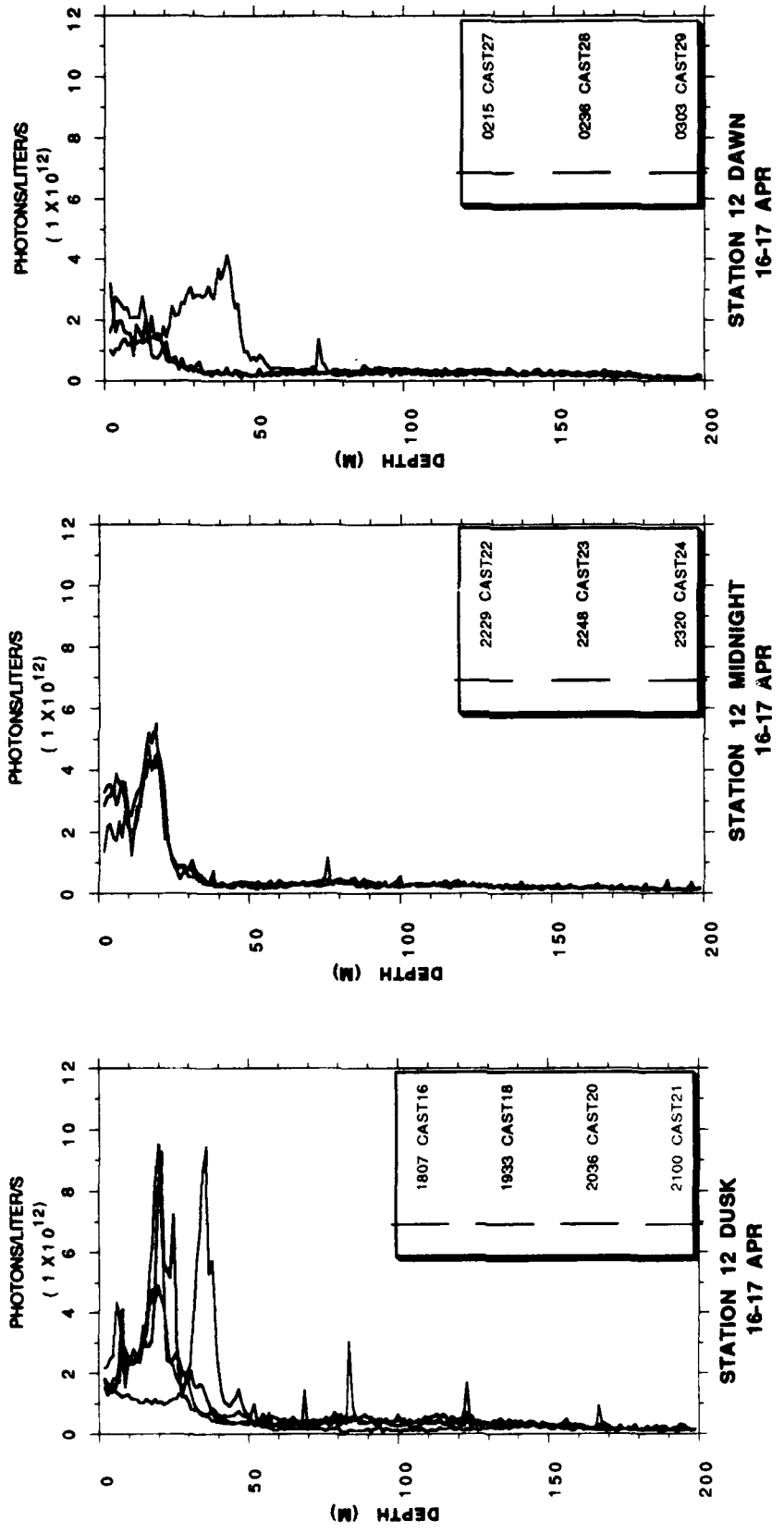

MED-OPS 91 Station 12 (16-17 Apr) Figure B-12d

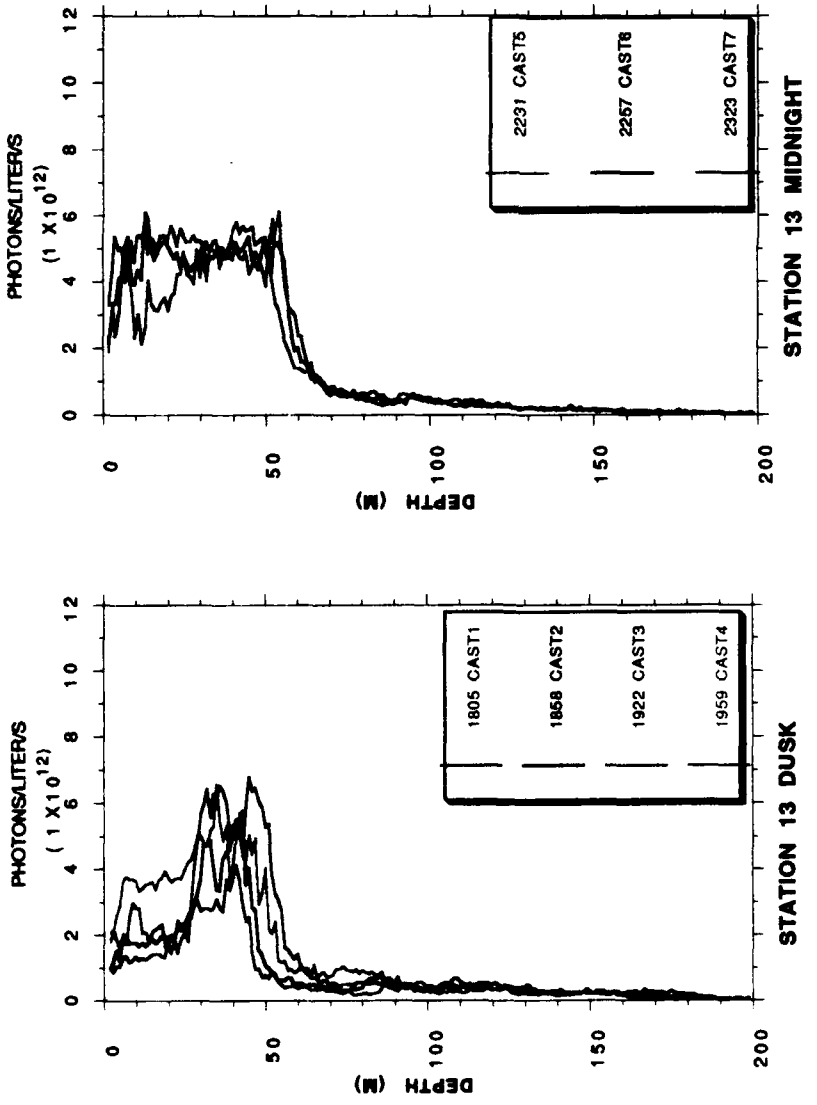

MED-OPS 91 Station 13

Figure B-13

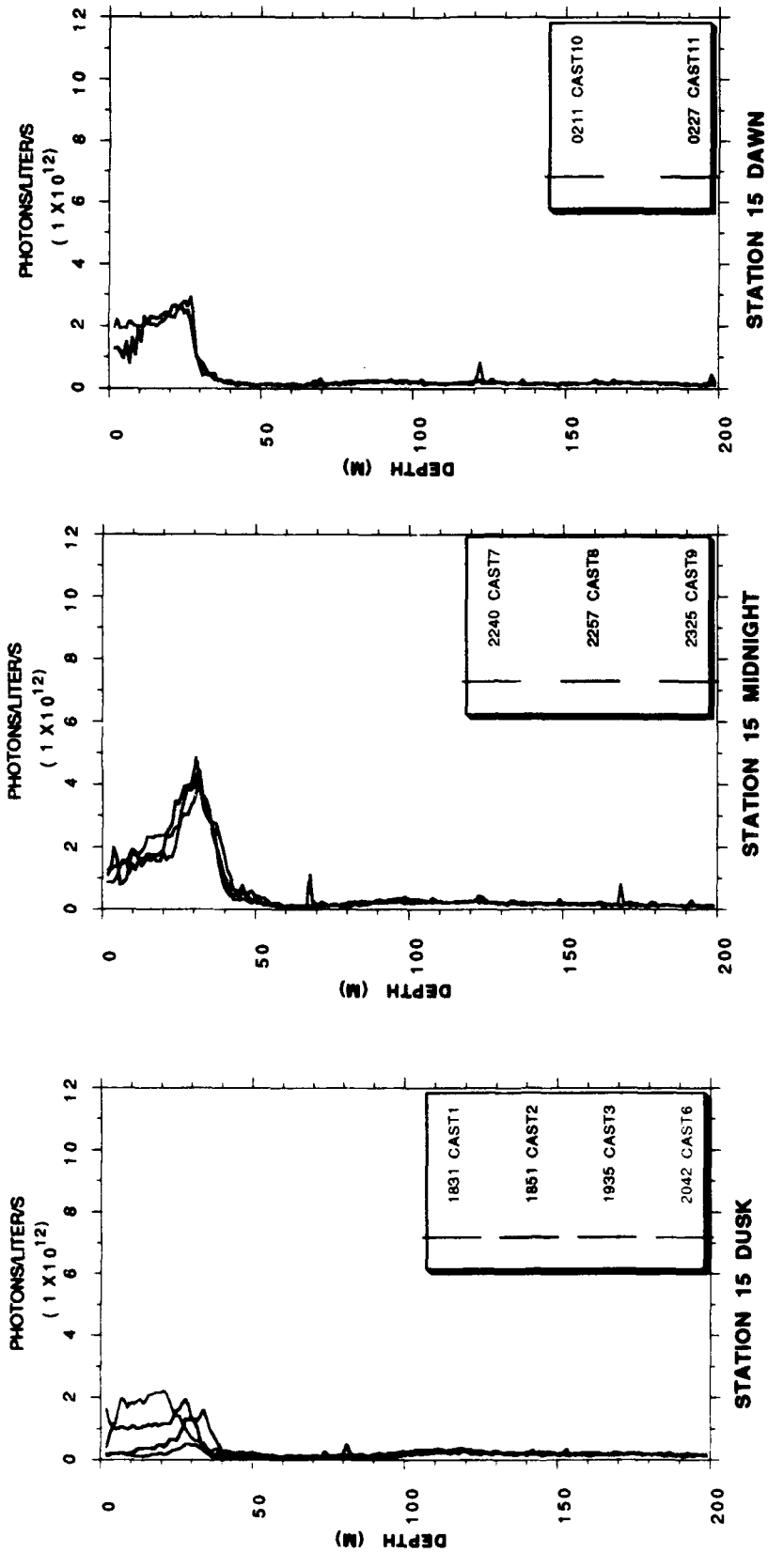

MED-OPS 91 Station 15

Figure B-15

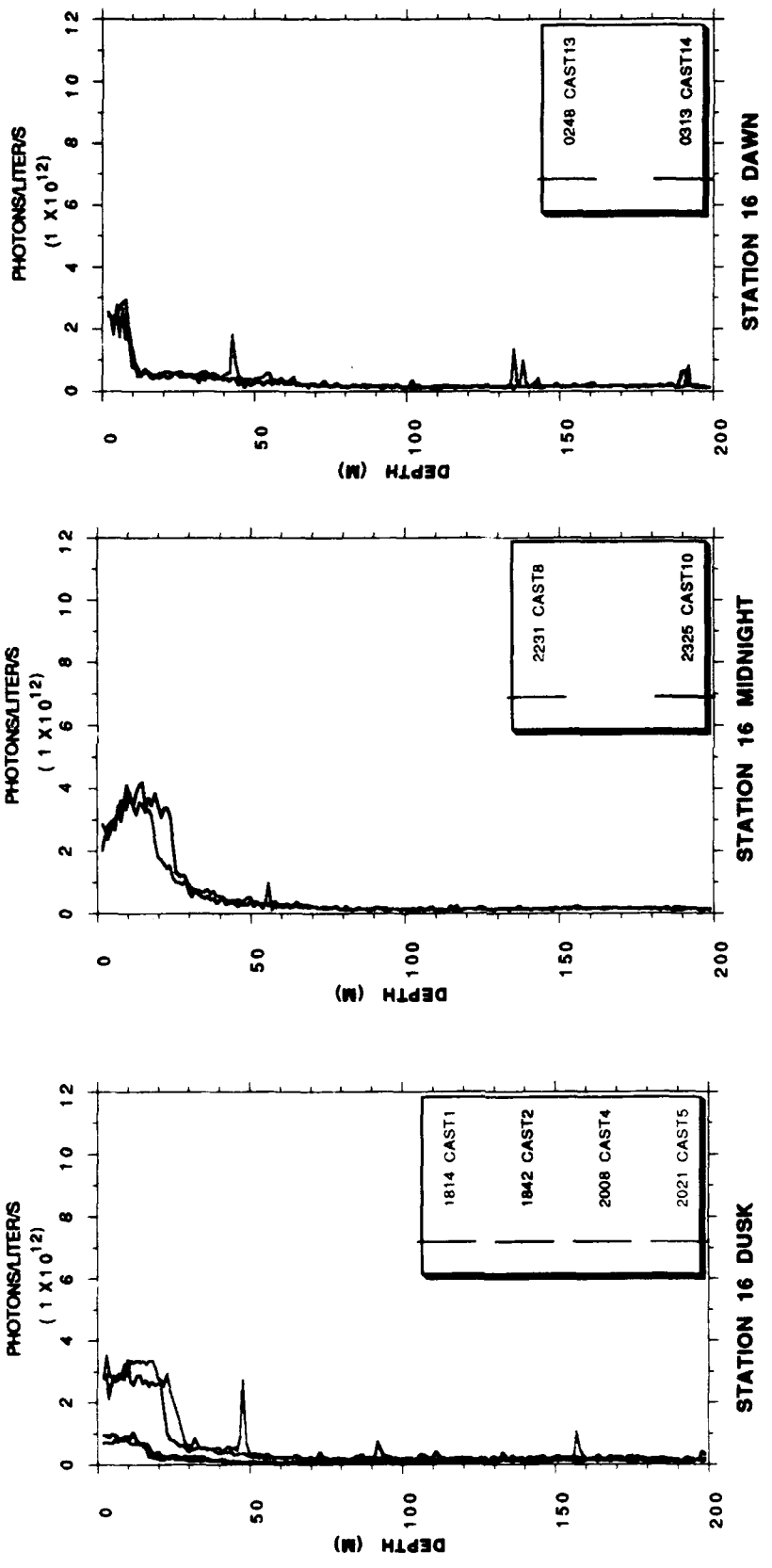

MED-OPS 91 Station 16

Figure B-16

APPENDIX C: Integrated Bioluminescence Intensity and Events

Bioluminescent light intensity and number of events were integrated for a column of water 1 m^2 and 200 m deep (the average value for each 1 m depth bin was multiplied by 10^3 to calculate the value for a m^3, and the results were totalled over the depth range). Data are presented for each cast at each station to indicate the change in the total light and events throughout the night. The light intensity scale is 10^{17} photons s^{-1} m^{-2}, and the events scale is 10^3 events m^{-2}. Due to technical uncertainties regarding the event counter that were unresolved as of this writing, the absolute value of the integrated events values may not be accurate; however it is believed that they do reflect relative changes in total events for the water column.

Station 1 MED-OP 91

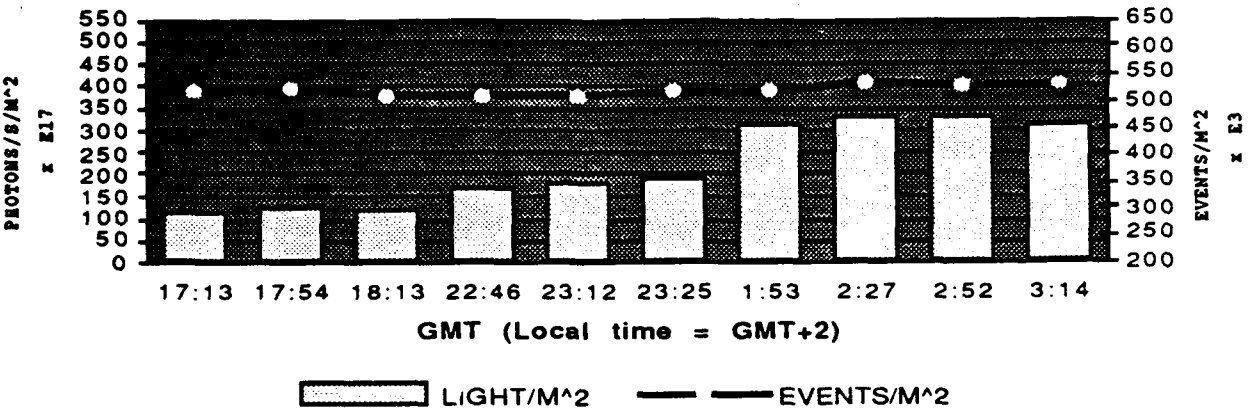

Station 2 MED-OPS 91

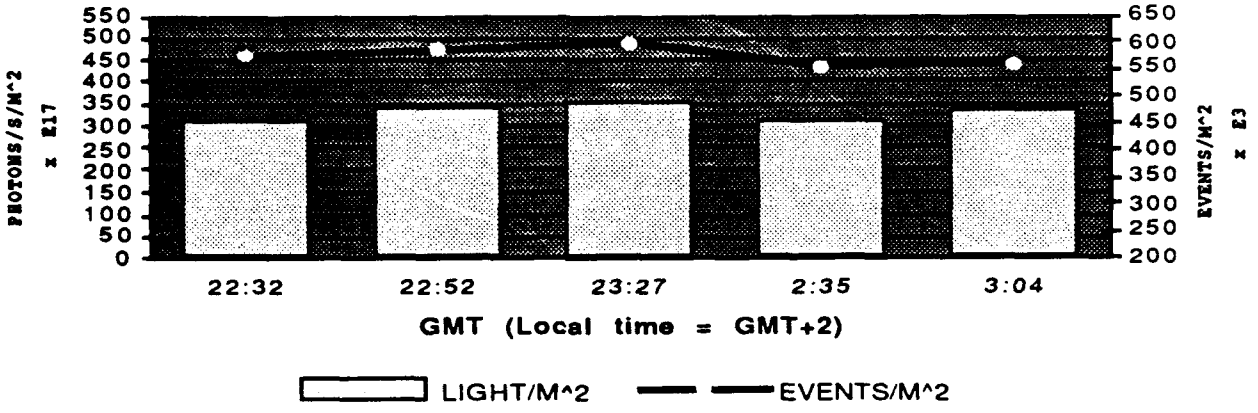

Station 5 MED-OPS 91

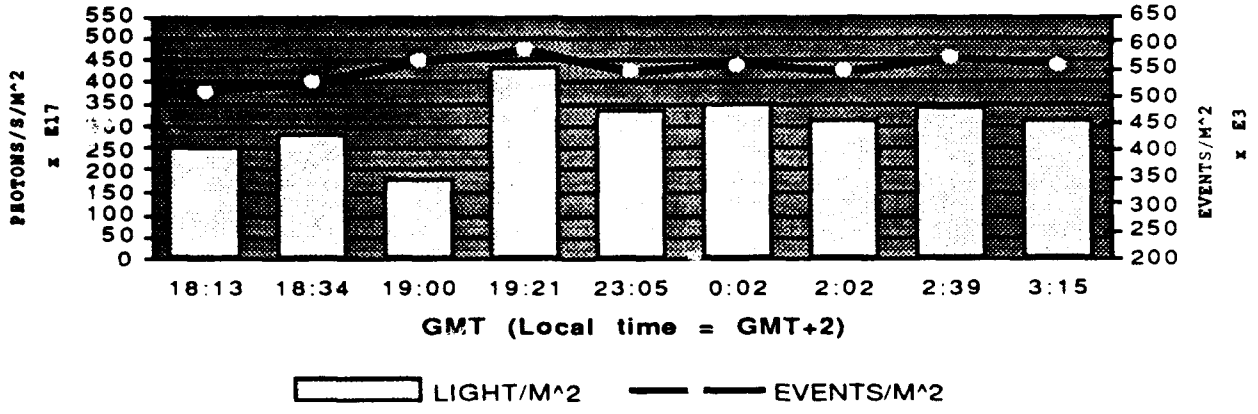

MED-OPS 91 Station 1,2, and 5 Figure C-1

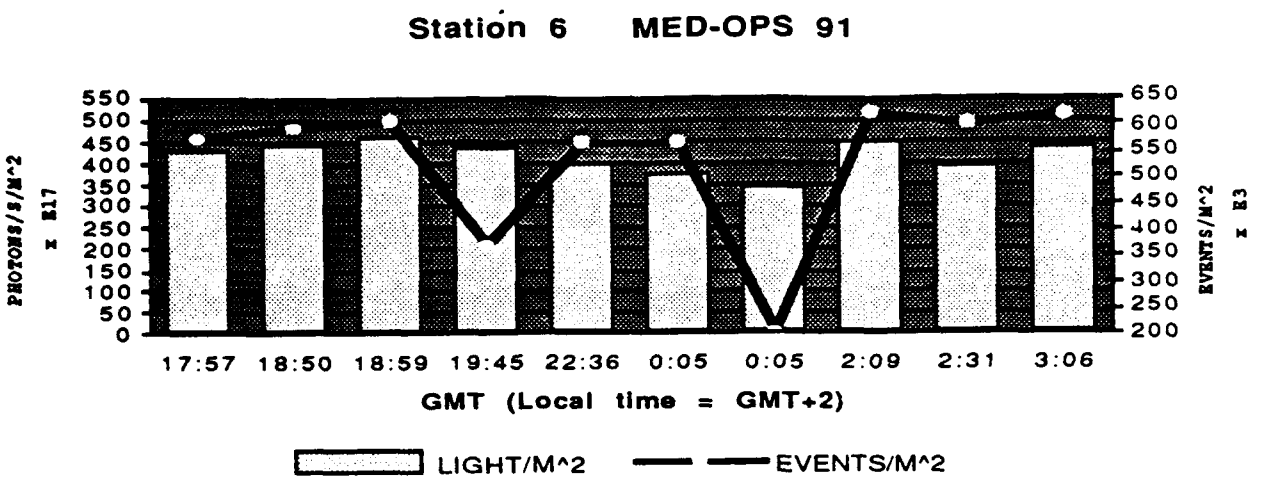

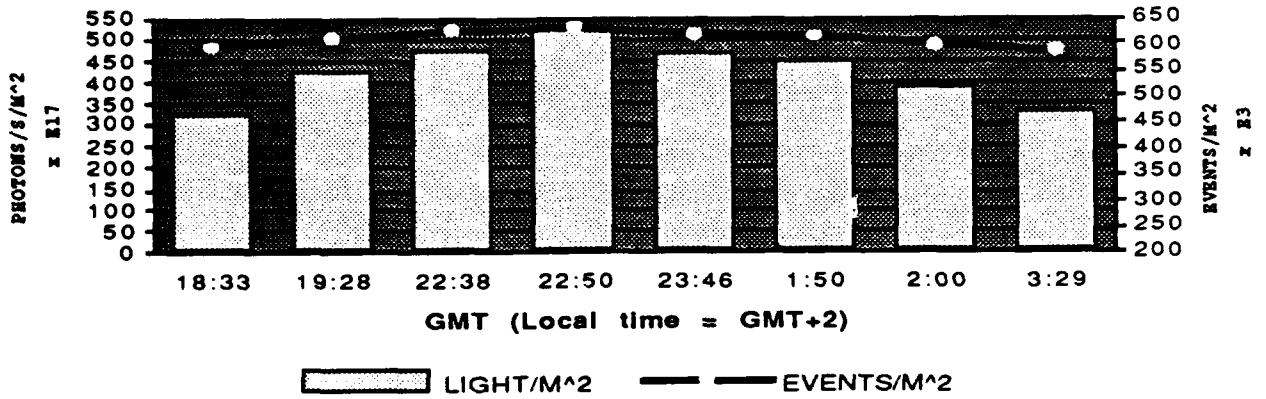

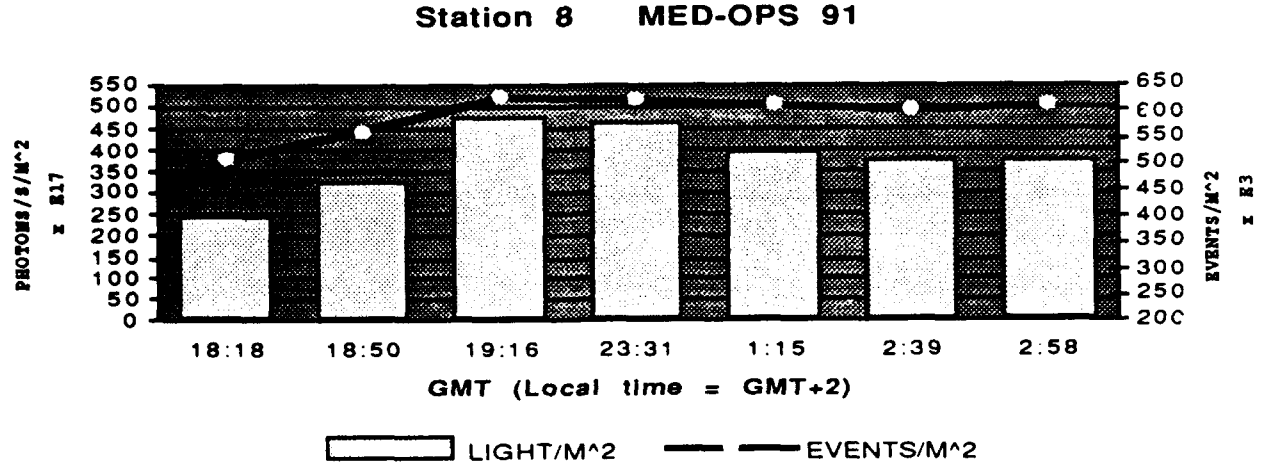

MED-OPS 91 Station 6, 7, and 8 Figure C-2

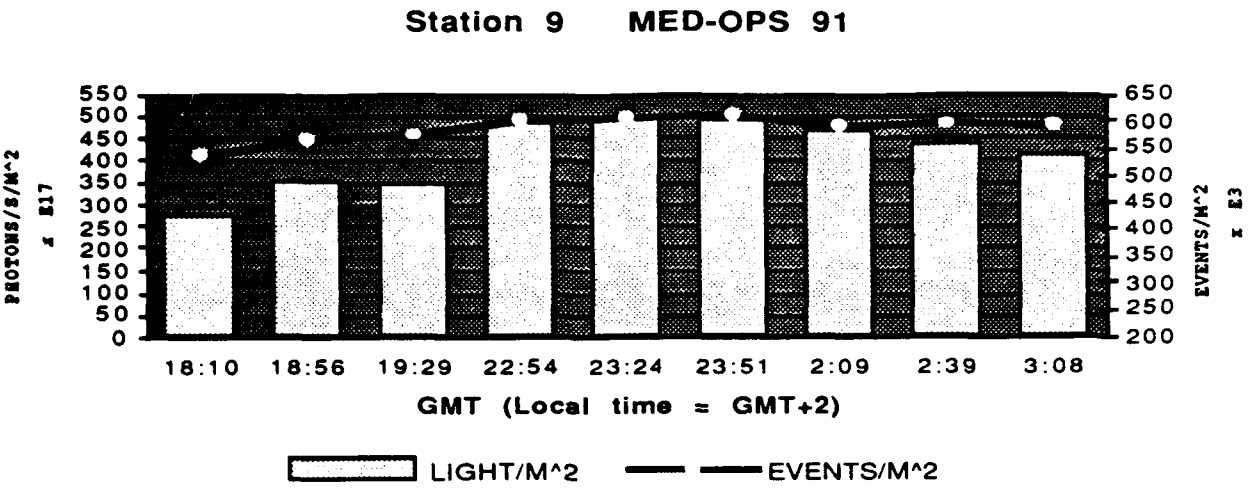

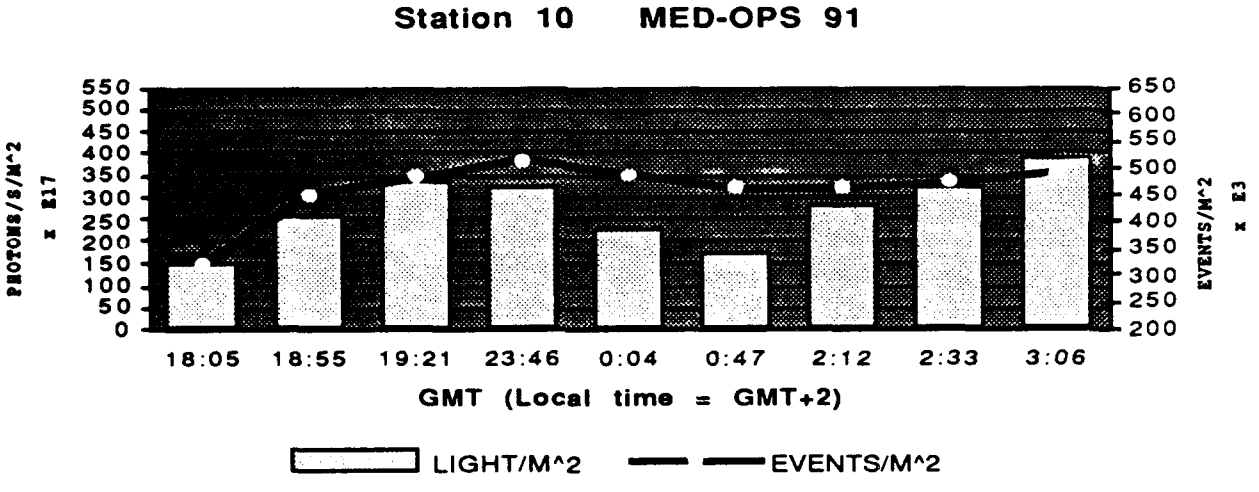

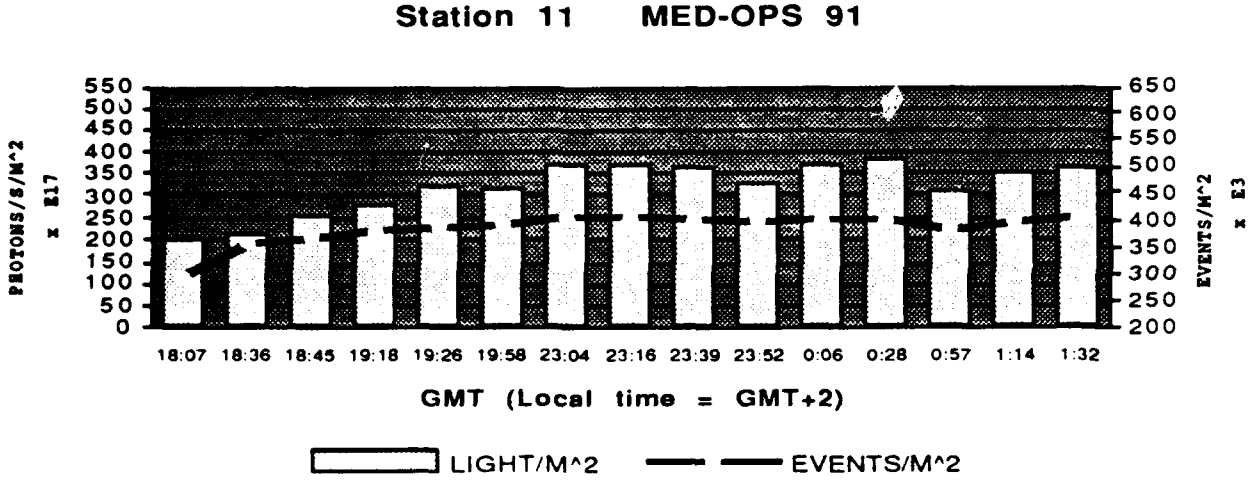

MED-OPS 91 Station 9, 10, and 11 Figure C-3

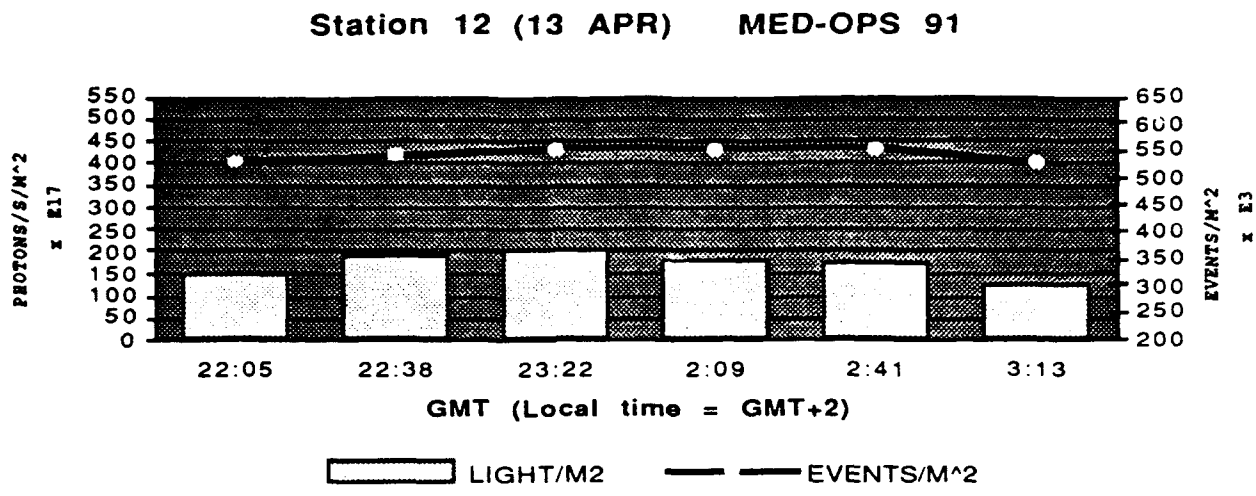

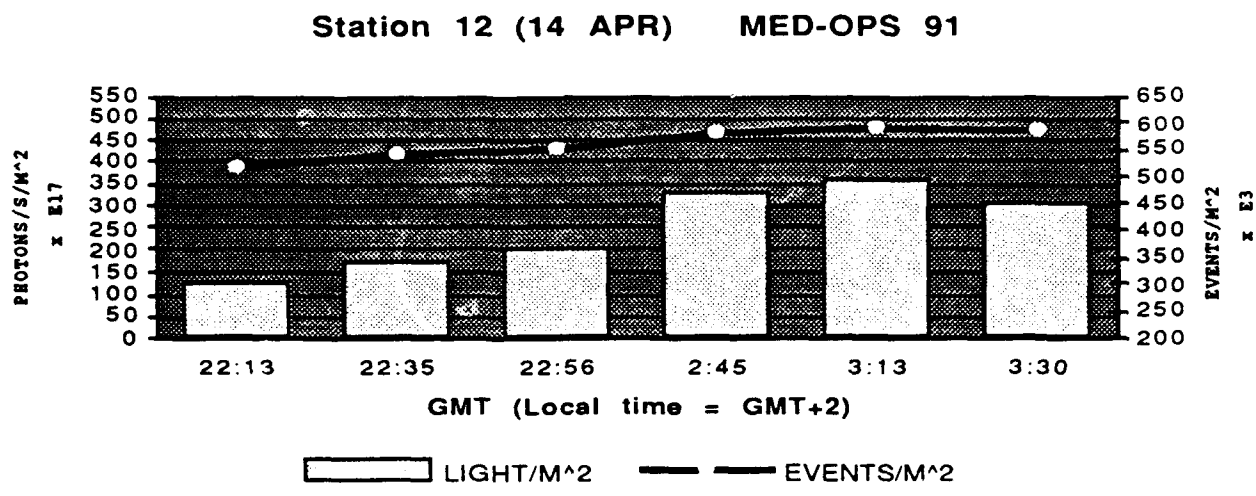

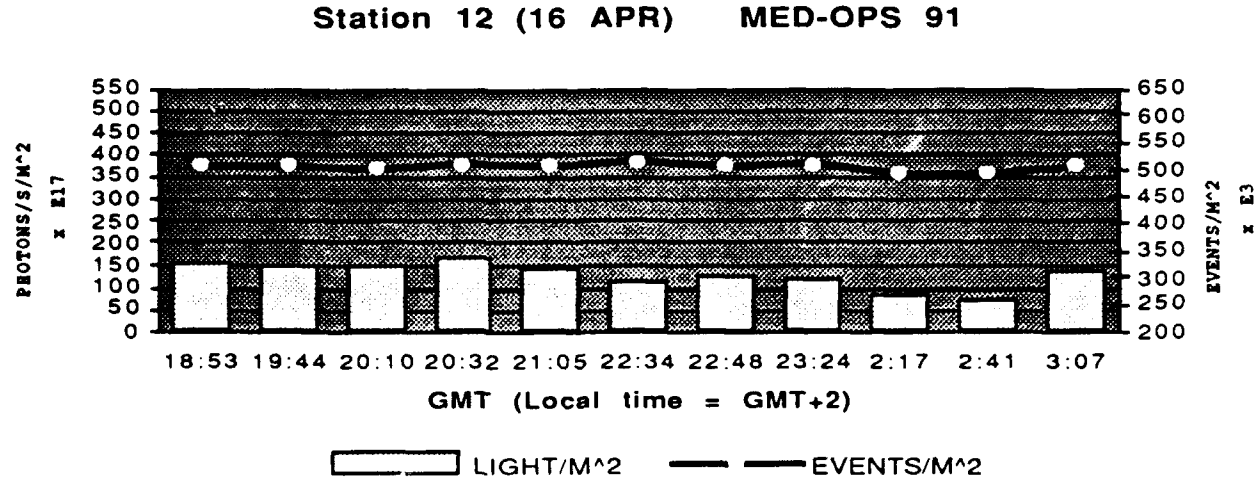

MED-OPS 91 Station 12 Figure C-4

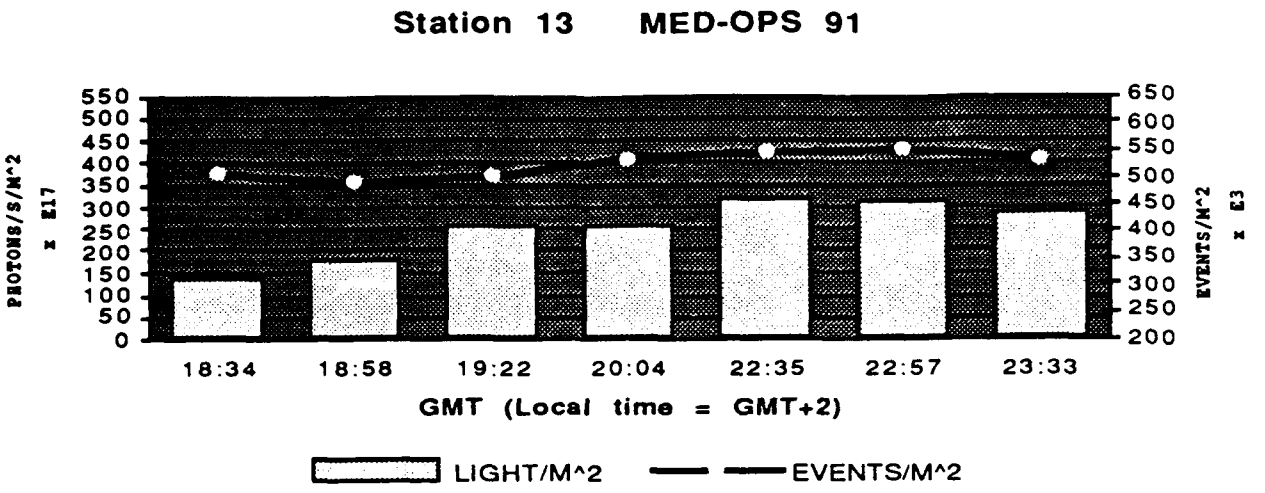

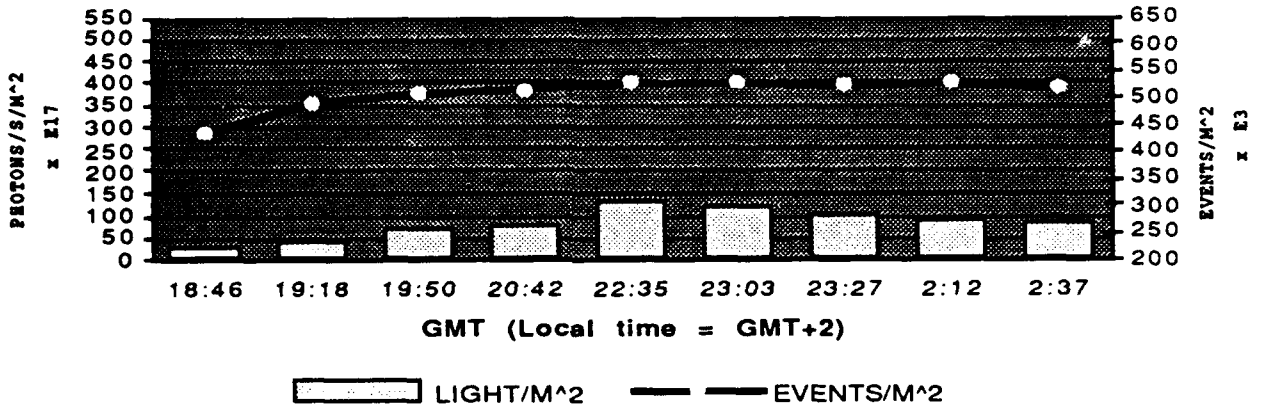

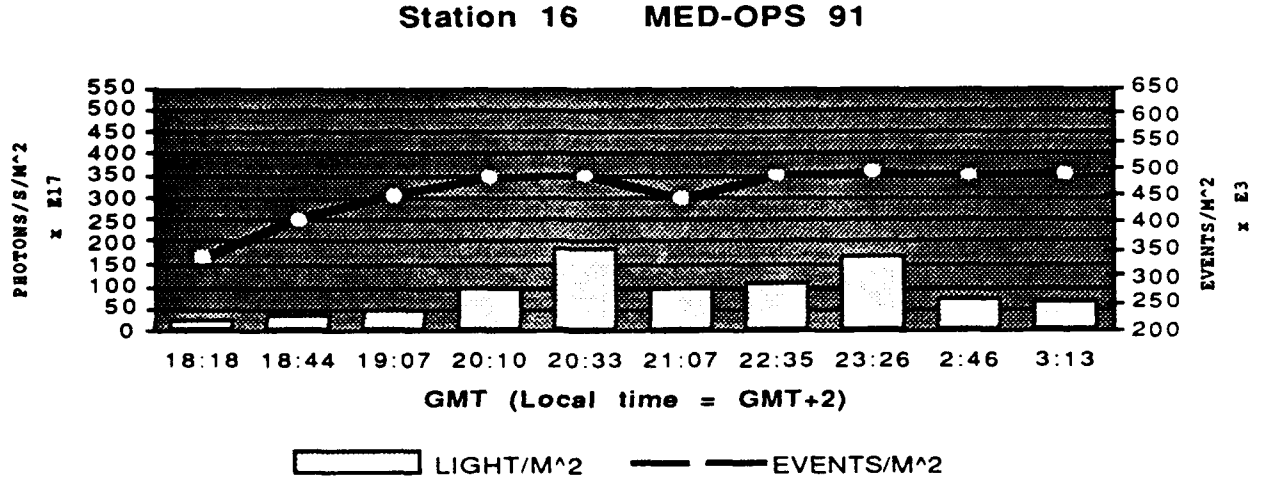

MED-OPS 91 Station 13, 15, and 16 Figure C-5

APPENDIX D: Plankton Counts

Zooplankton: Semiquantitative plankton samples were collected by vertical net hauls from 200 m to the surface using a 70 cm diameter net (62 µm mesh with 20 µm mesh cod end), and the major zooplankton groups were enumerated.

Dinoflagellates: For the quantitative dinoflagellate counts, the entire contents of 10 L Niskin sampling bottles were passed through a 20 µm mesh and the dinoflagellates in the sample (preserved in buffered formalin) were enumerated by the inverted microscope technique. All samples were collected at 1600 GMT.

Table D-1 : Zooplankton counts
Table D-2: Dinoflagellate counts, station 7, 8 April 91
Table D-3a: " station 12, 14 April 91
Table D-3b: " " 15 April 91
Table D-3c: " " 16 April 91

Densities (per cubic meter) of plankton collected from 200 m vertical tows of 70 cm diameter plankton net (62 μm cod end). Densities are derived from the mean of total counts of three subsamples from a Stempel pipette. Counts were made using a dissecting microscope.

Taxon	Station (date)											
	2 (4/3/91)	5 (4/7/91)	6 (4/8/91)	8 (4/10/91)	9 (4/11/91)	10 (4/12/91)	11 (4/13/91)	12 (4/14/91)	12 (4/15/91)	12 (4/17/91)	15 (4/20/91)	16 (4/21/91)
Foraminifera	2.4	1.7	3.3	1.3	0	0.7	0.6	1.5	0.2	0.3	0	0
Tintinnopsis	2.4	9.7	7.6	8.0	1.3	0.7	4.8	2.4	4.3	1.7	38.1	5.4
Harpacticoids	44.6	42.0	28.6	12.1	16.0	4.7	11.0	14.3	35.2	8.2	27.3	21.6
Calanoids	101.7	80.0	70.5	36.8	94.8	74.4	54.6	28.1	60.2	23.8	83.9	48.1
Cyclopoids	17.3	33.0	35.5	23.4	26.0	19.5	22.7	13.8	28.6	20.8	20.8	22.7
Pteropods	0.7	1.5	1.5	0.7	0.4	0.2	0.4	0	0.2	0	0	0.7
Phoronid larvae	0.7	0	0	0.2	0.2	0	0	0	0.2	0	0	0
Cladocerans	0.8	2.0	3.5	0.7	0.9	0.2	3.7	0.2	0.2	0	0	0.2
Bivalve larvae	1.3	0.8	0.9	0.2	0	0	1.3	0.4	0.4	1.5	0.2	0.4
Echinoderm larvae	1.7	0.7	1.5	1.3	0.6	0.2	0.4	0	0	0	0	0.9
Gastropod larvae	1.0	1.0	0.6	0.4	0.9	0.7	0.6	0.7	0	0.9	0.4	0
Nauplius larvae	5.4	1.3	14.5	27.3	14.0	28.6	25.1	24.5	14.3	8.4	36.4	9.7
Ostracods	4.9	3.9	3.7	2.6	1.3	0.4	2.4	1.3	5.2	4.1	0.4	4.1
Larvaceans	0	0.2	0.2	0.4	1.3	1.1	1.3	0.9	7.2	0	1.0	9.1
Salps	0	0	0	0.4	0	0	0	0.3	0.2	0.9	0	0
Ctenophores	0.2	0	0	0	0	0	0	0	0	0	0	0
Medusae	0.0	0	0.2	0	0.2	0	0.2	0	0.2	0.4	0	0.4
Siphonophores	1.3	0	0	0	0	0	0	0.2	0.2	0.2	0	0.7
Polychaete larvae	2.4	3.9	2.0	1.5	1.1	0.3	2.8	0	1.3	0.4	0.2	1.0
Cirripede larvae	0	0	0.2	0	0	0	0	0	0	0	0	0
Euphausiids	0	0.5	0.2	0.2	0	0.43	0.9	0.2	1.1	0	0.1	0
Carideans	2.6	0.2	0	0.8	1.3	0	0.2	0.2	0	0	0	1.1
Chaetognaths	2.8	2.0	3.0	0.8	0.9	0	0.2	0.2	0.4	0.7	1.1	0.7
Brachyuran larvae	0	0	0	0	0.4	0	1.3	0.2	0.4	0.2	0	0
Fish eggs	0	1.0	1.5	0.7	0.4	1.3	0.2	0.7	1.1	0.4	0	1.0

Mean densities (no. organisms/liter) and ranges (for 2 subsamples) of dinoflagellates from USNS BARTLETT Cruise 1306-91, Station 7 (1600Z cast), 8 April 1991. Water from Niskin bottles screened through 20 μm mesh. Total counts made with inverted microscope.

Taxon	5	10	20	50	85	120
Ceratium fusus	37 (34-39)	71 (69-73)	36 (33-40)	4 (3-6)	1 (1-2)	38 (35-41)
Ceratium (others)	138 (128-148)	270 (259-281)	102 (98-108)	24 (22-26)	2 (1-3)	99 (90-108)
Dinophysis sp.	18 (15-20)	17 (16-18)	12 (10-14)	7 (4-9)	1 (1-2)	2 (1-2)
Protoperidinium sp.	104 (103-106)	117 (115-119)	67 (61-71)	72 (70-74)	40 (39-41)	34 (29-40)
Noctiluca miliaris	48 (48-49)	60 (56-65)	47 (45-48)	5 (4-6)	1 (1-2)	2 (2-3)
TOTAL	345 (328-361)	535 (515-556)	264 (247-281)	112 (103-121)	45 (43-50)	175 (157-194)

MED-OPS 91 Station 7 Table D-2

Mean densities (no. organisms/liter) and ranges (for 2 subsamples) of dinoflagellates from USNS BARTLETT Cruise 1306-91, Station 12 (1600Z cast), 14 April 1991. Water from Niskin bottles screened through 20 μm mesh. Total counts made with inverted microscope.

Taxon	0	10	20	33	50	66	85
Ceratium fusus	9 (8-11)	10 (5-16)	24 (23-25)	4 (3-5)	12 (10-14)	1 (1-1)	6 (5-8)
Ceratium (others)	69 (67-70)	56 (55-56)	87 (76-98)	37 (36-38)	78 (75-82)	3 (2-3)	25 (18-31
Dinophysis sp.	12 (8-15)	11 (9-13)	11 (10-11)	3 (2-3)	10 (10-10)	<1 (0-<1)	2 (2-2)
Protoperidinium sp.	90 (88-93)	79 (73-85)	76 (70-82)	57 (54-60)	20 (20-20)	7 (6-8)	15 (13-17)
Noctiluca miliaris	35 (34-36)	39 (36-42)	20 (17-22)	4 (3-5)	2 (2-2)	1 (<1-1)	2 (1-3)
TOTAL	215 (205-225)	195 (178-212)	218 (196-238)	105 (98-111)	122 (117-128)	12 (9-13)	50 (39-61)

MED-OPS 91 Station 12 (14 Apr 91) Table D-3a

Mean densities (no. organisms/liter) and ranges (for 2 subsamples) of dinoflagellates from USNS BARTLETT Cruise 1306-91, Station 12 (1600Z cast), 15 April 1991. Water from Niskin bottles screened through 20 μm mesh. Total counts made with inverted microscope.

Taxon	0	10	20	33	50	66	85
Ceratium fusus	16 (14-18)	74 (71-77)	53 (49-57)	107 (103-111)	8 (7-8)	6 (6-7)	11 (9-13)
Ceratium (others)	61 (57-64)	71 (66-76)	68 (66-70)	96 (94-97)	30 (23-32)	23 (21-26)	2 (2-3)
Dinophysis sp.	24 (23-26)	10 (9-10)	10 (9-10)	6 (5-6)	3 (3-3)	2 (1-3)	1 (0-1)
Protoperidinium sp.	40 (31-48)	31 (31-32)	34 (32-36)	74 (73-75)	9 (8-10)	9 (7-11)	5 (4-6)
Noctiluca miliaris	18 (17-19)	15 (15-16	17 (17-18)	29 (24-35)	4 (3-4)	2 (2-3)	2 (2-2)
TOTAL	159 (142-175)	201 (192-211)	182 (173-191)	312 (299-324)	54 (49-57)	42 (37-50)	21 (17-25)

MED-OPS 91 Station 12 (15 Apr 91) Table D-3b

Mean densities (no. organisms/liter) and ranges (for 2 subsamples) of dinoflagellates from USNS BARTLETT Cruise 1306-91, Station 12 (1600Z cast), 16 April 1991. Water from Niskin bottles screened through 20 μm mesh. Total counts made with inverted microscope.

Taxon	0	10	20	40	50	66
Ceratium fusus	30 (27-33)	25 (21-29)	24 (19-30)	81 (78-83)	8 (6-10)	5 (5-5)
Ceratium (others)	34 (34-34)	40 (38-41)	54 (52-57)	98 (94-101)	26 (24-29)	8 (7-10)
Dinophysis sp.	4 (4-5)	2 (2-3)	6 (5-7)	7 (5-9)	5 (3-7)	2 (1-3)
Protoperidinium sp.	26 (25-27)	46 (43-49)	124 (111-137)	126 (111-140)	12 (12-13)	1 (9-12)
Noctiluca miliaris	1 1-1)	7 (3-11)	9 (6-12)	20 (17-22)	1 (1-2)	1 (0-1)
TOTAL	95 (91-100)	120 (107-133)	217 (193-243)	332 (305-355)	52 (46-61)	27 (22-31)

MED-OPS 91 Station 12 (16 Apr 91) Table D-3c

APPENDIX E: Photographic Survey

A 70 mm stereo underwater camera was used to image organisms and particles down to 1 cm in size. The camera and strobe lights were mounted on a frame that was lowered to each depth, pausing for 5 to 15 min. The interval between frames was set to 30 s. The volume of the field of focus was calculated to be approximately 0.125 m^{-3}. The data represents 2300 frames that were analyzed using a microscope and a loupe to identify organisms. Two general classes of detritus, "gelatinous blobs" and "streamers," were included in the counts.

CAMERA STATION #2													
DEPTH (M)	# OF FRAMES TAKEN	COPEPOD	EUPHAUSID	MISC CRUSTACEAN	CTENOPHORE	JELLYFISH	SALPS	SIPHONOPHORE	STREAMER	GELATINOUS BLOB	FISH	WORM	SQUID
6	1			1									
13	1												
19	1												
25	11				1	2							
50	10	1											
75	10			1					3				
100	10		1						9		1		
125	10					1			2				
150	10					2			6				
175	10		1	1		1			3				
200	10					1			4				
180	1											1	
160	1								1				
140	1												
120	1												
100	1								1				
80	1												
60	1					1			1				
40	1												
20	1												
0	1												

MED-OPS 91 Station 2 Table E-2

CAMERA STATION #5													
DEPTH (M)	# OF FRAMES TAKEN	COPEPOD	EUPHAUSID	MISC. CRUSTACEAN	CTENOPHORE	JELLYFISH	SALPS	SIPHONOPHORE	STREAMER	GELATINOUS BLOB	FISH	WORM	SQUID
4	1												
9	1								11				
13	1								4				
17	11								30			1	
29	20			1					18				
40	10			1					1				
44	10			1					7				
98	10								3				
134	1								1				
160	10		1						2				
180	10												
150	1												
120	1				1								
90	1												
60	1												
30	1												
0	1												

CAMERA STATION #6													
DEPTH (M)	# OF FRAMES TAKEN	COPEPOD	EUPHAUSID	MISC. CRUSTACEAN	CTENOPHORE	JELLYFISH	SALPS	SIPHONOPHORE	STREAMER	GELATINOUS BLOB	FISH	WORM	SQUID
5	1												
10	11		1		1								
17	10		1			3			1				
30	20		2			1			1				
50	10		1						2				
100	10			1					10				
133	10								11				
111	1												
89	1												
67	1												
45	1												
13	1												
0	1												

CAMERA STATION #8													
DEPTH (M)	# OF FRAMES TAKEN	COPEPOD	EUPHAUSID	MISC. CRUSTACEAN	CTENOPHORE	JELLYFISH	SALPS	SIPHONOPHORE	STREAMER	GELATINOUS BLOB	FISH	WORM	SQUID
3	1												
5	1												
8	1												
10	21			2		2		6			1		
17	20		21	5		8		4	1				
22	20		12	1		4	5	2	9		3		
80	10		1						7				
132	10		2						23				
110	1	1	1										
88	1		1										
66	1								1				
44	1							2					
22	1		2										
0	1		1			1							

CAMERA STATION #9													
DEPTH (M)	# OF FRAMES TAKEN	COPEPOD	EUPHAUSID	MISC. CRUSTACEAN	CTENOPHORE	JELLYFISH	SALPS	SIPHONOPHORE	STREAMER	GELATINOUS BLOB	FISH	WORM	SQUID
7	1												
13	21			1					3				
23	20		1		2				7				
29	20								8		1		
47	20		3						52		1		
73	10		1	1					28				
148	10		1						22				
133	1								1				
118	1		1						1				
103	1								1				
88	1												
73	1												
58	1												
43	1												
28	1												
13	1												
0	1												

CAMERA STATION #10													
DEPTH (M)	# OF FRAMES TAKEN	COPEPOD	EUPHAUSID	MISC CRUSTACEAN	CTENOPHORE	JELLYFISH	SALPS	SIPHONOPHORE	STREAMER	GELATINOUS BLOB	FISH	WORM	SQUID
1	1												
3	1												
4	1												
5	11			1				1					
9	10		1										
16	10		1	2					4				
37	30	1	7			1			28				
41	20		3	1					43				
52	10		1						45				
55	10		2						24				
46	1												
37	1												
28	1												
19	1												
10	1												
0	1												

CAMERA STATION #11													
DEPTH (M)	# OF FRAMES TAKEN	COPEPOD	EUPHAUSID	MISC. CRUSTACEAN	CTENOPHORE	JELLYFISH	SALPS	SIPHONOPHORE	STREAMER	GELATINOUS BLOB	FISH	WORM	SQUID
0	21		1	2	1	2		2			4	1	
8	20		50	1	1	1		1	1		9		
29	40		466	1	2			2	83		14		2
36	10		228						5		1		
49	10		34						21		4		
62	10		13			2		1	5				2
54	1												
46	1												
38	1												
30	1												
22	1												
14	1												
6	1												
0	1												

CAMERA STATION #12(10)													
DEPTH (M)	# OF FRAMES TAKEN	COPEPOD	EUPHAUSID	MISC. CRUSTACEAN	CTENOPHORE	JELLYFISH	SALPS	SIPHONOPHORE	STREAMER	GELATINOUS BLOB	FISH	WORM	SQUID
1	1												
3	1												
5	21		4	1		6	1			2	1		
12	20		8	1		2			5	25			
16	20	4	24						8	16			
22	20	15	1	6					6	3	1	1	
40	10	1	1			5	.		2	1	1		
50	10		2	1		1			1	1			
37													
25													
13													
0													

CAMERA STATION #12(11)													
DEPTH (M)	# OF FRAMES TAKEN	COPEPOD	EUPHAUSID	MISC. CRUSTACEAN	CTENOPHORE	JELLYFISH	SALPS	SIPHONOPHORE	STREAMER	GELATINOUS BLOB	FISH	WORM	SQUID
0	10							1					
9	20		1	3		2		1					
24	30	4	40	5		2		4	9	3	2	1	
29	20		2	1					24				
40	20	1	3					1	5			1	
35	1												
30	1												
25	1												
20	1												
15	1												
10	1												
5	1												
0	1												

CAMERA STATION #13													
DEPTH (M)	# OF FRAMES TAKEN	COPEPOD	EUPHAUSID	MISC CRUSTACEAN	CTENOPHORE	JELLYFISH	SALPS	SIPHONOPHORE	STREAMER	GELATINOUS BLOB	FISH	WORM	SQUID
0	20												
5	20												
25	20		11	1		1		1					
40	20		13	1	1	2	2		32			1	
55	20		5	1			3		38				
41	1												
27	1												
13	1												
0	1												

CAMERA STATION #15													
DEPTH (M)	# OF FRAMES TAKEN	COPEPOD	EUPHAUSID	MISC. CRUSTACEAN	CTENOPHORE	JELLYFISH	SALPS	SIPHONOPHORE	STREAMER	GELATINOUS BLOB	FISH	WORM	SQUID
0	20												
7	20		1					1					
32	30		7							1			
110	20			1									
97	1				1								
84	1												
71	1												
58	1												
45	1		1					1	1				
32	1												
19	1												
6	1												
0	1					1							

CAMERA STATION #16													
DEPTH (M)	# OF FRAMES TAKEN	COPEPOD	EUPHAUSID	MISC CRUSTACEAN	CTENOPHORE	JELLYFISH	SALPS	SIPHONOPHORE	STREAMER	GELATINOUS BLOB	FISH	WORM	SQUID
0	10					1							
10	20		7	1				8			1		
15	20					1		11	1				
20	20		6			1		2	1				
25	10		2		1				1				
50	10				1			2			1		
45	1												
40	1												
35	1												
30	1												
25	1												
20	1												
15	1												
10	1												
5	1				2								
0	1												

APPENDIX F: Extractable Algal Pigments

Water samples for pigment analysis were collected during the daylight casts for optical measurements. The water was prefiltered through a 210 µm mesh to remove larger zooplankton, then fractionated into <20 µm and >20 µm fractions using a 20 µm mesh before extracting the algal pigments with acetone. Values reported are for chlorophyll a, the primary photosynthetic pigment, and for phaepigments, the products of chlorophyll degradation that occur primarily in the digestive tracts of zooplankton. The precision of each value (the mean of 4 replicates) is stated as the 95% confidence interval (95% CI), i.e., the interval that will include the "true" mean 95% of the times that the population is sampled. In a normally distributed population, the 95% CI is equivalent to +/- 2 standard deviations. The statistics were determined using methods for small sample populations (Dean and Dixon, 1951). The proportion of chlorophyll a that occurred in the <20 µm fraction and the ratio of phaeopignments to chlorophyll a are also reported. Some of the ratios are slightly greater than 1, a condition attributable to the analytical error of the procedure.

REFERENCE

Dean, R.B. and W.J. Dixon (1951). Simplified statistics for small numbers of observations. *Analytical Chemistry* 23(4):636-638.

Station 1, April 2

Cast local time	DEPTH (m)	Chl "a" ($\mu g\ m^{-3}$)	+/- 95% CI	Phaeo ($\mu g\ m^{-3}$)	+/- 95% CI	Proportion of Chl "a" < 20 μm	Phaeo/ Chl
Cast A 0816	5	1.595	.111	.355	.119	.964	.223
	93	.820	.534	.318	.097	.413	.437
	145	1 021	.074	.514	.210	.923	.501
	250	.018	.015	.046	.015	.380	3.353
Cast B 1228	80	1.058	.447	.411	.067	.567	.480
	152	.661	.335	.384	.136	.563	.716
Cast C 1444	20	2.080	.420	.588	.091	.800	.283
	60	1.591	.736	.468	.229	.599	.298
	142	.708	.224	.349	.073	.663	.502

Station 2, April 3

Cast local time	DEPTH (m)	Chl "a" ($\mu g\ m^{-3}$)	+/- 95% CI	Phaeo ($\mu g\ m^{-3}$)	+/- 95% CI	Proportion of Chl "a" < 20 μm	Phaeo/ Chl
Cast A 0822	20	1.410	.260	.527	.027	.843	.375
	75	.294	.105	.232	.044	.625	.816
	250	.022	.006	.029	.004	1.000	1.313
Cast B 1135	5	1.296	.280	.462	.089	.760	.360
	20	1.496	.315	.512	.066	.809	.346
	60	.744	.189	.383	.015	.700	.531
	150	.048	.030	.057	.014	.400	1.336
Cast C 1432	2	1.070	.208	.444	.060	.779	.418
	10	1.033	.107	.456	.050	.952	.441
	10	.882	.123	.460	.025	.883	.523
	13	.866	.365	.410	.084	.636	.488

MED-OPS 91 Station 1 and 2 Table F-1

Station 3, April 4

Cast local time	DEPTH (m)	Chl "a" ($\mu g\ m^{-3}$)	+/- 95% CI	Phaeo ($\mu g\ m^{-3}$)	+/- 95% CI	Proportion of Chl "a" < 20 μm	Phaeo/ Chl
Cast A 095	10	.858	.123	.366	.081	.831	.426
Cast B 1150	10	1.332	.280	.504	.081	.766	.381
	20	1.356	.193	.519	.056	.874	.383

Station 5, April 6

Cast local time	DEPTH (m)	Chl "a" ($\mu g\ m^{-3}$)	+/- 95% CI	Phaeo ($\mu g\ m^{-3}$)	+/- 95% CI	Proportion of Chl "a" < 20 μm	Phaeo/ Chl
Cast A 0820	20	1.125	.127	.448	.357	.640	.403
	60	1.122	7.768	.425	.649	.673	.389
	60	1.045	1.981	.386	.149	.724	.374
	100	.622	.047	.271	.077	.842	.436
	150	.039	.008	.045	.010	.577	1.174
Cast B 1138	5	1.193	.044	.404	.418	.609	.355
	40	1.315	.065	.473	.409	.645	.378
	60	1.109	.075	.455	.163	.720	.406
	120	.246	.049	.215	.009	.949	.896
	100	.622	.047	.271	.077	.842	.436
	150	.039	.008	.045	.010	.577	1.174
Cast C C1500	40	1.298	.469	.465	.193	.770	.356
	90	.872	.084	.375	.155	.943	.458

Station 6, April 7

Cast local time	DEPTH (m)	Chl "a" (mg m^{-3})	+/- 95% CI	Phaeo (mg m^{-3})	+/- 95% CI	Proportion of Chl "a" < 20 µm	Phaeo/ Chl
Cast A 0829	1	1.083	.385	.314	.116	.664	.290
	5	1.217	.045	.306	.035	.945	.444
	20	.934	.238	.395	.051	.734	.429
	40	.679	.183	.364	.061	.785	.539
	100	.602	.163	.318	.042	.743	.534
Cast B 1145	5	.927	.168	.305	.035	.814	.332
	20	1.308	.946	.685	.804	.536	.641
	40	.791	.265	.386	.098	.626	.504
Cast C 1436	20	1.234	.230	.513	.035	.782	.420
	40	.783	.429	.332	.130	.481	.446
	120	.592	.148	.340	.067	.753	.580

Station 7, April 8

Cast local time	DEPTH (m)	Chl "a" (mg m^{-3})	+/- 95% CI	Phaeo (mg m^{-3})	+/- 95% CI	Proportion of Chl "a" < 20 µm	Phaeo/ Chl
Cast A 0851	20	2.336	1.674	1.187	.734	.350	.544
	30	1.997	1.795	1.153	.701	.240	.697
	40	2.063	1.922	1.356	.933	.221	.852
	60	.599	.416	.602	.250	.386	1.101
Cast B 1149	20	1.728	2.849	.844	1.149	.317	.501
	40	1.168	1.545	.978	.898	.247	1.112
	80	.074	1.578	.169	.636	.339	2.375

Station 8, April 9

Cast local time	DEPTH (m)	Chl "a" (mg m^{-3})	+/- 95% CI	Phaeo (mg m^{-3})	+/- 95% CI	Proportion of Chl "a" < 20 µm	Phaeo/ Chl
Cast A 0843	20	1.851	.130	.603	.038	.952	.326
	40	1.586	.223	.568	.089	.907	.358
	60	.549	.160	.413	.106	.702	.765
Cast B 1205	20	1.741	.186	.663	.165	.901	.379
	40	1.535	.186	.603	.067	.859	.394
	80	.611	.111	.431	.044	.788	.712
Cast C 1452	5	1.651	.149	.645	.072	.882	.392
	20	1.838	.111	.782	.056	.939	.426
	80	.509	.098	.553	.142	.845	1.083

Station 9, April 10

Cast local time	DEPTH (m)	Chl "a" (mg m^{-3})	+/- 95% CI	Phaeo (mg m^{-3})	+/- 95% CI	Proportion of Chl "a" < 20 µm	Phaeo/ Chl
Cast A 0827	5	.727	.068	.255	.028	.932	.351
	40	751	.102	.425	.014	.895	.567
	120	.035	.013	.063	.009	.642	1.865
Cast B 1136	5	.509	.248	.139	.178	.962	1.412
	40	.744	3.186	.467	2.180	.478	.633
	120	.115	.153	.184	.214	.811	1.583
Cast C 1450	20	.573	.060	.246	.022	.892	.429
	40	.744	.073	.396	.037	.912	.532
	80	.410	.015	.250	.065	1.046	.610

Station10, April 11

Cast local time	DEPTH (m)	Chl "a" (mg m^{-3})	+/- 95% CI	Phaeo (mg m^{-3})	+/- 95% CI	Proportion of Chl "a" < 20 µm	Phaeo/ Chl
Cast A 0824	5	.553	.041	.179	.010	.943	.323
	40	.689	.045	.306	.035	.945	.444
	120	.007	.001	.024	.004	.813	3.428
Cast B 1141	5	.488	.046	.139	.012	.906	.285
	30	.888	.105	.328	.098	.896	.370
	100	.010	.002	.023	.007	.818	2.336

Station 11, April 11

Cast local time	DEPTH (m)	Chl "a" (mg m^{-3})	+/- 95% CI	Phaeo (mg m^{-3})	+/- 95% CI	Proportion of Chl "a" < 20 µm	Phaeo/ Chl
Cast A 1151	5	.517	.081	.177	.025	.832	.345
	40	.617	.087	.366	.138	.889	.589
	80	.037	.003	.087	.022	1.000	2.327
Cast B 1447	5	.526	.064	.210	.006	.851	.402
	30	.766	.125	.311	.093	.824	.210
	80	.053	.011	.086	.025	.770	1.605

Station 12, Apr 13

Cast local time	DEPTH (m)	Chl "a" ($\mu g\ m^{-3}$)	+/- 95% CI	Phaeo ($\mu g\ m^{-3}$)	+/- 95% CI	Proportion of Chl "a" < 20 µm	Phaeo/ Chl
Cast A 1206	20	1.910	1.397	.919	.571	.429	.493
	30	.927	.356	.650	.105	.633	.728
	80	.311	.409	.224	.237	.110	1.075

Station 12 (Cont.), Apr 14

Cast local time	DEPTH (m)	Chl "a" ($\mu g\ m^{-3}$)	+/- 95% CI	Phaeo ($\mu g\ m^{-3}$)	+/- 95% CI	Proportion of Chl "a" < 20 µm	Phaeo/ Chl
Cast C 0849	10	1.709	.501	.670	.387	.732	.382
	20	1.066	.546	.461	.493	.584	.482
Cast D 1208	30	2.461	1.867	1.069	.560	.330	.479
Cast E 1504	30	1.780	.873	.974	.442	.559	.548
	20	2.662	1.547	1.302	.817	.439	.488

Station 12 (Cont.), Apr 15

Cast local time	DEPTH (m)	Chl "a" ($\mu g\ m^{-3}$)	+/- 95% CI	Phaeo ($\mu g\ m^{-3}$)	+/- 95% CI	Proportion of Chl "a" < 20 μm	Phaeo/ Chl
Cast F 0823	40	.455	.191	.485	.207	.614	1.075
Cast G 1150	20	.961	.111	.478	.040	.886	.499

Station 12 (Cont.), Apr 16

Cast local time	DEPTH (m)	Chl "a" ($\mu g\ m^{-3}$)	+/- 95% CI	Phaeo ($\mu g\ m^{-3}$)	+/- 95% CI	Proportion of Chl "a" < 20 μm	Phaeo/ Chl
Cast K 0835	20	.935	.093	.537	.027	.883	.576
Cast M 1215	14	1.077	.204	.553	.045	.835	.517
	20	.908	.189	.549	.120	.760	.603
Cast 0 1448	20	1.045	.019	.636	.210	1.025	.610
	40	.851	.111	.463	.040	.833	.550

Station 13, Apr 17

Cast local time	DEPTH (m)	Chl "a" ($\mu g\ m^{-3}$)	+/- 95% CI	Phaeo ($\mu g\ m^{-3}$)	+/- 95% CI	Proportion of Chl "a" < 20 μm	Phaeo/ Chl
Cast A 1150	4	.408	.012	.102	.018	.990	.249
	40	.609	.055	.215	.022	.887	.354
	60	.813	.096	.410	.106	.853	.502
Cast B 1610	4	1.122	.056	.550	.040	.933	.490
	40	.460	.018	.100	.018	.991	.218

Station 14, Apr 18

Cast local time	DEPTH (m)	Chl "a" ($\mu g\ m^{-3}$)	+/- 95% CI	Phaeo ($\mu g\ m^{-3}$)	+/- 95% CI	Proportion of Chl "a" < 20 μm	Phaeo/ Chl
Cast A 0828	4	.675	.095	.242	.026	.965	.359
	30	1.031	.062	.687	.208	1.000	.668
	80	.410	.089	.373	.060	.858	.910
Cast B 1142	4	.587	.029	.204	.022	.953	.348
	30	1.399	.123	.798	.120	.933	.571
	60	.676	.052	.412	.038	.914	.610
Cast C 1447	30	.684	.052	.250	.045	.904	.365
	60	.676	.041	.295	.011	.936	.437

Station 15, April 19

Cast local time	DEPTH (m)	Chl "a" ($\mu g\ m^{-3}$)	+/- 95% CI	Phaeo ($\mu g\ m^{-3}$)	+/- 95% CI	Proportion of Chl "a" < 20 μm	Phaeo/ Chl
Cast A 0828	4	1.161	.149	.528	.043	.856	.456
	20	1.220	.186	.561	.040	.847	.462
	80	.248	.029	.337	.016	.864	1.366
Cast B 1152	20	.1.247	.298	.628	.071	.737	.511
	60	.145	.135	.129	.104	.223	1.001
Cast C 1448	20	1.344	.368	.680	.061	.687	.519
	80	.194	.029	.246	.046	1.000	1.273

Station 16, April 20

Cast Local time	DEPTH (m)	Chl "a" ($\mu g\ m^{-3}$)	+/- 95% CI	Phaeo ($\mu g\ m^{-3}$)	+/- 95% CI	Proportion of Chl "a" < 20 μm	Phaeo/ Chl
Cast A 0859	4	1.253	.403	.434	.072	.635	.357
	20	.725	.367	.350	.103	.509	.513
	60	.016	.005	.062	.007	.722	3.89
Cast B 1156	4	1.028	.315	.353	.104	.690	.347
	30	1.679	.841	.550	.259	.508	.335
Cast C 1457	4	1.271	.175	.463	.015	.850	.367
	30	2.269	1.789	.865	.579	.313	.405

Station 17, April 21

Cast Local Time	DEPTH (m)	Chl "a" (mg m^{-3})	+/- 95% CI	Phaeo (mg m^{-3})	+/- 95% CI	Proportion of Chl "a" < 20 µm	Phaeo/ Chl
Cast A 0827	12	1.360	.111	.419	.021	.972	.308
	40	1.238	.371	.575	.132	.684	.495
	80	.399	.017	.282	.039	.960	.707

APPENDIX G: Underway Data

Seawater was pumped continuously from the ship's portside seachest at a depth of about 7 m and measured for bioluminescence and in situ fluorescence, an indicator of chlorophyll a. Two representative records are shown for 19 and 20 April 1991. Note the lack of correspondence between the two signals.

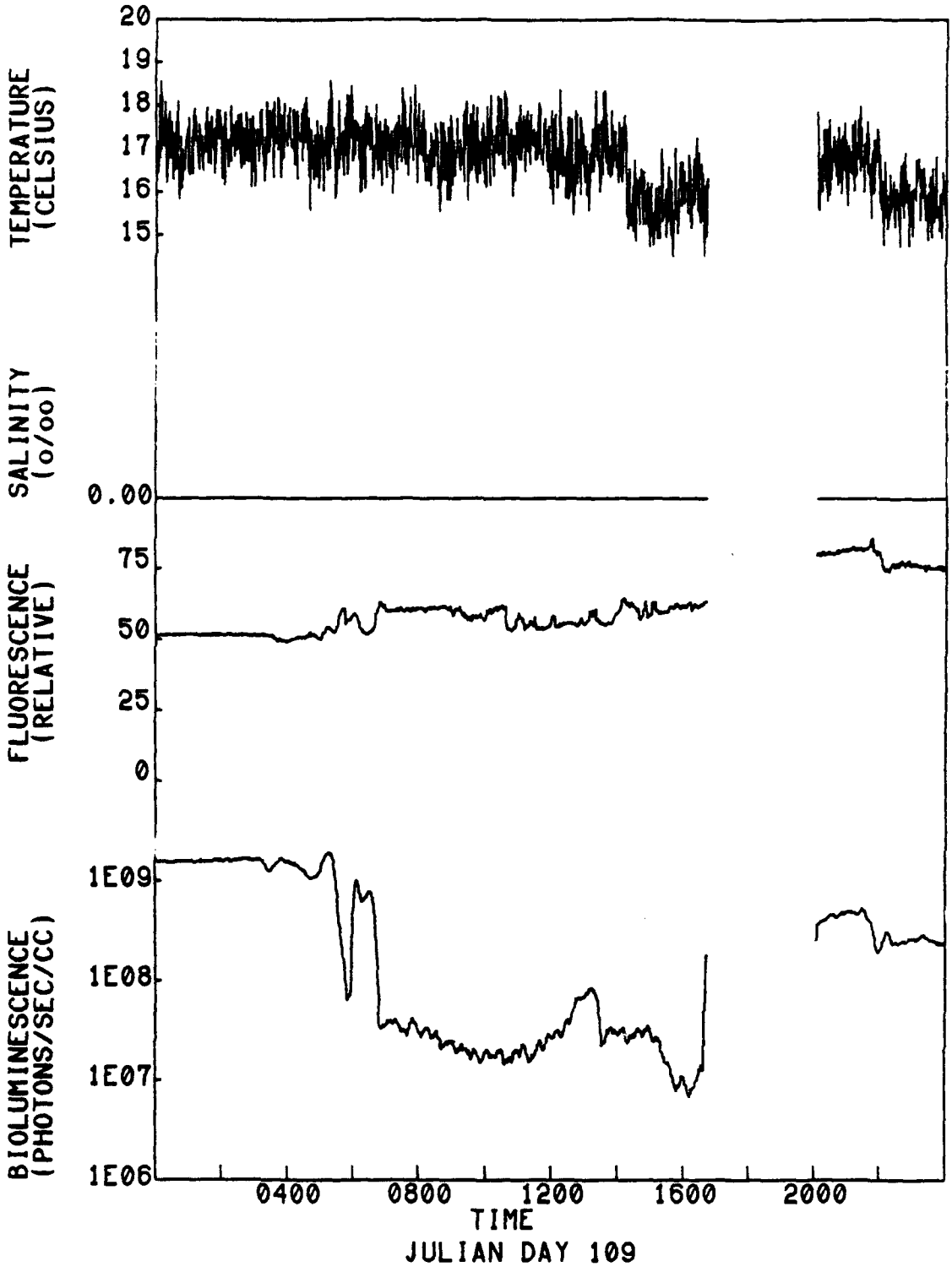

MED-OPS 91 19 April 91 Figure G-1

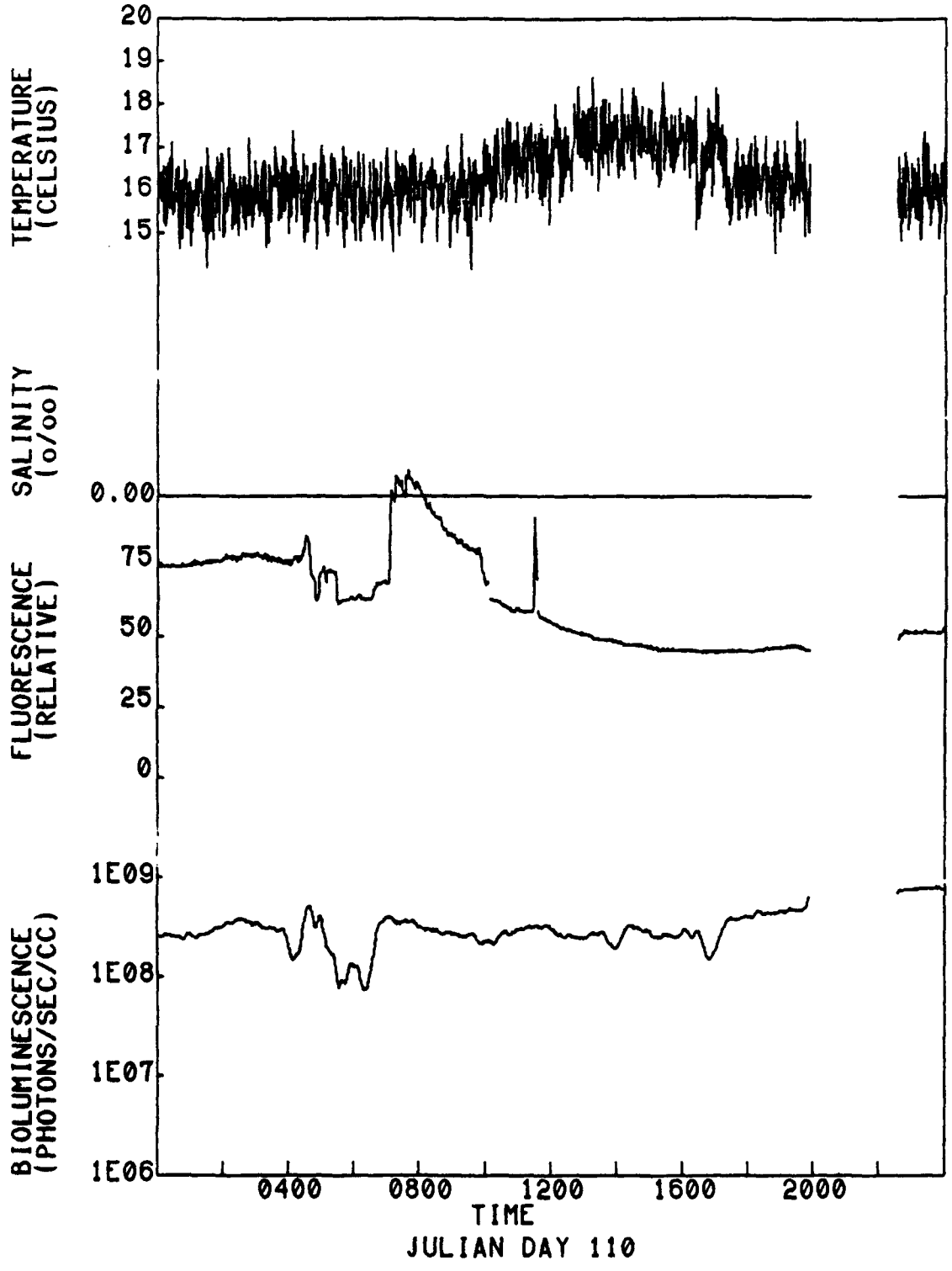

MED-OPS 91 20 April 91 Figure G-2

DISTRIBUTION LIST
TACTICAL OCEANOGRAPHY PROGRAM

CDR G. Berry
Asst. Secretary of the Navy
Research, Development, and
Acquisition
Pentagon Room 5E731, Code OCN
Navy Department
Washington, DC 20350-1000
Commercial: (703) 614-5091
Fax: (703) 697-0172

OP-096T Mr. R. Winokur
Chief of Naval Operations
Department of the Navy
Washington, DC 20350-2000
Commercial: (202) 653-1536
Fax: (202) 653-1435

OP-021T2 R. Lauer
Chief of Naval Operations
Department of the Navy
Washington, DC 20350-2000
Commercial: (703) 607-1642
Fax: (703) 607-1660

OP-021T2B E. Hashimoto
Chief of Naval Operations
Department of the Navy
Washington, DC 20350-2000
Commercial: (703) 607-1642
Fax: (703) 607-1660

Code 112 Dr. E. Hartwig
Director
Office of Naval Research
800 North Quincy Street
Arlington, VA 22217
Commercial: (703) 696-4398
Ocean Sciences

Code 1123 Dr. Spinrad
Director
Office of Naval Research
800 North Quincy Street
Arlington, VA 22217
Commercial: (703) 696-4732
Ocean Sciences

Code 1123B Mary Altalo
Director
Office of Naval Research
800 North Quincy Street
Arlington, VA 22217
Commercial: (703) 696-4590
Ocean Sciences

Code N2 CAPT Laduce
Commander
Naval Oceanography Command
SSC, MS 39529-5000
Commercial: (601) 688-4500

Code N532 J. Ownbey, Jr.
Commander
Naval Oceanography Command
SSC, MS 39522-5001
Commercial: (601) 688-4819

Code OP V. Sprague
Commanding Officer
Naval Oceanographic Office
SSC, MS 39522-5001
Commercial: (601) 688-4257

Code 23 CDR L. Bounds
Director
Office of Naval Technology
800 North Quincy Street
Arlington, VA 22217
Commercial: (202) 696-5120

J. Griffin
Commander
Space and Naval Warfare
Systems Command
2511 Jefferson Davis Highway
Building NC1
Arlington, VA 22202
Commercial: (202) 602-4869
Fax: (703) 602-4420

Code 8213 Dr. P. Temple
Commander
Naval Undersea Warfare Center
(NUWC)
(formerly NUSC)
Newport Division
Newport, RI 02841
Commercial: (401) 841-3158
Fax: (401) 841-1131

LCDR B. Williams
Commander
Submarine Group NINE
Bremerton, WA 98315-5100
Commercial: (202) 396-6095

Code 014 CDR T. Donaldson
Commander, Sub Force
U.S. Atlantic Fleet
Norfolk, VA 23511
Commercial: (804) 444-3265
AUTOVON: 564-3265

Code 225 LCDR E. Long
Commander
Submarine Development Squadron
Twelve
Box 70, Naval Submarine Base,
New London
Groton, CT 06340
Commercial: (203) 449-3378
AUTOVON: 241-3378

Dr. Charles Sinex
Applied Physics Laboratory
Johns Hopkins University
Johns Hopkins Road
Laurel, MD 20723-6099
Commercial: (301) 953-5617

Dr. J. Case
University of California, Santa
Barbara
Marine Science Institute
Santa Barbara, CA 93106
Commercial: (805) 893-2913
Fax: (805) 893-2611

Dr. Edith Widder
Harbor Branch Oceanographic
Institute
Division of Marine Sciences
5600 Old Dixie Highway
Fort Pierce, FL 34946
Commercial: (407) 465-2400, ext.
315
Fax: (407) 465-2446

Dr. T. Bell
Arete Associates
P.O. Box 16287
Arlington, VA 22215
or: 1725 Jefferson Davis Highway
Arlington, VA 22202
Commercial: (703) 892-1900
Fax: (703) 892-1906

Naval Oceanographic and
Atmospheric Research Laboratory
SSC, MS 39529-5004
Attn: Code 300
330
333 (5)
311 (3)
125P
125L (6)

Naval Research Laboratory
Washington, DC 20375
Attn: Library (2)

Naval Oceanographic Office
SSC, MS 39522-5001
Attn: Code TD
Library (2)

REPORT DOCUMENTATION PAGE

Form Approved
OBM No. 0704-0188

1. Agency Use Only *(Leave blank).*	2. Report Date. February 1992	3. Report Type and Dates Covered. Final

4. Title and Subtitle.
Bioluminescence in the Western Alboran Sea in April 1991

5. Funding Numbers.
Program Element No. 0603704N
Project No.
Task No.
Accession No. DN251016
Work Unit No. 13332Y

6. Author(s).
D.M. Lavoie, D.K. Young, and M.S. Hulbert

7. Performing Organization Name(s) and Address(es).
Naval Oceanographic and Atmospheric Research Laboratory
Ocean Science Directorate
Stennis Space Center, MS 39529-5004

8. Performing Organization Report Number.
NOARL Technical Note 212

9. Sponsoring/Monitoring Agency Name(s) and Address(es).
Naval Oceanographic and Atmospheric Research Laboratory
ASW Oceanography Office
Stennis Space Center, Mississippi 39529-5004

10. Sponsoring/Monitoring Agency Report Number.
NOARL Technical Note 212

11. Supplementary Notes.

12a. Distribution/Availability Statement.
Approved for public release; distribution is unlimited.

12b. Distribution Code.

13. Abstract *(Maximum 200 words).*

This document reports on the results of an expedition to study bioluminescence in the western Alboran Sea of the Mediterranean in April of 1991. Two oceanographic research vessels and a research submersible were involved in making extensive measurements of bioluminescence and optical properties, as wall as related biological and physical parameters. The primary research tool used was the HIDEX, a high resolution, state-of-the-art bathyphotometer. The results reported here cover only bioluminescence and related biological measurements made from the USNS Bartlett. Recommendations are given for survey requirements needed to extend measurements seasonally and geographically in this region of the Mediterranean.

14. Subject Terms.
Bioluminescence, Optical Properties

15. Number of Pages. 99

16. Price Code.

17. Security Classification of Report.	18. Security Classification of This Page.	19. Security Classification of Abstract.	20. Limitation of Abstract.
Unclassified	Unclassified	Unclassified	SAR